

3-29-2010

Tailoring Heme-Thiolate Proteins into Efficient Biocatalysts with High Specificity and Selectivity

Hui Tian

Florida International University, htian001@fiu.edu

DOI: 10.25148/etd.FI10041624

Follow this and additional works at: <https://digitalcommons.fiu.edu/etd>

Recommended Citation

Tian, Hui, "Tailoring Heme-Thiolate Proteins into Efficient Biocatalysts with High Specificity and Selectivity" (2010). *FIU Electronic Theses and Dissertations*. 172.

<https://digitalcommons.fiu.edu/etd/172>

This work is brought to you for free and open access by the University Graduate School at FIU Digital Commons. It has been accepted for inclusion in FIU Electronic Theses and Dissertations by an authorized administrator of FIU Digital Commons. For more information, please contact dcc@fiu.edu.

FLORIDA INTERNATIONAL UNIVERSITY

Miami, Florida

TAILORING HEME-THIOLATE PROTEINS INTO EFFICIENT BIOCATALYSTS
WITH HIGH SPECIFICITY AND SELECTIVITY

A dissertation submitted in partial fulfillment of the

requirements for the degree of

DOCTOR OF PHILOSOPHY

in

CHEMISTRY

by

Hui Tian

2010

To: Dean Kenneth Furton
College of Arts and Sciences

This dissertation, written by Hui Tian, and entitled Tailoring Heme-Thiolate Proteins into Efficient Biocatalysts with High Specificity and Selectivity, having been approved in respect to style and intellectual content, is referred to you for judgment.

We have read this dissertation and recommend that it be approved.

John Landrum

David Chatfield

Fenfei Leng

Martin Tracey

Xiaotang Wang, Major Professor

Date of Defense: March 29, 2010

The dissertation of Hui Tian is approved.

Dean Kenneth Furton
College of Arts and Sciences

Interim Dean Kevin O'Shea
University Graduate School

Florida International University, 2010

© Copyright 2010 by Hui Tian

All rights reserved.

DEDICATION

I dedicate this dissertation to my husband Xiao and my parents. Without their understanding, patience, support, and most of all love, the completion of this work would not have been possible.

ACKNOWLEDGMENTS

My graduate study and research at FIU in the past few years have been an amazing and rewarding experience in my life. I am indebted to so many people that have helped me to grow professionally and personally during the journey.

First of all, I wish to express my sincerest and deepest gratitude to my major professor, Dr. Xiaotang Wang, for his incredible guidance, support, patience and encouragement through the years of my graduate study. I thank him for having faith in me and providing me with such an excellent atmosphere for doing research. I cannot ask for a better mentor and cannot thank him enough for what he has done for me.

I would like to extend my appreciation to my committee members: Dr. Fenfei Leng who helped me at the very beginning of my research projects and gave me so many valuable pieces of advices and guidance; Dr. John Landrum who has guided and supported my research and study in a lot of ways; and Dr. David Chatfield and Dr. Tracey Martin who have given me so many critical comments and helpful suggestions.

Special thanks go to Dr. Andrew Terentis at Florida Atlantic University who helped me with the resonance Raman experiments for more than two years which are indispensable parts of this work. His knowledge and guidance have led me to a new technique area. Many thanks to Dr. Chenzhong Li for his support and help with the electrochemical studies, and valuable suggestions with my original proposal.

I would like to extend my heartfelt appreciation to Dr. Stanislaw Wnuk for all the care, support and encouragement he has given me along the years.

Special thanks must go to Yali HSu for the help with operation and maintenance of CD and NMR instruments, and Dr. Yucheng Jiang, Dr Yazhong Xiao, and Dr. Hedong Bian, the visiting professors in our department, for their kind assistance and inspiration to my research projects.

I thank all members of the Wang lab for their support, help, advice and friendship. I am really happy and lucky to spend the years with them who I have learned a lot from. I extend my thanks to all my friends in the chemistry department, biology department and biomedical engineering department for their generous help and encouragement, especially Shradha Prabhulkar for her kind help with the electrochemistry experiments.

I would like to acknowledge the organizations that have helped fund my research: National Science Foundation, Department of Chemistry & Biochemistry and University Graduate School at Florida International University for the financial support of a Dissertation Evidence Acquisition Fellowship. Last, I offer my regards and gratitude to all of those who have supported me in any respect during the completion of this dissertation.

ABSTRACT OF THE DISSERTATION

TAILORING HEME-THIOLATE PROTEINS INTO EFFICIENT BIOCATALYSTS

WITH HIGH SPECIFICITY AND SELECTIVITY

by

Hui Tian

Florida International University, 2010

Miami, Florida

Professor Xiaotang Wang, Major Professor

Cytochrome P450 monooxygenases, one of the most important classes of heme-thiolate proteins, have attracted considerable interest in the biochemical community because of its catalytic versatility, substrate diversity and great number in the superfamily. Although P450s are capable of catalyzing numerous difficult oxidation reactions, the relatively low stability, low turnover rates and the need of electron-donating cofactors have limited their practical biotechnological and pharmaceutical applications as isolated enzymes. The goal of this study is to tailor such heme-thiolate proteins into efficient biocatalysts with high specificity and selectivity by protein engineering and to better understand the structure-function relationship in cytochromes P450.

In the effort to engineer P450cam, the prototype member of the P450 superfamily, into an efficient peroxygenase that utilizes hydrogen peroxide via the “peroxide-shunt” pathway, site-directed mutagenesis has been used to elucidate the critical roles of

hydrophobic residues in the active site. Various biophysical, biochemical and spectroscopic techniques have been utilized to investigate the wild-type and mutant proteins. Three important P450cam variants were obtained showing distinct structural and functional features. In P450camV247H mutant, which exhibited almost identical spectral properties with the wild-type, it is demonstrated that a single amino acid switch turned the monooxygenase into an efficient preoxidase by increasing the peroxidase activity nearly one thousand folds. In order to tune the distal pocket of P450cam with polar residues, Leu 246 was replaced with a basic residue, lysine, resulting in a mutant with spectral features identical to P420, the inactive species of P450. But this inactive-species-like mutant showed catalytic activities without the facilitation of any cofactors. By substituting Gly 248 with a histidine, a novel Cys-Fe-His ligation set was obtained in P450cam which represented the very rare case of His ligation in heme-thiolate proteins. In addition to serving as a convenient model for hemoprotein structural studies, the G248H mutant also provided evidence about the nature of the axial ligand in cytochrome P420 and other engineered hemoproteins with thiolate ligations. Furthermore, attempts have been made to replace the proximal ligand in sperm whale myoglobin to construct a heme-thiolate protein model by mimicking the protein environment of cytochrome P450cam and chloroperoxidase.

TABLE OF CONTENTS

CHAPTER	PAGE
I	LITERATURE REVIEW1
	1.1 Introduction of Metalloproteins.....1
	1.2 Cytochromes P450.....8
	1.3 Heme Peroxidases.....17
	1.4 Protein Engineering of P450 and Heme Peroxidases24
	1.5 References29
II	SINGLE AMINO ACID SWITCH TURNS P450CAM FROM A MONOOXYGENASE INTO AN EFFICIENT PEROXIDASE.....42
	2.1 Summary42
	2.2 Introduction.....43
	2.3 Experimental Procedures48
	2.4 Results54
	2.5 Discussion and Conclusion66
	2.6 References70
III	ENGINEERING CYTOCHROME P450 INTO P420 WITH CATALYTIC ACTIVITIES76
	3.1 Summary.....76
	3.2 Introduction77
	3.3 Experimental Procedures83
	3.4 Results and Discussion86
	3.5 References98
IV	SPECTROSCOPIC STUDY OF A NOVEL HEME IRON LIGAND SET IN ENGINEERED CYTOCHROME P450CAM105
	4.1 Summary105
	4.2 Introduction106
	4.3 Experimental Procedures111
	4.4 Results114
	4.5 Discussion and Conclusion125
	4.6 References130
V	PROTEIN ENGINEERING OF MYOGLOBIN WITH THIOLATE PROXIMAL LIGATION.....135
	5.1 Summary.....135
	5.2 Introduction.....136

5.3 Experimental Procedures	142
5.4 Results and Discussion	144
5.5 References	150
APPENDICES	154
VITA	175

LIST OF TABLES

TABLE	PAGE
1.1 Heme-thiolate proteins and heme-thiolate protein mimics with redox-potential axial ligand switches	7
1.2 Cytochrome P450-catalyzed reactions	9
2.1 Wavelength and extinction coefficients of absorption maxima for wild type and V247H mutant of P450cam	56
3.1 Wavelength and extinction coefficients of absorption maxima for P450cam, P420cam, L246K and L246K 3H mutants	90
4.1 Wavelength and extinction coefficients of absorption maxima for wild type and G248H mutant of P450cam	117
5.1 Proximal sequence alignment of Mb and its P450 and CPO mimics	142
5.2 Wavelength and extinction coefficients of absorption maxima for P450cam, Mb, MbP, and MbP H64G	149

LIST OF FIGURES

FIGURE	PAGE
1.1 Structure of iron protoporphyrin IX, heme <i>b</i>	4
1.2 Heme centers of heme- thiolate proteins and heme- imidazole proteins	6
1.3 The cytochrome P450 catalytic cycle including the “peroxide-shunt” pathway	12
1.4 Cytochrome P450cam putative oxygen complex, Compound I	13
1.5 Crystal structure of cytochrome P450cam	16
1.6 Mechanism of Compound I formation in heme peroxidases with distal His	20
1.7 “Push-pull” mechanisms for O-O bond cleavage of both heme-imidazole proteins and heme-thiolate proteins.....	21
1.8 Proposed mechanism of Compound I formation catalyzed by chloroperoxidase	23
2.1 The active site structure of camphor-bound cytochrome P450cam (V247).....	47
2.2 UV-vis spectra of P450camV247H in various oxidation states	55
2.3 UV spectra of P450camV247H and its KCN bound complex	57
2.4 Far-UV CD and visible CD spectra of substrate-bound forms of the WT and V247H mutant of P450cam	58
2.5 Resonance Raman spectra of ferric and ferrous WT P450cam and V247H mutant with and without camphor binding	61
2.6 600-MHz ¹ H Nuclear Magnetic Resonance spectra of the low spin cyanide complexes of WT P450 and V247H mutant	62
2.7 Cyclic voltammograms of WT P450cam and V247H mutant in the presence and absence of substrate camphor	63

2.8	ABTS assay of WT P450cam, V247H and CPO at different pH values	65
3.1	Heme environmental structure of ferric cytochrome P450cam and chloroperoxidase	80
3.2	UV-visible spectra of P450H in various oxidation states	87
3.3	ABTS assay of wild-type P450cam and P450H	87
3.4	UV-visible spectra of P450camL246K in various oxidation states	89
3.5	Resonance Raman spectra of ferric and ferrous WT P450cam (with and without camphor), P420, L246K, L246K 3H mutants	92
3.6	Resonance Raman spectra of Fe ^{II} -CO complexes of P450cam L246K and L246K 3H mutants in low and high frequency regions	93
3.7	Fe ²⁺ -CO - Fe ²⁺ - ¹³ C ¹⁸ O difference spectra of P450camL246K in both low and high frequency regions	95
3.8	Correlation of Fe-CO and C-O stretching frequencies for different heme proteins and porphyrin derivatives (P450L246K)	96
3.9	ABTS assay of P450camL246K, P420 and CPO	97
4.1	The active site structure of camphor-bound cytochrome P450cam (G248).....	110
4.2	UV-vis spectra of P450camG248H in various oxidation states	115
4.3	Resonance Raman spectra of ferric and ferrous WT P450cam and G248H mutant with and without camphor binding	119
4.4	Resonance Raman spectra of ferrous-CO complexes of WT P450cam and G248H mutant in both low and high frequency	120
4.5	CD spectra of both camphor-free and camphor-bound forms of the WT and G248H mutant of P450cam	123
4.6	Cyclic voltammograms of P450cam and G248H	124
5.1	A ribbon diagram of sperm whale myoglobin crystal structure	140
5.2	Crystal structure of sperm whale myoglobin active site	141

5.3	UV spectra of Mb and P450cam in various oxidation states	145
5.4	UV spectra of MbP in various oxidation states	147
5.5	UV spectra of MbP H64G in various oxidation states	148

LIST OF ABBREVIATIONS

ACRONYM	FULL NAME
CYP	cytochromes P450
CPO	chloroperoxidase
HRP	horseradish peroxidase
CIP	<i>Coprinus cinereus</i> peroxidase
CBS	cystathionine β -synthase
CcP	cytochrome c peroxidase
NOS	nitric oxide synthase
iNOS	inducible nitric oxide synthase
CooA	CO-sensing transcriptional activator
Pdx	Putidaredoxin
Cpd 0	compound 0
Cpd I	compound I
Cpd II	compound II
WT	wild type
CO	carbon monoxide
SDS	sodium dodecyl sulfate
PAGE	polyacrylamide gel electrophoresis
ITPG	isopropyl β -D-1-thiogalactopyranoside

PMSF	phenylmethylsulfonyl fluoride
DEAE	diethylaminoethyl (cellulose)
DTT	dithiothreitol
NMR	nuclear magnetic resonance
RR	resonance Raman
NAD(P)H	nicotinamide adenine dinucleotide (phosphate), reduced
NHE	normal hydrogen electrode
Tris	Tris-(hydroxymethyl)-aminomethane
SWCNT	single-walled carbon nanotubes
Mb	myoglobin
MbP	myoglobin P450cam mimic
MbO	myoglobin CPO mimic
Hb	hemoglobin
Ala/A	alanine
Arg/R	arginine
Asp/D	aspartic acid
Cys/C	cysteine
Glu/E	glutamic acid
Gly/G	glycine

His/H	histidine
Leu/L	leucine
Lys/K	lysine
Ser/S	serine
Thr/T	threonine
Val/V	valine

CHAPTER I. LITERATURE REVIEW

1.1 INTRODUCTION OF METALLOPROTEINS

It is an old wisdom that metals are indispensable for life. Nature uses metal ions extensively for both structural and functional roles. By incorporating metal ions into proteins, a diverse class of biologically significant macromolecules termed metalloproteins is created. In fact, about one third to one half of all proteins require metals to carry out their functions (1). Metalloproteins can catalyze some of the most difficult and yet important transformations in nature, such as photosynthesis, respiration, electron transfer, water oxidation, molecular oxygen transport and reduction, and nitrogen fixation (2). The significance of iron, copper, and zinc in biological systems together with other metals including cobalt, manganese, molybdenum, and nickel has been evident for decades (3). The catalytic activities of these metal-containing systems depend on both the nature of the metal and the influence of the protein environment including the type of ligands provided by the protein, the geometry of the coordination sphere and the protein structure in the vicinity of the metal ion.

A great deal of effort has been devoted to the understanding of the structure and function of metalloproteins because of their indispensable roles in biological systems and their ability to catalyze some of the most difficult chemical reactions under mild and environmentally friendly conditions. Furthermore, such enzymes are able to catalyze

regio- and stereo-selective transformations and thus offer products that are critical to the production of fine chemicals, pharmaceuticals, and many other value-added materials. To better understand the critical roles of metalloproteins, protein engineering has been used to study their structure-function relationships by either rational design or directed evolution.

1.1.1 Heme-containing proteins

Heme is comprised of a tetrapyrrole ring system complexed with an iron atom in the center. One or two axial ligands complete the coordination requirement of the heme iron. A heme protein (also known as hemoprotein or haemoprotein) contains a heme prosthetic group, bound either covalently or non-covalently to the protein. As one of the largest classes of metalloproteins, the heme-containing proteins have attracted a great deal of attention from the scientific community since the beginning of modern enzymology. They have diverse biological functions and are able to catalyze a broad spectrum of biological processes ranging from electron transfer (cytochromes) to oxygen storage (myoglobin) / transport (hemoglobin) / activation (P450) and molecular sensing (CooA) (4-6).

Many biochemical and biophysical studies of heme proteins and their variants have suggested that the type of reaction catalyzed by different hemoproteins is normally controlled by: 1) the nature of the proximal ligand and its surrounding residues, 2) the distal environment including conserved significant residues, and 3) the type of heme (7).

The most common heme prosthetic group is iron protoporphyrin IX also known as heme *b* (Fig. 1.1), which is the prosthetic group found in all the heme proteins discussed in this dissertation. The ferriprotoporphyrin IX is made up of four pyrrol rings joined by methine bridges with ferric iron in the center of the molecule replacing the two hydrogen atoms attached to pyrrol nitrogens. The remaining two axial ligands to the heme iron are located above (distal) and below (proximal) the porphyrin plane respectively. Different types of heme have different side chains. There are eight side chains in ferriprotoporphyrin IX (heme *b*): four methyl groups at positions 1, 3, 5, and 8, two vinyl groups at positions 2 and 4, and two propionate groups at positions 6 and 7. The carbon atoms of the methine bridges are symbolized as α , β , γ , and δ (8). In many heme proteins, oxygen or hydrogen peroxide will bind to the heme iron in the distal site as the proximal site is normally occupied by certain amino acid heteroatoms. For example, in most heme peroxidases, there is a histidine nitrogen serving as the proximal ligand; while chloroperoxidase, as an exception, possesses a cysteinate sulfur ligated to the heme iron. The distal side in these cases is the catalytic center, and its coordination state varies in different states of the enzyme during catalytic cycles. In some other heme proteins with no directly bound oxygen or hydrogen peroxide, both of the axial coordination sites are occupied by heteroatoms from the nearby amino acids, like cytochrome *c* which has a histidine and methionine as the axial ligands (9).

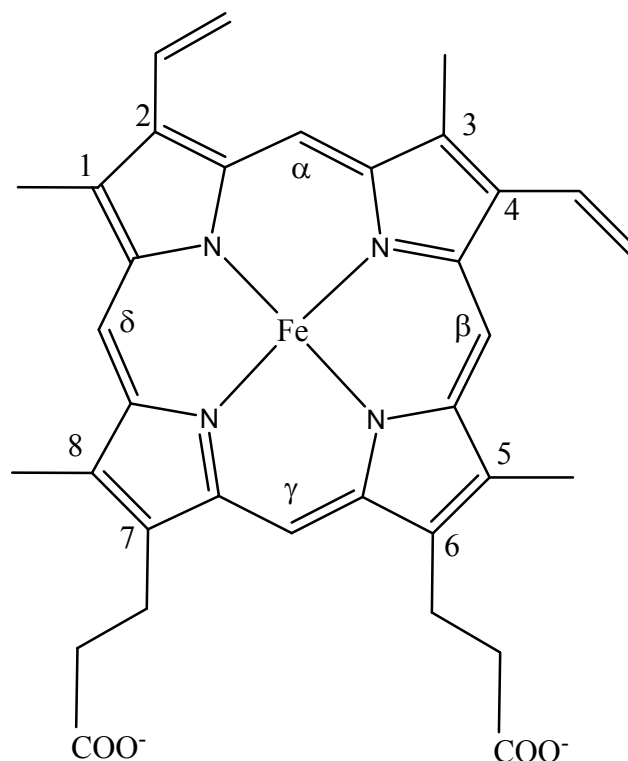


Figure 1.1 Structure of iron protoporphyrin IX, heme *b*. A-D indicate the location of each pyrrole ring and α to δ identify the site of each methane bridge.

One of the most important questions about heme proteins is how different heme proteins achieve such structural and functional diversity by using the same heme prosthetic group (5-7). For instance, hemoglobin and myoglobin are O₂ carriers and can bind O₂ reversibly (10, 11); heme oxygenase (HO) and cytochromes P450 activate O₂, and transfer the oxygen atom to the heme prosthetic group or to other organic molecules (12-15); FixL protein, CoxA protein and guanylate cyclase serve as biological sensors for O₂, CO and NO respectively (16). The protein environment, especially near the active site, clearly plays an essential role in governing the reactivity of the metal iron, and it could be the determining factor that controls the functionalities of the distinct hemoproteins with

essentially identical metal centers. Therefore, the redesign of heme proteins, from one type into another, not only provides a test of the known factors governing their structure and function but also allows the direct comparison of two different heme proteins in the same framework to achieve protein variants with better efficiency and selectivity (7).

1.1.2 Heme-Thiolate Proteins and their structural mimics

Heme-thiolate proteins are a group of heme proteins with a thiolate anion from a deprotonated cysteine residue serving as the proximal heme ligand (Fig. 1.2 (A)). They constitute one of the two major categories of heme-containing proteins found in living organisms. The other group is the heme-imidazole proteins whose axial ligand is an imidazole group from a histidine residue (Fig. 1.2 B). Their difference in the axial ligand is also indicated in the optical properties of their reduced forms with carbon monoxide bound: the heme-thiolate proteins usually show a characteristic absorption maximum at around 450nm, whereas the corresponding absorption spectrum of heme-imidazole proteins give a Soret peak at around 420nm (17). Therefore, the optical features of CO complexes have generally been used as a probe for the nature of proximal ligation in hemoproteins.

There are several classes of heme-thiolate proteins reported such as cytochromes P450, chloroperoxidase (CPO), nitric oxide synthases (NOS), cystathionine β -synthase, the sensor protein CooA and eIF2 α kinase (17). Heme-thiolate proteins are essentially among the most versatile biocatalysts of the hemoprotein family. They serve as

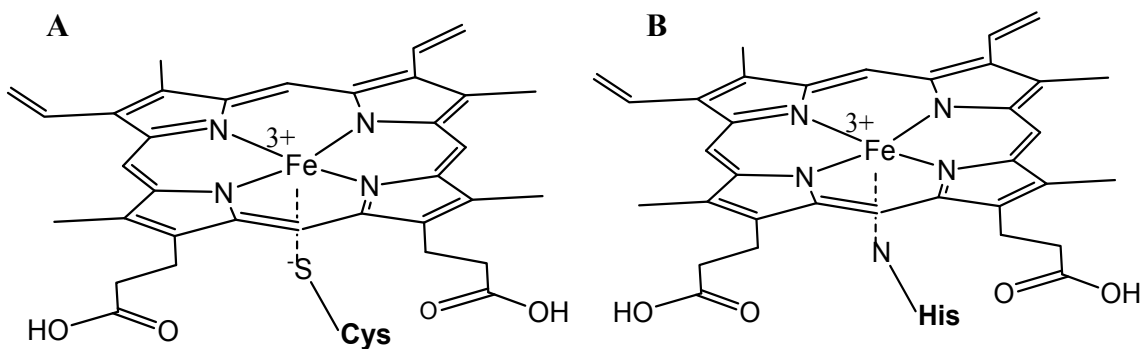


Figure 1.2 Heme centers of heme-thiolate proteins with Cys as the proximal ligand (A), and heme-imidazole proteins with His as the proximal ligand (B).

oxidoreductases that perform essential functions in the biological systems. The hallmark reaction catalyzed by these enzymes is the substrate oxidation, converting R-H to R-OH (18). It has been suggested that the identity of the axial ligands to the heme iron, the nature of the heme environment, and the accessibility of the substrate to the active site combine to play crucial roles in determining the enzyme activities. Because of the similarity of the protein environment that heme-thiolate proteins and heme-imidazole proteins share, many studies have been carried out to engineer the heme-imidazole proteins by replacing the proximal histidine with a cysteine residue to mimic heme-thiolate proteins, in order to better understand the structure-function relationships in these heme-containing enzymes.

In fact, the proximal thiolate ligation is not kept intact in various oxidation states in all heme-thiolate proteins, and in some cases the Fe-thiolate ligation is lost upon reduction and carbon monoxide binding. That also happens in many hemoproteins with

engineered iron-thiolate ligands. Table 1.1 listed some examples of the heme-thiolate proteins and their mimics with redox-dependent axial ligands in various oxidation states.

Table 1.1. Heme-thiolate proteins and their mimics with redox-dependent axial ligand switches.

Protein	Fe (III)	Fe (II)	Fe (II)-CO	Ref
Heme-thiolate proteins				
P450	Cys/OH ⁻	Cys	Cys/CO	(13)
CPO	Cys/OH ⁻	Cys	Cys/CO	(19-21)
NOS	Cys/OH ⁻	Cys	Cys/CO	(22, 23)
CooA	Cys/Pro	His/Pro	His/CO	(24, 25)
CBS	Cys/His	Cys/His	His/CO	(26, 27)
Engineered heme-thiolate protein mimics				
Mb H93C	Cys	His	His/CO	(28, 29)
CcP H175C/D235L	Cys	Cysteic acid	Cysteic acid/CO	(30)
Cytochrome c M80C	Cys/His	His	His/CO	(9)
Heme oxygenase H25C	Cys/H ₂ O		CO	(31)
NP1 H60C	Cys	H ₂ O	CO	(32)
Cytochrome <i>b5</i> H39C	Cys/His	His	His/CO	(33)

For instance, in the CO-sensing transcriptional activator CooA, the Cys75 axial ligand of the ferric heme is exchanged to His77 upon reduction and CO activation. Therefore, the electronic absorption spectrum of CO-complex of CooA exhibits the Soret band at around 420nm instead of 450nm, typical of thiolate-ligated hemoproteins (25). In the listed hemoproteins with engineered heme-thiolate ligations in their ferric forms (Table 1.1), upon reduction the iron-thiolate ligands are all lost either by oxidation, dissociation or protonation, resulting in ferrous-CO complexes with 420-nm Soret

absorption maxima. Heme oxygenase uses His-25 as its proximal iron ligand. The substitution of His-25 with a cysteine results in a 6-coordinated ligation of the iron to a cysteinate and water molecule, but the Fe-Cys bond is lost upon being reduced and the ferrous heme is only loosely bound to a postulated water molecule (31).

1. 2 CYTOCHROMES P450

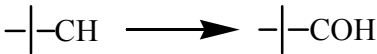
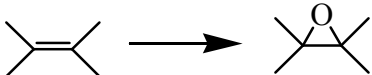
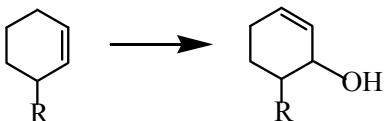
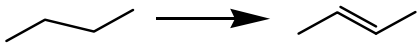
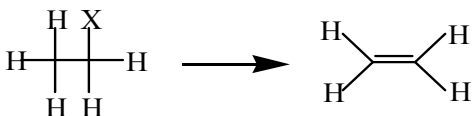
Cytochrome P450 (CYP) monooxygenase, a red pigment first found in liver microsomes and named for its spectral properties, is one of the most important heme-thiolate proteins. The ability of P450s to functionalize unactivated hydrocarbon at physiological conditions has attracted considerable interests from the chemical and biological communities (13). There are several books dedicated to the superfamily of P450 enzymes (14, 34-39). Many reviews have elaborated the chemistry, structure and functions of P450s (13, 40-44). The P450 enzymes have been identified in all domains of life and more than 11,500 distinct CYP proteins had been known and named as of Feb. 2009 (45). In all P450s, the heme-thiolate ligation is highly conserved in the proximal side of the active site and is considered to play critical roles in the catalytic mechanisms. The cytochromes P450 perform regio- and stereo-specific reactions under physiological conditions and the most common reaction catalyzed by cytochrome P450 is a

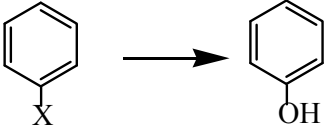
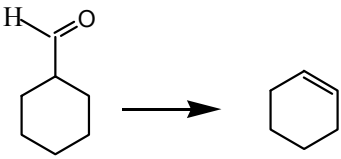
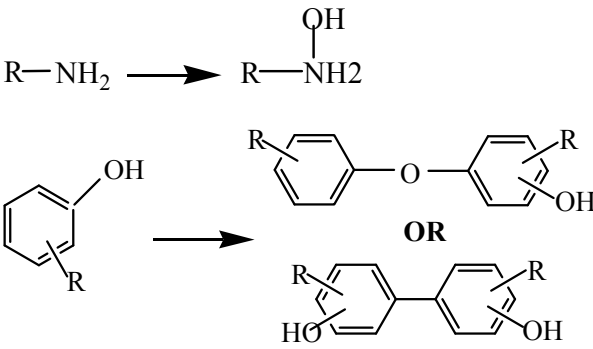
monooxygenase reaction in which one atom of oxygen is inserted into an organic substrate (RH) while the other oxygen atom is reduced to water (Eq. 1).



The P450s generally require two electrons from either NADH or NAD(P)H to activate O₂, and the electrons are transferred to the heme of P450 via a protein electron transport system, usually a reductase and an iron-sulfur protein, depending on the type of P450s. In addition to hydroxylation, P450s are able to catalyze a number of other significant reactions as listed in Table 1.2. The catalytic versatility, substrate diversity and sheer number of P450s have lead to considerable interest over the last few decades in the engineering of P450 enzymes for a variety of purposes.

Table 1.2 Cytochrome P450-catalyzed reactions (34, 46).

C-H hydroxylation	
Epoxidation	
Allylic Rearrangement	
Desaturation	
Reductive Dehalogenation	

Oxidative Dehalogenation	
Alcohols oxidation	$\text{H}_3\text{C}-\underset{\text{OH}}{\underset{ }{\text{CH}}}-\text{H} \longrightarrow \text{H}_3\text{C}-\overset{\text{O}}{\parallel}{\text{CH}}$
Aldehyde oxidation	$\text{H}_3\text{C}-\overset{\text{O}}{\parallel}{\text{CH}} \longrightarrow \text{H}_3\text{C}-\overset{\text{O}}{\parallel}{\text{C}}-\text{OH}$
Deformylation	
Oxidative deformylation	$\begin{array}{c} \text{R}_1 \\ \\ \text{H}-\text{C}-\text{CHO} \\ \\ \text{R}_2 \end{array} \begin{array}{c} \text{R}_3 \\ \\ \text{C} \\ \\ \text{R}_4 \end{array} \longrightarrow \begin{array}{c} \text{R}_1 \\ \\ \text{C}=\text{C} \\ \quad \\ \text{R}_2 \quad \text{R}_3 \\ \quad \\ \quad \text{R}_4 \end{array} + \text{HCOOH}$
Sulfoxidation	$\text{R}-\text{S}-\text{R}' \longrightarrow \text{R}-\overset{\text{O}}{\parallel}{\text{S}}-\text{R}'$
N-Dealkylation	$\begin{array}{c} \\ \text{N}-\text{R} \\ \end{array} \longrightarrow \begin{array}{c} \\ \text{N}-\text{H} \\ \end{array}$
O-Dealkylation	$\text{R}-\text{O}-\text{CH}_2\text{R}' \longrightarrow \text{ROH} + \text{R}'\text{COH}$
N-Oxygenation	$\text{R}-\text{NH}_2 \longrightarrow \text{R}-\overset{\text{OH}}{\underset{ }{\text{NH}}}_2$
Peroxidase-type oxidation	
NO Synthase-type oxidation	$\begin{array}{c} \text{R}_1 \\ \\ \text{C}=\text{N}-\text{OH} \\ \\ \text{R}_2 \end{array} \longrightarrow \begin{array}{c} \text{R}_1 \\ \\ \text{C}=\text{O} \\ \\ \text{R}_2 \end{array} + \text{NO (or N}_x\text{O}_y)$

1.2.1 Catalytic cycle of P450s

The generally accepted catalytic cycle of P450 enzymes is shown in Fig. 1.3 (34). The resting state **(1)** is a six-coordinate, low-spin ferric heme, with porphyrin nitrogen atoms occupying the four equatorial position and cysteine and water serving as the axial ligands at the proximal and distal sides, respectively. The catalytic cycle is initiated by the substrate binding in the protein active site followed by the displacement of the distal water molecule, converting the six-coordinate low-spin ferric heme to a predominantly five-coordinate high-spin form (intermediate **(2)**) (47). In the meantime, the reduction potential is increased by greater than +100mV (substrate-dependent) upon substrate binding, which has been shown to initiate electron transfer to the heme from NAD(P)H via native reductase proteins (48). The first electron transfer leads to the reduction of ferric to ferrous heme (intermediate **(3)**), followed by dioxygen binding at the ferrous heme iron, yielding an unstable ferrous-oxy species (intermediate **(4)**). The second electron transfer is suggested to be the rate-limiting step in the cycle followed by protonation and the formation of the hydroperoxo-iron complex (intermediate **(6)**, Compound 0). Then this species is further protonated to generate highly reactive Compound I (49), ferryl-oxo porphyrin π -radical cation, the key intermediate **(7)** in the catalysis (Fig. 1.4). This step involves the heterolytic splitting of the oxygen-oxygen bond and the releasing of a water molecule. A highly conserved threonine residue near the heme has been suggested to play an essential role to relay protons from the solvent to

the heme (50, 51). Finally, the Fe-ligated oxygen atom is transferred to the substrate through intermediate (8) followed by hydroxylation and regeneration of the resting state.

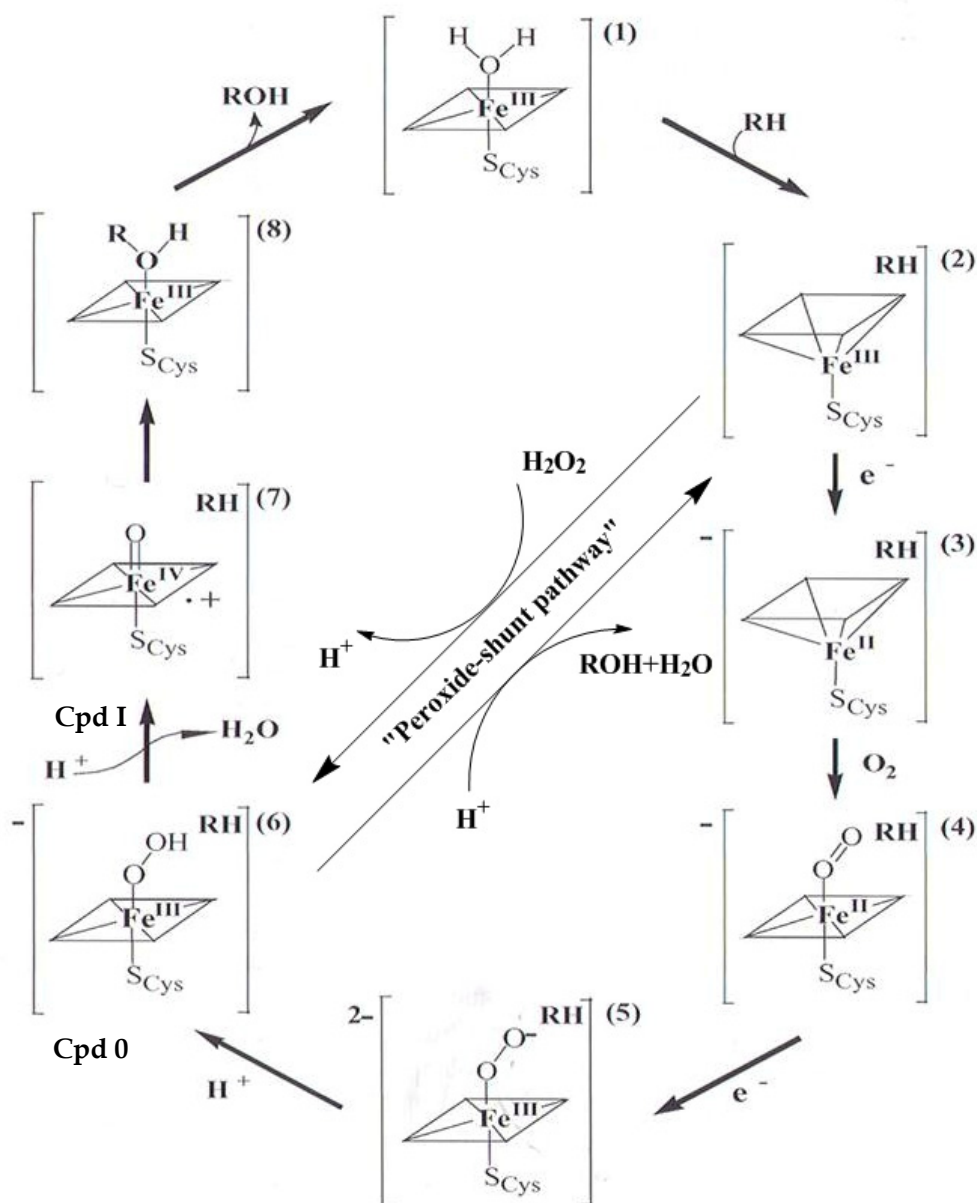


Figure 1.3 The cytochrome P450 catalytic cycle including the “peroxide-shunt pathway”. RH is substrate and ROH is the product. The porphyrin molecule is represented as a parallelogram. Intermediates (6) and (7) are Compound 0 and Compound I respectively.

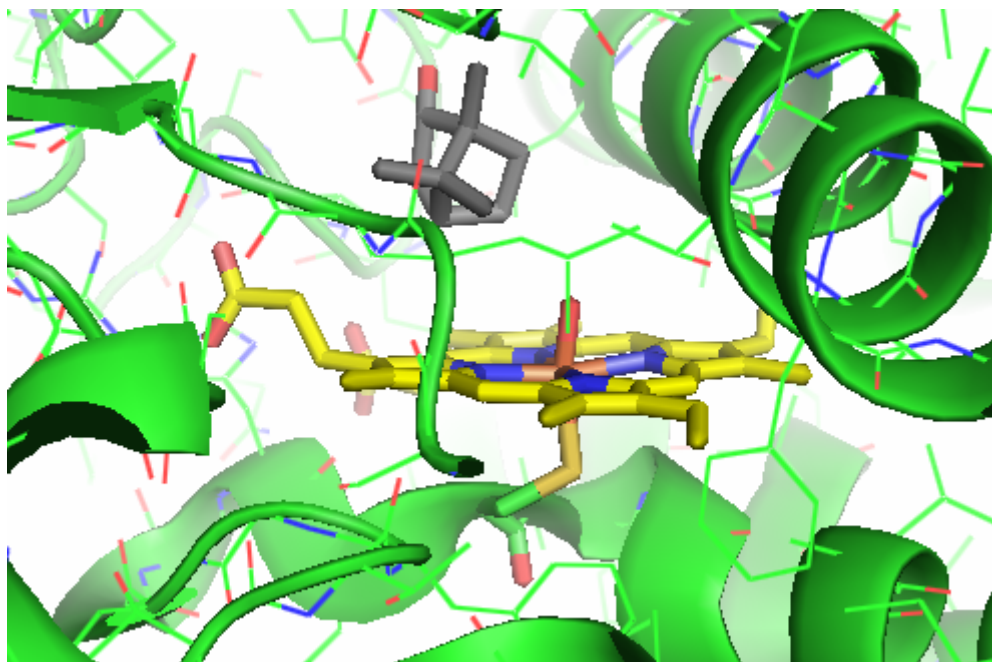


Figure 1.4 P450cam putative oxygen complex, Compound I. The heme prosthetic group is colored in yellow, the substrate is in gray and the bound dioxygen is in red. All other amino acids are depicted in lines and ribbons. This image was created from the crystal data (PDB code 1DZ9) using PYMOL (52).

In the standard catalytic cycle, Compound I would hydroxylate the substrate and regenerate the P450 resting state. Although the main steps mentioned above are similar for all P450 enzymes, each step is far from being simple and many side reactions exist leading to the leakage of the cycle (34).

1.2.2 “Peroxide-shunt” pathway

In the absence of reducing cofactors, partner proteins and dioxygen, P450s are capable of utilizing hydrogen peroxide or organic peroxy compound as the oxidant to hydroxylate substrates through the “peroxide-shunt” pathway (Eq. 2) (14):



As illustrated in Fig. 1.3, the shunt pathway bypasses a large portion of the standard catalytic cycle by eliminating the rate-limiting electron transfer steps and directly results in the generation of the $\text{Fe}^{\text{III}}\text{-OOH-}$ complex (**Cpd. 0**). There are many studies about the P450 peroxide shunt pathway (53-59). This type of reaction is not suggested to be physiological, since the turnover rate is quite low and high concentrations of peroxide are needed to achieve the optimal reaction rate. But on the other hand, some unique P450 enzymes have been reported to function as peroxxygenases by utilizing hydrogen peroxide or the peroxide groups of their substrates as the oxygen donor with high catalytic turnover rates, compared with a normal monooxygenation reaction or the peroxide-shunt reaction catalyzed by common P450s (60-66). The “peroxxygenase” activity of P450s has definitely broadened the versatility of the superfamily and offers a possibility to utilize cell-free P450-dependent catalysis without the requirement of NAD(P)H, and auxiliary proteins.

1.2.3 P450 Structure

In the massive superfamily of cytochrome P450s, there are more than 11,500 distinct CYP proteins known to date, while the sequence identities between the P450 families are generally low (about 10-30%) (45, 67). Despite the sequence diversities, P450 in many different families and many different organisms share a high degree of structural conservation in their secondary and tertiary folds (34, 68, 69). So far, there are over 300 unique P450 structures available in the Protein Data Bank. Most P450 enzymes are normally described as consisting of α helical and β sheet domains. Unlike peroxidases which clearly fold into N- and C-terminal helical-rich domains with the heme sandwiched between the helices from each domain, P450s do not fold into distinctly divided N- and C-terminal domains. For example, cytochrome P450cam, the first protein to be crystallized in the P450 superfamily, divides into a helix-rich domain on the right side and a β -sheet-rich domain on the left side (Fig. 1.5). The heme group is bracketed between the proximal helix L and distal helix I in the C terminal half of the molecule, while a majority of the β -structure is also in the C-terminal half but located far from heme (70, 71).

The heme prosthetic group is deeply embedded in the hydrophobic interior, which itself provides the largest hydrophobic surface for interactions with the substrates. The heme is oriented nearly parallel to the surfaces between helices L and I with no significant exposure to the protein surface (13). The most distinct structural feature of

P450 is the presence of an unusual proximal ligation, thiolate sulfur provided by a deprotonated cysteine residue. It has been generally agreed that the Cys thiolate ligand to the heme iron and its surrounding protein environment play unique and critical roles in P450 catalysis. In P450s, the protein architecture surrounding the proximal Fe-Cys ligation is highly conserved. In almost all P450s with known structures, the peptide NH of the Cys ligand is the proton donor in an H-bond with a peptide carbonyl O atom, which forms a tight structure placing the Cys sulfur atom in a position surrounded by

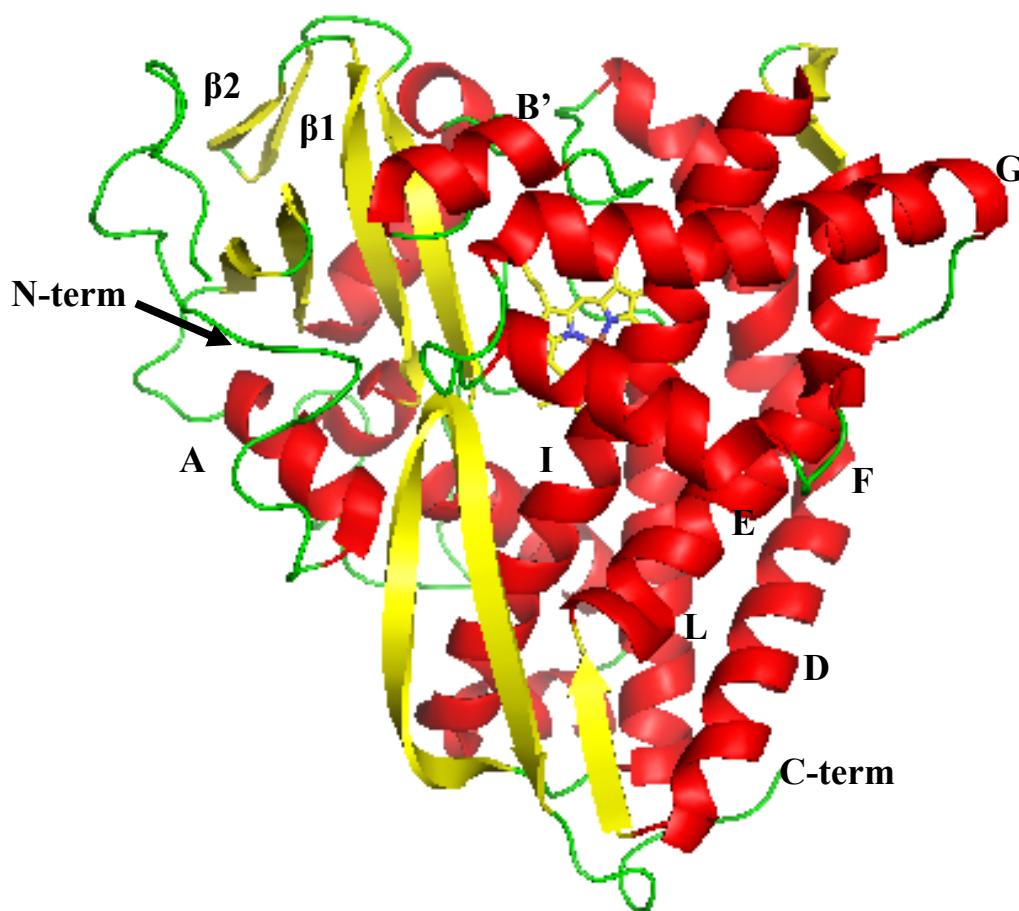


Figure 1.5 Crystal Structure of cytochrome P450cam showing the key elements of secondary structure in different colors. This figure was generated from the crystal data (PDB code 2CPP) using PYMOL (70).

peptide NH groups forming H-bonds with the thiolate ligand (34). For instance in cytochrome P450cam, the sulfur from Cys357 is surrounded by three amide protons from Leu358, Gly359 and Gln360, which have been reported to stabilize the coordination of the anionic thiolate ligand to the reduced heme iron and also control the “push” effect of the thiolate ligand (70, 72). Other P450 enzymes including P450BM3, P450eryF, and P450terp also possess such NH-S hydrogen bonds (67, 73, 74). This characteristic feature has also been found in other heme thiolate enzymes, such as CPO utilizing two of the three NH-S hydrogen bonds and NOS accepting an additional H-bond from the indole NH of Trp (20, 75).

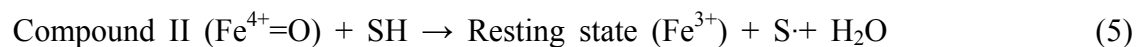
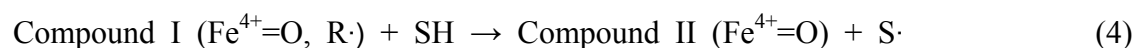
1.3. HEME PEROXIDASES

Nonmammalian heme peroxidases and cytochrome P450s are often grouped together because they both contain a single low-potential ferriprotoporphyrin IX (Fig. 1.1) and share similar intermediates in their respective catalytic cycles (76). The first heme peroxidase crystal structure solved was yeast cytochrome *c* peroxidase (CcP) (77) followed by the first P450 structure (70). Heme peroxidases have played a key role in the development of modern enzymology. They are ubiquitous enzymes that catalyze one electron oxidation of various micro- and macromolecular substrates by utilizing hydrogen peroxide or lipid hydroperoxides as the oxidant, except for chloroperoxidase which is a heme-thiolate protein and performs two-electron oxidations as well (8, 78-80). Almost all

functionally related peroxidases, such as horseradish peroxidase or cytochrome *c* peroxidase, possess a histidine proximal ligand. The crystal structure studies of the heme peroxidases have firmly established the similarity in their active site architecture: histidine and arginine in the distal side serving as a proton acceptor from hydrogen peroxide and a charge stabilizer, respectively, and heme-bound histidine and hydrogen-bonded aspartic acid in the proximal side of the heme prosthetic group (81-85).

1.3.1 Catalytic cycles

Most heme peroxidases follow the reaction scheme as shown in equations (3-5) and share common reaction intermediates, Compound I and Compound II (8, 86, 87)



The catalytic cycle begins with the coordination of one equivalent of hydrogen peroxide to the resting ferric peroxidase. The bound peroxide undergoes rapid heterolytic cleavage to produce the active intermediate Cpd I, the ferryl-oxo porphyrin cation radical, where R is the organic moiety of the heme or an amino acid residue, similar to cytochrome P450s (88). This is a two-electron oxidation/reduction reaction, in which the enzyme is oxidized and hydrogen peroxide is reduced to water. In the following steps, Cpd I is reduced by an organic substrate, usually an aromatic molecule to give a substrate radical, to the resting state in two sequential one-electron transfer reactions via a second

active intermediate, Cpd II, a ferryl-oxo porphyrin complex (87, 89). It is different from P450s which oxidize substrates by inserting one O₂-derived oxygen atom into a substrate C-H bond.

The ability to react rapidly with hydrogen peroxide to form Cpd I has distinguished peroxidases from other hemoproteins. This characteristic reactivity has a great deal to do with the influence of the protein environment around the heme center. In most heme peroxidases, there is a highly conserved histidine residue in the distal pocket of the active site (82-85, 87, 90-93). Many studies have shown that the distal His plays a critical role as a general acid-base catalyst in the formation of Cpd I in the peroxidase catalytic cycles (87, 94-97). It is proposed that the conserved His facilitates the generation of the initial Fe-OOH complex by deprotonating an approaching hydrogen peroxide as a base and subsequently heterolytically cleaving the O-O bond by protonating the departing distal oxygen as an acid (Fig .1.6) (98). Also, a network of hydrogen bonds is reported to assist the distal histidine in its catalytic role in many heme peroxidases such as horseradish peroxidase (Asn-70 H-bonded to His-42), cytochrome *c* peroxidase, lignin peroxidase and *Arthromyces ramosus* peroxidase, and others (81, 84, 91, 99).

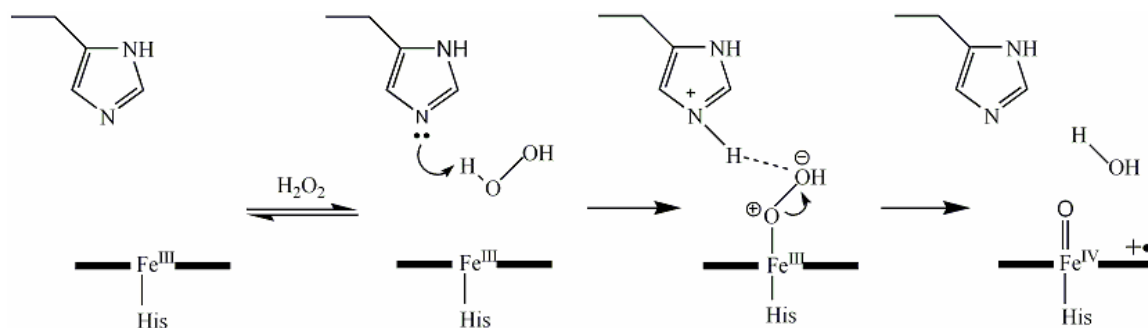


Figure 1.6 Mechanism of Compound I formation in heme peroxidases with distal His.

1.3.2 “Push-Pull” mechanism compared with P450s

It is intriguing that heme peroxidases and cytochrome P450 enzymes perform distinct physiological functions while using the same cofactor. Nevertheless, they do share the same key, highly reactive intermediate in their catalytic cycles, Cpd I. It has been reported that the proximal ligand and some distal residues in these heme proteins play significant roles in the promotion of the heterolytic rupture of the O-O bond of dioxygen or peroxides and the following formation of Cpd I, but through different mechanisms because of different structural features. For many heme peroxidases, a general “push-pull” mechanism has been proposed for this process (Fig. 1.7 (A)) (80, 88, 100). The “push” effect is provided by the proximal histidine ligand whose electron donor capabilities are enhanced through the H-bonding to a nearby carboxylate group (e.g., Asp). Meanwhile, the distal histidine accepts a proton from the oxygen atom of hydrogen peroxide that binds to the heme iron and transfers it to the other oxygen to form a leaving group. A nearby cationic residue (e.g., protonated Arg) in the distal pocket

works in concert with the histidine to facilitate the O-O bond cleavage. The combination of the distal histidine and arginine has been suggested to provide the “pull” effect (13).

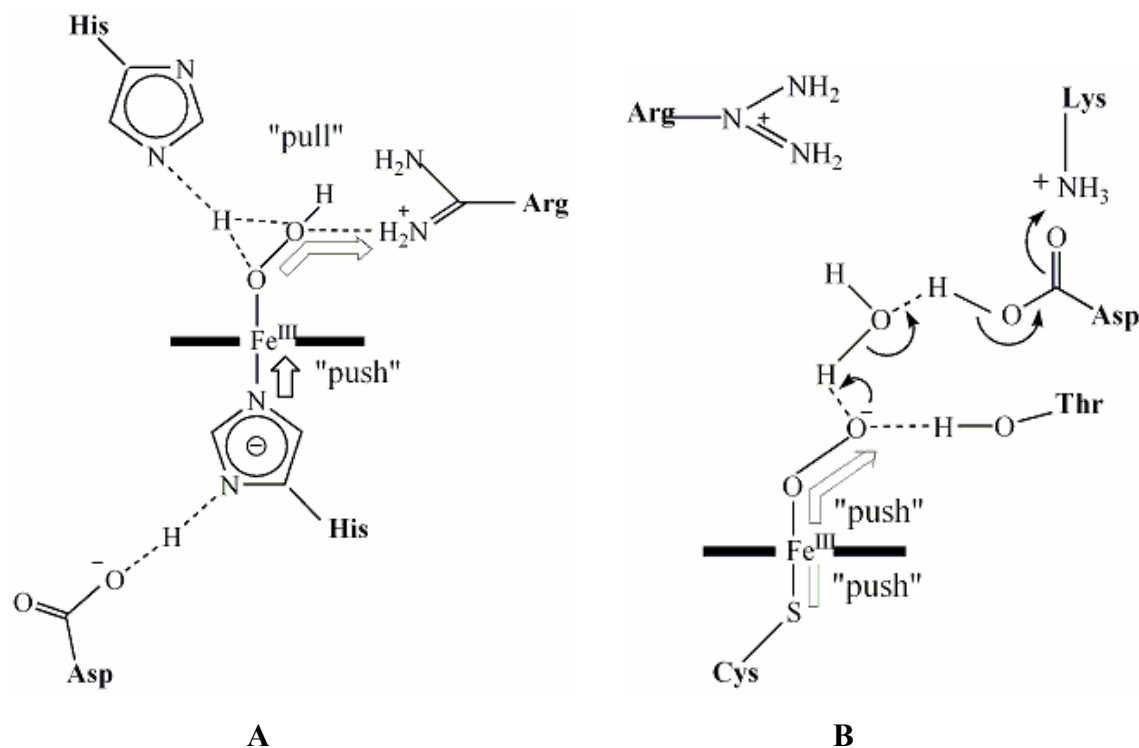


Figure 1.7 “Push-pull” mechanisms for O-O bond cleavage of both heme-imidazole protein (A) and heme-thiolate protein (B), such as horseradish peroxidase and P450 respectively. (13)

However, cytochrome P450 lacks such distal machinery. It possesses a cysteine proximal ligand, rather than a histidine typical of most peroxidases. This proximal thiolate ligand has been implicated as a crucial factor to facilitate the heterolytic scission of the O-O bond through its “push” effect by serving as a strong internal electron donor (Fig. 1.7 (B)) (13, 80, 101-104). The cysteine thiolate enables the protonation of Cpd 0 by the facilitation of Asp and Thr that exist in the protein pocket (14). Once the O-O bond is

heterolytically cleaved, the electron-releasing axial thiolate ligand would help to stabilize the high-valent nature of Cpd I (13).

1.3.3. Chloroperoxidase: a P450-peroxidase hybrid

Chloroperoxidase is an enzyme discovered by Hager and coworkers about 50 years ago from the marine fungus *Calduriomyces fumugo* (105). CPO serves as one of the most diverse and versatile known heme peroxidases. CPO and cytochromes P450 share a number of physiochemical properties, but they do have clear functional and structural differences (106). In addition to its biological role in halogenation of organic molecules, CPO is also able to use hydrogen peroxide as the oxidant to catalyze one- and two-electron classical peroxidase reactions and P450- and catalase-type reactions under acidic conditions. These enzymatic properties have made CPO a very promising industrial biocatalyst. Cytochrome P450, on the other hand, is a monooxygenase that activates dioxygen to catalyze the hydroxylation of hydrocarbons. Therefore, it is important to define the structural details that differentiate the chemical activities demonstrated by CPO and P450.

CPO, with 299 amino acids, is a single polypeptide consisting of eight helical segments and one small β pair. Structurally CPO has a P450-like proximal heme environment with cysteinate sulfur as the axial ligand and a peroxidase-like distal heme pocket in that polar residues form the peroxide-binding site, and was thus considered as a P450-peroxidase hybrid (20). Despite the functional properties shared with other

peroxidases and P450s, the tertiary structure of CPO bears little resemblance to either peroxidases or P450s. In the CPO distal pocket, though polar as in other peroxidases, a glutamic acid instead of a histidine is responsible for the cleavage of the O-O bond in the formation of Cpd I (Fig. 1.8).

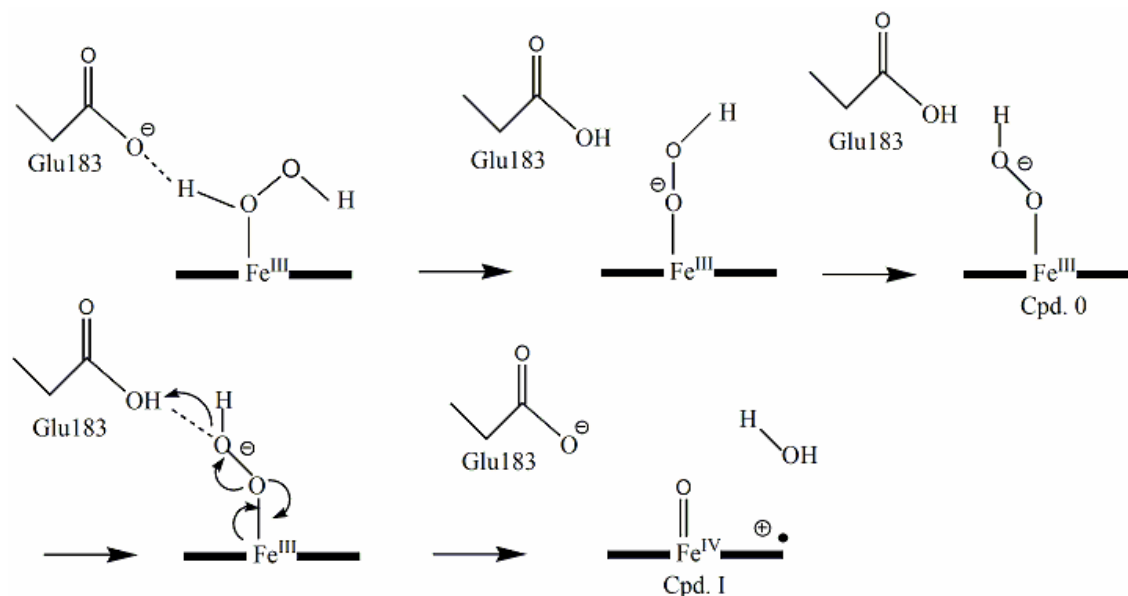


Figure 1.8 Proposed mechanism of compound I formation catalyzed by Chloroperoxidase.

In this mechanism, the activation of hydrogen peroxide is initiated by its binding to the heme in the distal side. The deprotonated Glu183 abstracts a proton from the substrate hydrogen peroxide, and then the formed hydroperoxo-anion binds to the heme iron, yielding a ferric-hydroperoxo species known as Compound 0. Glu183 then protonates the distal oxygen of Cpd 0 and the peroxide O-O is cleaved heterolytically to generate Cpd I and release a water molecule, similar to other peroxidase mechanisms (107, 108). CPO is adept in catalyzing a number of chiral oxidations with high yields and high

enantioselectivity, in addition to alkyne hydroxylation and heteroatom dealkylation (109-114). The stereoselective ability of CPO in catalysis is suggested to be based on its unique active site structure and unique catalytic mechanism, which make it the promising candidate for industrial catalysts.

1.4 PROTEIN ENGINEERING OF P450S AND HEME PEROXIDASES

Heme-containing proteins are primary targets of enzyme engineering because of their distinct activities and versatile functions. The diversity of function and spectroscopic characteristics of this class of proteins have been attributed to the structural components and interactions around the heme prosthetic group, especially the identity of the proximal axial ligation and the residues located in the distal pocket. The hemoproteins have been extensively studied by protein engineering to help test structure-based mechanistic hypotheses and evaluate the roles of important residues in enzyme catalysis, which often involves the change of substrate specificity, reaction selectivity and efficiency of the enzymes.

As mentioned before, cytochromes, globins, and most peroxidases utilize histidine as the proximal ligand, while cytochromes P450, chloroperoxidase and nitric oxide synthase use a cysteine thiolate ligand. Together with biochemical, biophysical and X-ray crystallographic techniques, site-directed mutagenesis studies have greatly contributed to the understanding of the structure-function relationships of hemoproteins and the key

structural features governing the variability by achieving structural mimics of different proteins. Substitution of the amino acids in the active site could make it possible to alter the protein axial ligand and to explore the interconversion of functions among hemoproteins, based on structure comparisons. In the following section, the mutagenesis results that demonstrate the importance of protein structure in controlling heme activity and the ability to engineer functions in some important examples of peroxidases and P450 are described.

1.4.1 Cytochrome *c* peroxidase H52L & H175C

Like many other heme peroxidases, cytochrome *c* peroxidase (CcP) belongs to the heme-imidazole protein family with a histidine serving as the axial ligand (H175) to the heme iron. In the distal side of the heme group, there is a conserved histidine residue (His52) (81). To investigate the role that histidine plays in the reaction of CcP with peroxide, His52 was replaced with a nonpolar leucine residue. Although no dramatic changes in the structure or in the accessibility of heme binding sites were observed, the H52L mutant displayed a 10^5 -fold decrease in catalytic rate compared with that of the wild type (115). In addition, the reactivity of the H52L mutant with peroxide was pH dependent and affected by the buffer. The pH-dependent study of this mutant has indicated that the distal histidine plays crucial roles in the rapid reaction of CcP with peroxide and it is more complex than simply being a base catalyst during the initial formation of Cpd I (116).

On the other hand, the proximal histidine ligand has been substituted by a cysteine. The successful introduction of a thiolate ligand into a peroxidase system naturally with histidine axial ligation would shed light on the roles of His and Cys in the catalytic activities of peroxidases by comparing the structure and function of the two heme ligations in similar surroundings. In addition, by monitoring the changes in the structural, functional and spectroscopic properties of the switched thiolate ligation could offer insight into the question about how the thiolate-heme center performs such distinct and diverse functions in various hemoproteins. The initial attempt to prepare a thiolate-ligated CcP H175C mutant led to Cys oxidation to cysteic acid (117). In the crystal structure studies of P450 and CcP, it has been shown that P450 has a hydrophobic environment surrounding the proximal thiolate ligand provided by a conserved Phe residue, while in CcP there is a negatively charged Asp which forms hydrogen bonds to the proximal His175 ligand. The Asp235 residue was proposed to be critical in forming a stable heme-thiolate ligation in the resting state of the CcP H175C variant (30).

1.4.2 P450cam C357H

In cytochrome P450cam, the crystal structure has demonstrated that the specific cysteine bound to the heme iron is Cys357 (70). To investigate the functional and structural roles of the proximal thiolate ligand in P450cam, the axial Cys357 has been replaced by a histidine (118, 119). The importance of the thiolate coordination for the P450 activities has been exemplified by their inactive forms P420, in which the thiolate

ligation is lost (120, 121). The P450cam C357H mutant exhibits greatly decreased camphor oxidation activity, and the heterolytic/ homolytic ratio of the O-O bond cleavage in the reaction with cumene hydroperoxide, also the electron transfer rate is much slower than that of the wild type. However, the mutant shows greater peroxidase activity because of the axial ligand alteration. To clarify the roles of the thiolate coordination in the heme-thiolate proteins, the axial histidine of myoglobin has been replaced with a cysteine (Mb H93C) and the altered thiolate ligand accelerates the heterolytic scission of peroxide O-O bond and enhances the styrene epoxidation activity aided by hydrogen peroxide. These results have confirmed the important roles of the thiolate ligand plays in hemoproteins play in facilitating the O-O bond cleavage to form the active intermediate Cpd I and in protein folding, substrate binding and electron transfer.

1.4.3 CPO C29H & CPO E183H

Chloroperoxidase (CPO) is unique in structure since it shares features with both peroxidases and P450 enzymes. As in cytochromes P450, CPO has a cysteine heme ligand (Cys29) in the proximal side of the heme prosthetic group. However, in contrast to the results of P450cam C357H, the thiolate coordination in chloroperoxidase is suggested to be not as important as in P450. After substituting the proximal thiolate ligand (Cys 29) with a histidine, the CPO C29H was found to retain most (around 80%) of its chlorination, peroxidation, epoxidation and catalase activities compared to those of the wild type protein (114). These are surprising observations in consideration of many suggestions for

the significance of the proximal thiolate ligand in P450. These unexpected results could be interpreted by the different mechanisms of the heterolytic O-O bond cleavage in CPO and P450 catalytic cycles.

As the results of CPO C29H mutant downplayed the importance of thiolate ligation in CPO activity, it has been suggested that the distal environment of the heme active site plays the major role in controlling the versatile functions of this enzyme. Although, like peroxidases that have polar distal pocket, CPO does not possess a histidine residue which is normally conserved in the distal helix as the general acid-base catalyst in the formation of Compound I. Instead, a glutamic acid at position 183 distal to the heme group takes over this function, based on the crystal structure of CPO (20). To investigate the role E183 plays in CPO catalysis, it has been replaced by a histidine residue. The results have shown that this substitution is destructive to CPO activity, especially its chlorination and dismutation activity, which are reduced by 85% and 50%, respectively (122). This indicated that Glu-183 is important but not essential to the chlorination and the catalase activity of CPO. However the epoxidation activity of the CPO E183H mutant was surprisingly increased by about 2.5 times than that of the wild type. The crystal structure of CPO identified a proton shuttle among Glu183, His105, and Asp106. Replacement of glutamic acid with a histidine could partially destroy the triad, resulting in the inhibition of chlorination activity but acceleration epoxidation activity.

In summary, mutagenesis studies have shown that the axial ligands in P450s and peroxidases do play essential roles in their catalysis. Key factors that determine the functional specificity of hemoproteins include the nature of the proximal ligands as well as the architecture of the distal site. The remainder of the dissertation details my effort to tailor heme-thiolate proteins, specifically cytochrome P450cam, into efficient biocatalysts with high specificity and selectivity by redesigning the protein through change of residues in the distal pocket, in an effort to elucidate the key structural and functional roles of critical amino acids in this protein.

1.5 REFERENCES

1. Thomson, A. J., Gray, H. B. (1998) Bioinorganic chemistry: editorial overview, *Curr. Opin. Chem. Biol.* 2, 155-158.
2. Lu, Y., Yeung, N., Sieracki, N., and Marshall, N. M. (2009) Design of functional metalloproteins, *Nature* 460, 855-862.
3. Williams, R. J. P. (1987) Missing information in bio-inorganic chemistry, *Coord. Chem. Rev.* 79, 175-193.
4. Turano, P., and Lu, Y. (2001) in *Handbook on Metalloproteins* (Bertini, I., Sigel, H. & Sigel, A., Ed.), pp 269-356, Dekker, New York.
5. Bertini, I., Gray, H. B., Lippard, S. J. & Valentine, J. S. (1994) Bioinorganic Chemistry Univ. Sci. Books, Mill Valley, CA.
6. Lippard, S. J., and Berg, J.M. (1994) *Principles of Bioinorganic Chemistry*, Univ. Sci. Books, Mill Valley, CA.

7. Lu, Y., Berry, S. M., and Pfister, T. D. (2001) Engineering novel metalloproteins: Design of metal-binding sites into native protein scaffolds, *Chemical Reviews* 101, 3047-3080.
8. Dunford, H. B. (1999) *Heme Peroxidases*, John Wiley & Sons, New York.
9. Raphael, A. L. a. G., H. B. (1991) Semisynthesis of Axial-Ligand (Position 80) Mutants of Cytochrome c, *J. Am. Chem. Soc.* 113, 1038-1040.
10. Antonini, E. a. B., M. (1971) *Hemoglobin and Myoglobin in Their Reactions with Ligands*, Elsevier, New York.
11. Perutz, M. F. (1989) Myoglobin and haemoglobin: role of distal residues in reactions with haem ligands, *Trends. Biochem. Sci.* 14, 42-44.
12. Ortiz de Montellano, P. R. (1998) Heme oxygenase mechanism: Evidence for an electrophilic, ferric peroxide species, *Acc. Chem. Res.* 31, 543-549.
13. Sono, M. R., M. P.; Coulter, E. D.; and Dawson, J. H. (1996) Heme-Containing Oxygenases, *Chemical Reviews* 96, 2841-2887.
14. Ortiz de Montellano, P. R. (2005) *Cytochrome P450: structure, mechanism, and biochemistry*, 3 ed., Kluwer Academic/Plenum Publishers, New York.
15. Poulos, T. L., Li, H. Y., Raman, C. S., and Schuller, D. J. (2001) Structures of gas-generating heme enzymes: Nitric oxide synthase and heme oxygenase, in *Advances in Inorganic Chemistry*, Vol 51, pp 243-293.
16. Chan, M. K. (2000) Heme protein biosensors, *J. Porphyrins Phthalocyanines* 4, 358-361.
17. Omura, T. (2005) Heme-thiolate proteins, *Biochem. Biophys. Res. Commun.* 338, 404-409.
18. Udit, A. K., and Gray, H. B. (2005) Electrochemistry of heme-thiolate proteins, *Biochemical and Biophysical Research Communications* 338, 470-476.

19. Sono, M., Dawson, J. H., Hall, K., Hager, L. P. (1986) Ligand and Halide Binding Properties of Chloroperoxidase: Peroxidase-Type Active Site Heme Environment with Cytochrome P-450 Type Endogenous Axial Ligand and Spectroscopic Properties, *Biochemistry* 25, 347-356.
20. Sundaramoorthy, M., Turner, J., and Poulos, T. L. (1995) The crystal structure of chloroperoxidase: A heme peroxidase-cytochrome P450 functional hybrid, *Structure* 3, 1367-1377.
21. Hollengerg, P. F., Hager, L. P. (1973) The P450-nature of the carbon monoxide complex of ferrous chloroperoxidase, *J. Biol. Chem.* 248, 2630-2633.
22. White, K. A., Marletta, M. A. (1992) Nitric oxide synthase is a cytochrome P-450 type hemoprotein, *Biochemistry* 31, 6627-6631.
23. Sono, M., Stuehr, D. J., Ikeda-Saito, M., Dawson, J. H. (1995) Identification of Nitric Oxide Synthase as a Thiolate-ligated Heme Protein Using Magnetic Circular Dichroism Spectroscopy: COMPARISON WITH CYTOCHROME P-450-CAM AND CHLOROPEROXIDASE, *J. Biol. Chem.* 270, 19943-19948.
24. Nakajima, H., Nakagawa, E., Kobayashi, K., Tagawa, S., and Aono, S. (2001) Ligand-switching intermediates for the CO-sensing transcriptional activator CooA measured by pulse radiolysis, *Journal of Biological Chemistry* 276, 37895-37899.
25. Reynolds, M. F., Shelver, D., Kerby, R. L., Parks, R. B., Roberts, G. P., Burstyn, J. N. (1998) EPR and Electronic Absorption Spectroscopies of the CO-Sensing CooA Protein Reveal a Cysteine-Ligated Low-Spin Ferric Heme *J. Am. Chem. Soc.* 120, 9080-9081.
26. Meier, M., Janosik, M., Kery, V., Kraus, J. P., and Burkhard, P. (2001) Structure of human cystathionine β -synthase: a unique pyridoxal 5'-phosphate-dependent heme protein., *EMBO Journal* 20, 3910-3916.
27. Ojha, S., Hwang, J., Kabil, O., Penner-Hahn, J. E., and Banerjee, R. (2000) Characterization of the Heme in Human Cystathionine β -Synthase by X-ray Absorption and Electron Paramagnetic Resonance Spectroscopies, *Biochemistry* 39, 10542-10547.
28. Matsui, T., Nagano, S., Ishimori, K., Watanabe, Y., and Morishima, I. (1996) Preparation and reactions of myoglobin mutants bearing both proximal cysteine

ligand and hydrophobic distal cavity: Protein models for the active site of P-450, *Biochemistry* 35, 13118-13124.

29. Adachi, S., Nagano, S., Ishimori, K., Watanabe, Y., Morishima, I., Egawa, T., Kitagawa, T., and Makino, R. (1993) Roles of Proximal Ligand in Heme-Proteins - Replacement of Proximal Histidine of Human Myoglobin with Cysteine and Tyrosine by Site-Directed Mutagenesis as Models for P-450, Chloroperoxidase, and Catalase, *Biochemistry* 32, 241-252.
30. Sigman, J. A., Pond, A. E., Dawson, J. H., and Lu, Y. (1999) Engineering cytochrome c peroxidase into cytochrome P450: A proximal effect on heme-thiolate ligation, *Biochemistry* 38, 11122-11129.
31. Liu, Y., Moenne-Loccoz, P., Hildebrand, D. P., Wilks, A., Loehr, T. M., Mauk, A. G., and Ortiz de Montellano, P. R. (1999) Replacement of the Proximal Histidine Iron Ligand by a Cysteine or Tyrosine Converts Heme Oxygenase to an Oxidase, *Biochemistry* 38, 3733-3743.
32. Vetter, S. W., Terentis, A. C., Osborne, R. L., Dawson, J. H., and Goodin, D. B. (2009) Replacement of the axial histidine heme ligand with cysteine in nitrophorin 1: spectroscopic and crystallographic characterization, *Journal of Biological Inorganic Chemistry* 14, 179-191.
33. Wang, W., Lu, J., Yao, P., Xie, Y., and Huang, Z. (2003) The distinct heme coordination environments and heme-binding stabilities of His39Ser and His39Cys mutants of cytochrome b5, *Protein Engineering* 16, 1047-1054.
34. Sigel, A., Sigel, H., and Sigel, R. K.O. (2007) The ubiquitous roles of cytochrome P450 proteins in *Metal Ions in Life Sciences* (Sigel, A., Sigel, H., and Sigel, R. K.O. , Ed.), Wiley, Chichester.
35. Lewis, D. F. V. (1996) *Cytochromes P450: Structure, Function, and Mechanism*, Taylor & Francis, London.
36. Lechner, M. C., Ed. (1993) *Cytochrome P-450: Biochemistry, Biophysics, and Molecular Biology*, John Libbey Eurotext, Paris.
37. Waterman, M. R., Johnson, E. F., Eds. (1991) Cytochrome P450 (Part A), in *Methods in Enzymology*, Academic Press, San Diego.

38. Johnson, E. F., Waterman, M. R., Eds. (1996) Cytochrome P450 (Part B), in *Methods in Enzymology*, Academic Press, San Diego.
39. Phillips, I. R., Shephard, E. A., Eds. (1998) Cytochrome P450 Protocols, in *Methods in Molecular Biology*, Humana Press, Totowa
40. Denisov, I. G., Makris, T. M., Sligar, S. G., and Schlichting, I. (2005) Structure and chemistry of cytochrome P450, *Chemical Reviews* 105, 2253-2277.
41. Hasemann, C. A., Kurumbail, R.G., Boddupalli, S.S., Peterson, J.A. and Deisenhofer, J. (1995) Structure and function of cytochromes P450: a comparative analysis of three crystal structures, *Structure* 3, 41-62.
42. Wong, L. L. (1998) Cytochrome P450 monooxygenases, *Curr. Opin. Chem. Biol.* 2, 263-268.
43. Guengerich, F. P. (1991) Reactions and Significance of Cytochrome P-450 Enzymes, *Journal of Biological Chemistry* 266, 10019-10022.
44. Sligar, S. G., Makris, T. M., Denisov, I. G. (2005) Thirty years of microbial P450 monooxygenase research: Peroxo-heme intermediates— The central bus station in heme oxygenase catalysis, *Biochemical and Biophysical Research Communications* 338, 346-354.
45. Nelson, D. R. (2009) The Cytochrome P450 Homepage, *Human Genomics* 4, 59-65.
46. Mansuy, D. (1998) The great diversity of reactions catalyzed by cytochromes P450, *Comp Biochem Physiol C Pharmacol Toxicol Endocrinol* 121, 5-14.
47. Sligar, S. G., Gunsalus I.C. (1976) A thermodynamic model of regulation: modulation of redox equilibria in camphor monooxygenase, *Proc Natl Acad Sci USA* 73, 1078-1082.
48. Daff, S. N., Chapman, S. K., Turner, K. L., Holt, R. A., Govindaraj, S., Poulos, T. L., and Munro, A. W. (1997) Redox Control of the Catalytic Cycle of Flavocytochrome P-450 BM3, *Biochemistry* 36, 13816-13823.

49. Newcomb, M., Zhang, R., Chandrasena, R. E. P., Halgrimson, J. A., Horner, J. H., Makris, T. M., and Sligar, S. G. (2006) Cytochrome P450 Compound I, *Journal of the American Chemical Society* 128, 4580-4581.
50. Imai, M., Shimada, H., Watanabe, Y., Matsuthima-Hibiya, Y., Makino, R., Koga, H., Horiuchi, T., Ishimura, Y. (1989) Uncoupling of the cytochrome P-450cam monooxygenase reaction by a single mutation, threonine-252 to alanine or valine: A possible role of the hydroxy amino acid in oxygen activation, *Proc Natl Acad Sci USA* 86, 7823-7827.
51. Harris, D. L., Loew, G.H. (1994) A Role for Thr 252 in Cytochrome P450cam Oxygen Activation, *J. Am. Chem. Soc.* 116, 11671-11674.
52. Schlichting, I., Berendzen, J., Chu, K., Stock, A. M., Maves, S. A., Benson, D. E., Sweet, B. M., Ringe, D., Petsko, G. A., and Sligar, S. G. (2000) The catalytic pathway of cytochrome P450cam at atomic resolution, *Science* 287, 1615-1622.
53. Capdevila, J., Estabrook, R.W., Prough, R.A. (1980) Differences in the mechanism of NADPH and cumene hydroperoxide-supported reactions of cytochrome P-450, *Arch. Biochem. Biophys.* 200, 186-195.
54. McCarthy, M. B., White, R.E. (1983) Functional differences between peroxidase compound I and the cytochrome P-450 reactive oxygen intermediate, *J. Biol. Chem.* 258.
55. Coon, M. J., Blake, R.C. 2nd, White, R.E., Nordblom, G.D. (1990) Assays for cytochrome P-450 peroxygenase activity, *Methods Enzymol* 186, 273-278.
56. Cirino, P. C., and Arnold, F. H. (2002) Regioselectivity and activity of cytochrome P450 BM-3 and mutant F87A in reactions driven by hydrogen peroxide, *Advanced Synthesis & Catalysis* 344, 932-937.
57. Joo, H., Lin, Z. L., and Arnold, F. H. (1999) Laboratory evolution of peroxide-mediated cytochrome P450 hydroxylation, *Nature* 399, 670-673.
58. Cirino, P. C., and Arnold, F. H. (2003) A self-sufficient peroxide-driven hydroxylation biocatalyst, *Angew. Chem. Int. Ed.* 42, 3299-3301.

59. Prasad, S., and Mitra, S. (2004) Substrate modulates compound I formation in peroxide shunt pathway of *Pseudomonas putida* cytochrome P450(cam), *Biochemical And Biophysical Research Communications* 314, 610-614.
60. Matsui, K., Shibutani, M., Hase, T., Kajiwara, T. (1996) Bell pepper fruit fatty acid hydroperoxide lyase is a cytochrome P450 (CYP74B), *FEBS Lett* 394, 21-24.
61. Song, W. C., Funk, C.D., Brash, A.R. (1993) Molecular cloning of an allene oxide synthase: a cytochrome P450 specialized for the metabolism of fatty acid hydroperoxides, *Proc Natl Acad Sci USA* 90, 8519-8523.
62. Miyata, A., Hara, S., Yokoyama, C., Inoue, H., Ullrich, V., Tanabe, T. (1994) Molecular cloning and expression of human prostacyclin synthase, *Biochem. Biophys. Res. Commun.* 200, 1728-1734.
63. Matsunaga, I., and Shir, Y. (2004) Peroxide-utilizing biocatalysts: structural and functional diversity of heme-containing enzymes, *Current Opinion in Chemical Biology* 8, 127-132.
64. Shoji, O., Fujishiro, T., Nakajima, H., Kim, M., Nagano, S., Shiro, Y., Watanabe, Y. (2007) Hydrogen Peroxide-Dependent Monooxygenations by Tricking the Substrate Recognition of Cytochrome P450BS β , *Angew. Chem. Int. Ed.* 46, 3656-3659.
65. Lee, D., Yamada, A., Sugimoto, H., Matsunaga, I., Ogura, H., Ichihara, K., Adachi, S., Park, S. and Shiro, Y. (2003) Substrate Recognition and Molecular Mechanism of Fatty Acid Hydroxylation by Cytochrome P450 from *Bacillus subtilis*, *J. Biol. Chem.* 278, 9761-9767.
66. Matsunaga, I., Sumimoto, T., Ayata, M., Ogura, H. (2002) Functional modulation of a peroxygenase cytochrome P450: novel insight into the mechanisms of peroxygenase and peroxidase enzymes, *FEBS Lett* 528, 90-94.
67. Hasemann, C. A., Kurumbail, R.G., Boddupalli, S.S., Peterson, J.A., and Deisenhofer, J. (1995) Structure and function of cytochromes P450: a comparative analysis of three crystal structures, *Structure* 3, 41-62.
68. Graham, S. E., Peterson, J.A. (1999) How Similar Are P450s and What Can Their Differences Teach Us?, *Arch. Biochem. Biophys.* 369, 24-29.

69. Johnson, E. F., and Stout, C.D. (2005) Structural diversity of human xenobiotic-metabolizing cytochrome P450 monooxygenases, *Biochem. Biophys. Res. Commun.* 338, 331-336.
70. Poulos, T. L., Finzel, B. C., and Howard, A. J. (1987) HIGH-RESOLUTION CRYSTAL-STRUCTURE OF CYTOCHROME-P450CAM, *Journal of Molecular Biology* 195, 687-700.
71. Poulos, T. L., Finzel, B. C., Gunsalus, I. C., Wagner, G. C., and Kraut, J. (1985) THE 2.6-Å CRYSTAL-STRUCTURE OF PSEUDOMONAS-PUTIDA CYTOCHROME-P-450, *Journal of Biological Chemistry* 260, 6122-6130.
72. Poulos, T. L. (1996) The role of the proximal ligand in heme enzymes, *J. Biol. Inorg. Chem.* 1, 356-359.
73. Ravichandran, K. G., Boddupalli, S. S., Hasemann, C. A., Peterson, J. A., Deisenhofer, J. (1993) Crystal structure of hemoprotein domain of P450BM-3, a prototype for microsomal P450's, *Science* 261, 731-736.
74. Cupp-Vickery, J., Poulos, T. L. . (1995) Structure of cytochrome P450yp involved in erythromycin biosynthesis, *Nat. Struct. Biol.* 2, 144-153.
75. Crane, B. R., Arvai, A. S., Gachhui, R., Wu, C., Ghosh, D. K., Getzoff, E.D., Stuehr, D. J., Tainer, J. A. . (1997) The Structure of Nitric Oxide Synthase Oxygenase Domain and Inhibitor Complexes, *Science* 278, 425-431.
76. Poulos, T. L. (2000) Peroxidase and cytochrome P450 structures, in *Porphyrin Handbook* (Kadish, K. M., Smith, K. M., Guillard, R., Ed.), pp 189-218, Academic Press, San Diego, Calif.
77. Poulos, T. L., Freer, S. T., Alden, R. A., Edwards, S. L., Skogland, U., Takio, K., Eriksson, B., Xuong, N. H., Yonetani, T., and Kraut, J. (1980) Crystal-Structure of Cytochrome-c Peroxidase, *J. Biol. Chem.* 255, 575-580.
78. Welinder, K. G. (1992) Superfamily of plant, fungal and bacterial peroxidases, *Curr. Opin. Struct. Biol.* 2, 388-393.
79. Poulos, T. L. (1987) Heme enzyme crystal structures, *Adv. Inorg. Biochem.* 7, 1-36.

80. Dawson, J. H. (1988) Probing structure-function relations in hemecontaining oxygenases and preoxidases, *Science* 240, 433-439.
81. Finzel, B. C., Poulos, T. L., and Kraut, J. (1984) Crystal structure of yeast cytochrome c peroxidase refined at 1.7-Å resolution, *J. Biol. Chem.* 259, 13027-13036.
82. Patterson, W. R., and Poulos, T. L. (1995) Crystal structure of recombinant pea cytosolic ascorbate peroxidase, *Biochemistry* 34, 4331-4341.
83. Gajhede, M., Schuller, D. J., Henriksen, A., Smith, A. T., and Poulos, T. L. (1997) Crystal Structure of Horseradish Peroxidase C at 2.15 Å Resolution, *Nat. Struct. Biol.* 4, 1032-1038.
84. Poulos, T. L., Edwards, S. L., Wariishi, H., and Gold, M. G. (1993) Crystallographic refinement of lignin peroxidase at 2 Å, *J. Biol. Chem.* 268, 4429-4440.
85. Sundaramoorthy, M., Kishi, K., Gold, M. H., and Poulos, T. L. (1994) The crystal structure of manganese peroxidase from *Phanerochaete chrysosporium* at 2.06-Å resolution, *J. Biol. Chem.* 269, 32759-32767.
86. Li, H. Y., Poulos, T.L. (1994) Structural variation in heme enzymes: a comparative analysis of peroxidase and P450 crystal structures, *Structure* 2, 461-464.
87. Tanaka, M., Ishimori, K., Mukai, M., Kitagawa, T., and Morishima, I. (1997) Catalytic activities and structural properties of horseradish peroxidase distal His42->Glu or Gln mutant, *Biochemistry* 36, 9889-9898.
88. Al-Mustafa, J., Kincaid, J.R. (1994) Resonance Raman Study of Cyanide-Ligated Horseradish Peroxidase. Detection of Two Binding Geometries and Direct Evidence for the "Push-Pull" Effect, *Biochemistry* 33, 2191-2197.
89. Yamada, H., and Yamazaki, I. (1974) Proton balance in conversions between five oxidation-reduction states of horseradish peroxidase, *Arch. Biochem. Biophys.* 165, 728-738.

90. Fukuyanma, K., Kunishima, N. Amada, F., Kubota, T., Matsubara, H. (1995) Crystal Structures of Cyanide- and Triiodide-bound Forms of *Arthromyces ramosus* Peroxidase at Different pH Values, *J. Biol. Chem.* 270, 21884-21892.
91. Kunishima, N., Fukuyama, K., Matsubara, H., Hatanaka, H., Shibano, Y., and Amachi, T. (1994) Crystal structure of the fungal peroxidase from *Arthromyces ramosus* at 1.9 Å resolution: Structural comparisons with the lignin and cytochrome c peroxidases, *J. Mol. Biol.* 235, 331-344.
92. Edwards, S. L., Raag, R., Wariishi, H., Gold, M. H., and Poulos, T. L. (1993) Crystal structure of lignin peroxidase, *Proc. Natl. Acad. Sci. U.S.A.* 90, 750-754.
93. Schuller, D. J., Ban, N., van Huystee, R. B., McPherson, A., and Poulos, T. L. (1996) The crystal structure of peanut peroxidase, *Structure* 4, 311-321.
94. Newmyer, S. L. a. O. d. M., P.R. (1996) Rescue of the Catalytic Activity of an H42A Mutant of Horseradish Peroxidase by Exogenous Imidazoles, *J. Biol. Chem.* 271, 14891-14896.
95. Howes, B. D., RodriguezLopez, J. N., Smith, A. T., and Smulevich, G. (1997) Mutation of distal residues of horseradish peroxidase: Influence on substrate binding and cavity properties, *Biochemistry* 36, 1532-1543.
96. Foshay, M. C., Vitello, L.B., and Erman, J.E. (2009) Relocation of the Distal Histidine in Cytochrome c Peroxidase: Properties of CcP(W51H), CcP(W51H/H52W), and CcP(W51H/H52L), *Biochemistry* 48, 5417-5425.
97. Poulos, T. L., and Kraut, J. (1980) THE STEREOCHEMISTRY OF PEROXIDASE CATALYSIS, *J. Biol. Chem.* 255, 8199-8205.
98. Poulos, T. L., and Kraut, J. (1980) The Stereochemistry of Peroxidase Catalysis, *J. Biol. Chem.* 255, 8199-8205.
99. Newmyer, S. L., and Ortiz de Montellano, P. R. (1996) Rescue of the Catalytic Activity of an H42A Mutant of Horseradish Peroxidase by Exogenous Imidazoles, *J. Biol. Chem.* 271, 14891-14896.
100. Poulos, T. L. (1988) Heme enzyme crystal structures, *Adv. Inorg. Biochem.* 7, 1-36.

101. Kimata, Y., Shimada, H., Hirose, T., Ishimura, Y. (1995) Role of Thr-252 in cytochrome P450cam: a study with unnatural amino acid mutagenesis, *Biochem. Biophys. Res. Commun.* 209, 96-102.
102. Gerber, N., C., Sligar, S. G. (1994) A role for Asp-251 in cytochrome P-450cam oxygen activation, *J. Biol. Chem.* 269, 4260-4266.
103. Gerber, N. C., Sligar, S. G. (1992) Catalytic mechanism of cytochrome P-450: evidence for a distal charge relay, *J. Am. Chem. Soc.* 114.
104. Dawson, J. H., Holm, R. H., Trudell, J. R., Barth, G., Linder, R. E., Bunnenberg, E., Djerassi, C., Tang, S. C. (1976) Oxidized cytochrome P-450. Magnetic circular dichroism evidence for thiolate ligation in the substrate-bound form. Implications for the catalytic mechanism, *J. Am. Chem. Soc.* 98, 3707-3709.
105. Morris, D. R., Hager, L. P. (1966) Chloroperoxidase: I. Isolation and Properties of the Crystalline Glycoprotein *J. Biol. Chem.* 241, 1763-1768.
106. Dawson, J. H., and Sono, M. (1987) Cytochrome P-450 and Chloroperoxidase: Thiolate-Ligated Heme Enzymes. Spectroscopic Determination of Their Active Site Structures and Mechanistic Implications of Thiolate Ligation, *Chemical Reviews* 87, 1255-1276.
107. Wang, X., Tachikawa, H., Yi, X., Manoj, K. M., and Hager, L. P. (2003) Two-dimensional NMR Study of the Heme Active Site Structure of Chloroperoxidase, *J. Biol. Chem.* 278, 7765-7774.
108. Kuhnelt, K., Blankenfeldt, W., Turner, J., Schlichting, I. (2006) Crystal Structures of Chloroperoxidase with Its Bound Substrates and Complexed with Formate, Acetate, and Nitrate, *J. Biol. Chem.* 281, 23990-23998.
109. Hu, S. H., Hager, L.P. (1999) Highly enantioselective propargylic hydroxylations catalyzed by chloroperoxidase, *J. Am. Chem. Soc.* 121, 872-873.
110. Hu, S. H., Hager, L.P. (1999) Asymmetric epoxidation of functionalized cis-olefins catalyzed by chloroperoxidase, *Tetrahedron Lett.* 40, 1641-1644.
111. Kedderis, G. L., Hollenberg, P.F. (1984) Peroxidase-catalyzed N-demethylation reactions. Substrate deuterium isotope effects, *J. Biol. Chem.* 259, 3663-3668.

112. Kedderis, G. L., Koop, D.R., Hollenberg, P.F. (1980) N-Demethylation reactions catalyzed by chloroperoxidase, *J. Biol. Chem.* 255, 10174-10182.
113. Hager, L. P., Lakner F.J., Basavapathruni, A. (1998) Chiral synthons via chloroperoxidase catalysis, *J. Mol. Catal. B: Enzym.* 5, 95-101.
114. Yi, X., Mroczko, M., Manoj, K.M., Wang, X., Hager, L.P. (1999) Replacement of the proximal heme thiolate ligand in chloroperoxidase with a histidine residue, *Proc Natl Acad Sci USA* 96, 12412-12417.
115. Erman, J. E., Vitello, L. B., Miller, M. A., Shaw, A., Brown, K. A., and Kraut, J. (1993) Histidine-52 is A Critical Residue for Rapid Formation of Cytochrome-c Peroxidase Compound-I, *Biochemistry* 32, 9798-9806.
116. Palamakumbura, A. H., Vitello, L. B., and Erman, J. E. (1999) Oxidation of the His-52 ->Leu Mutant of Cytochrome c Peroxidase by p-Nitroperoxybenzoic Acid: Role of the Distal Histidine in Hydroperoxide Activation, *Biochemistry* 38, 15653-15658.
117. Choudhury, K., Sundaramoorthy, M., Hickman, A., Yonetani, T., Woehl, E., Dunn, M. F., and Poulos, T. L. (1994) Role of the Proximal Ligand in Peroxidase Catalysis *J. Biol. Chem.* 269, 20239-20249.
118. Auclair, K., Moenne-Loccoz, P., and Ortiz de Montellano, P. R. (2001) Roles of the Proximal Heme Thiolate Ligand in Cytochrome P450cam, *J. Am. Chem. Soc.* 123, 4877-4885.
119. Yoshioka, S., Takahashi, S., Hori, H., Ishimori, K., and Morishima, I. (2001) Proximal cysteine residue is essential for the enzymatic activities of cytochrome P450cam, *Eur. J. Biochem.* 268, 252-259.
120. Yu, C.-A., Gunsalus, I. C. (1974) Cytochrome P-450cam: II. Interconversion with P-420, *J. Biol. Chem.* 249, 102-106.
121. Martinis, S. A., Blanke, S. R., Hager, L. P., Sligar, S. G., Hoa, G. H. B., Rux, J. J., and Dawson, J. H. (1996) Probing the heme iron coordination structure of pressure-induced cytochrome P420cam, *Biochemistry* 35, 14530-14536.

122. Yi, X., Conesa, A., Punt, J. P., Hager, L. P. (2003) Examining the Role of Glutamic Acid 183 in Chloroperoxidase Catalysis, *J. Biol. Chem.* 278, 13855-13859.

Chapter II. SINGLE AMINO ACID SWITCH TURNS P450CAM FROM A MONOOXYGENASE INTO AN EFFICIENT PEROXIDASE

2.1 SUMMARY

Most heme peroxidases contain a highly conserved histidine that serves as the general acid-base catalyst at the distal side of the heme prosthetic group in the formation of compound I. In contrast, cytochromes P450 do not have such obvious acid-base groups in their hydrophobic distal heme pockets. To explore the possibility of engineering cytochrome P450cam into an efficient peroxygenase via the “peroxide-shunt” pathway, Val247 located closely to the heme iron in the distal helix has been substituted with a histidine residue. The V247H mutant shows essentially identical optical spectral features compared to those of wild type P450cam in the absence of substrate camphor, suggesting that the heme-Cys ligation in the parent protein is kept intact in the mutant. Surprisingly this mutant does not bind camphor like the wild type, possibly due to unfavorable conformational changes in the distal helix which prevents camphor from entering the substrate binding site in the same way. However, the V247H mutant has acted as a self-sufficient enzyme with significantly higher peroxidase activity compared with wild type protein, showing even higher activity than chloroperoxidase. Various spectroscopic studies including UV, RR, CD and NMR coupled with electrochemical studies have

provided insights into the structural changes that correlate with the observed catalytic activities of this mutant.

2.2 INTRODUCTION

Cytochromes P450 constitute a superfamily of heme-containing monooxygenases that are found ubiquitously in many bacteria, all archaea, fungi and many higher eukaryotes. The P450 enzymes are involved in the activation of dioxygen for the insertion or addition of one atom of oxygen to a wide variety of substrates, making them crucial to many biotransformations such as steroid hormone biosynthesis, drug metabolism, detoxification of xenobiotics, and molecular signaling (1-3). The reactions catalyzed by P450s include epoxidation, dealkylation, hydroxylation, dehalogenation, and heteroatom oxidation (4). The most distinctive structural feature of cytochromes P450 is the coordination of a deprotonated cysteine to the heme iron as the proximal ligand, while many other hemoproteins possess a histidine at the proximal side. Thus P450s belong to the family of so-called heme-thiolate proteins, together with chloroperoxidase (CPO) from *Caldariomyces fumago*, nitric oxide synthase (NOS), cystathionine β -synthase, and etc. The proximal thiolate ligand in P450s has been proposed to play a vital mechanistic role in providing the “push” effect which enables the heterolytic O-O bond cleavage to generate activated iron (IV)-oxo porphyrin radical cation species commonly called CpdI, leading to subsequent substrate oxidation (5-7).

The typical P450 catalytic cycle involves substrate binding, dioxygen binding, two-electron transfers, followed by CpdI formation and substrate oxidation. With a few exceptions, the catalysis of the diverse reactions by P450s all require an external source of reducing equivalents and auxiliary proteins (e.g., putidaredoxin, and puridaredoxin reductase for P450cam). The requirement of expensive cofactors and the complication caused by additional proteins is the limitation to the application of P450s as oxygenases. Some P450s are capable of accepting hydrogen peroxide or an organic peroxy compound as an oxidant to catalyze oxygen insertion through the so-called “peroxide-shunt” pathway in the absence of electron transport proteins and the NAD(P)H cofactor (8-13). However, P450s are typically not efficient in their utilization of hydrogen peroxide, the natural substrate for peroxidases, as the source of oxygen atom in the monooxygenation reactions.

Serving as the prototype member in the superfamily, cytochrome P450cam from *Pseudomonas putida* has been extensively studied using various physical and chemical techniques. It catalyzes the regio- and stereo-specific hydroxylation of its natural substrate *d*-camphor to 5-exo-hydroxy-camphor (15). A great deal of effort has been made to suitably engineer this enzyme by directed evolution and active site modification for the oxygenation of significant unnatural substrates. It is still quite important to understand the roles of the active-site components in the reactivity, stability, specificity and substrate recognition of this enzyme after its discovery decades ago.

To explore the possibility of converting P450cam into an efficient self-sufficient peroxidase, we attempted to modify the heme distal side elements that play crucial mechanistic roles in this protein's catalytic functions. In most heme peroxidases, a distal histidine is highly conserved in the active site and serves as a general acid-base catalyst that is necessary for the formation of CpdI by donating a proton to the Fe^{3+} -OOH moiety to promote the heterolytic cleavage of the O-O bond in the peroxidase reaction cycles (16-19). It has also been proposed that a functional nitrogen (such as the nitrogen of His42 in HRP or His52 in CcP), located at a suitable distance from the heme iron, can behave as an acid-base catalyst in hemoproteins (16, 20). Additionally, some unique P450 enzymes have been shown to function as peroxygenases by utilizing hydrogen peroxide as the oxygen donor with extremely high catalytic turnover rates compared to their normal monooxygenation reactions as well as the peroxide shunt reaction catalyzed by the common P450s (12, 21). A common structural feature about these proteins is that the distal side of the heme molecule is quite hydrophilic, which allows H_2O_2 to enter the active site followed by the formation of CpdI with the interaction of the carboxyl group of substrate and the Arg residue located near the heme (12).

In contrast, P450cam possesses a very hydrophobic distal environment that lacks the distal machinery of the peroxidases mentioned above. Therefore, to probe the roles of the nonpolar amino acids in the distal helix and to make an efficient peroxygenase, we substituted a distal residue with a hydrophilic histidine which is highly conserved in other

heme peroxidases. In the distal pocket of P450cam, camphor is bound in a specific orientation above the heme iron, with a hydrogen bond between the camphor carbonyl and the phenol side chain of Tyr96 as well as numerous non-covalent contacts with active site residues (22). Val247 is one of the neighboring residues in the distal pocket that have hydrophobic contact with the substrate camphor (23). In light of its proximity to the heme prosthetic group, it served as a logical choice for our target (Fig. 2.1). The substitution of Val247 with a histidine was anticipated to provide a functional nitrogen from the imidazole group of His247 that could act as an acid-base catalyst via the peroxide-shunt pathway to facilitate the generation of Cpd I that affords substrate oxidation.

Various spectroscopic techniques were utilized in the present work for the structural and functional characterizations of the P450cam V247H mutant. In addition to electronic absorption spectroscopy, resonance Raman spectroscopy is well established as a highly sensitive probe of the active-site structure of heme proteins by providing detailed structural information on iron spin and ligation states. Circular dichroism was performed to examine the secondary and tertiary structural changes of the mutant. Proton nuclear magnetic resonance spectroscopy, one of the most powerful methods for high resolution structural characterization of paramagnetic metalloproteins, was also utilized to characterize the active site structure of the cyanide complexes of the wild type and mutant proteins.

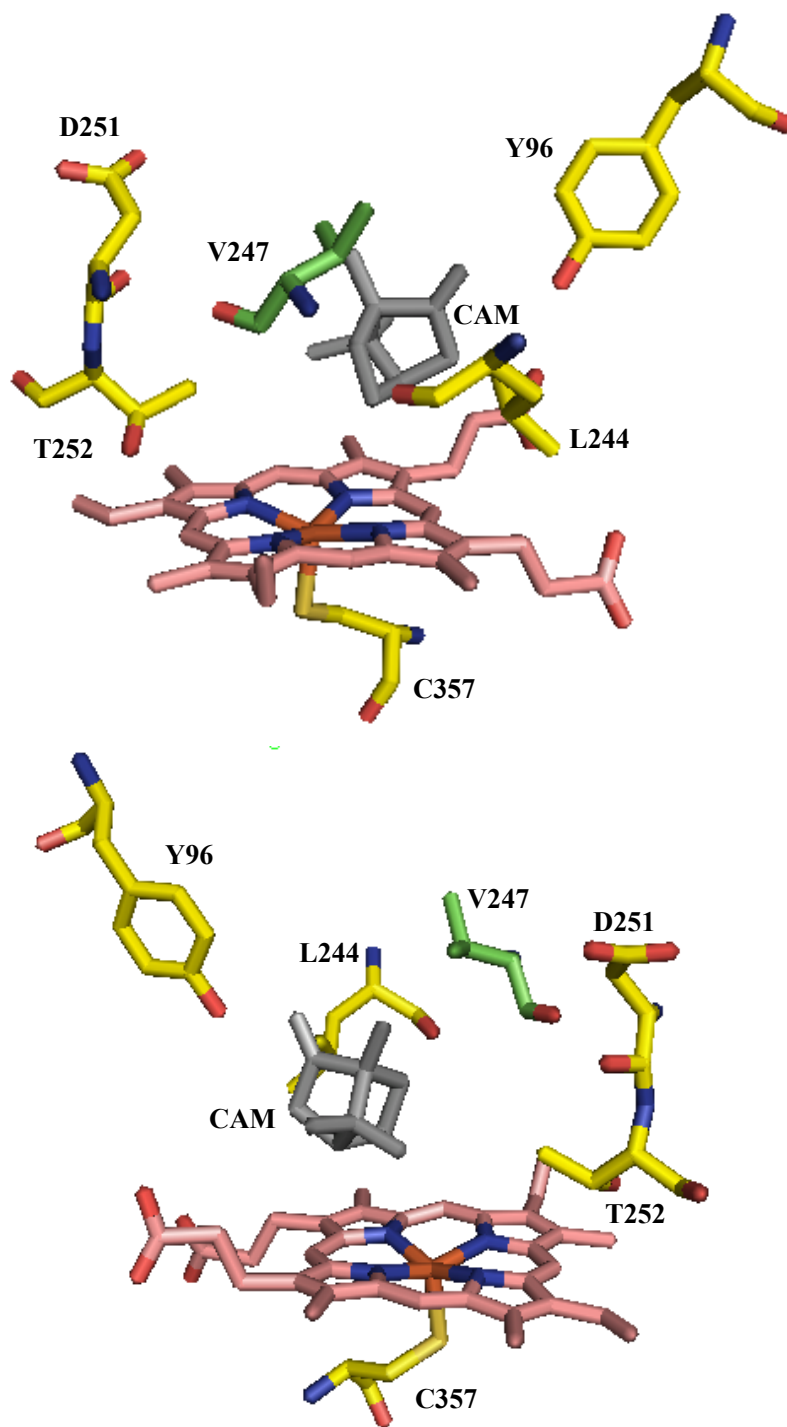


Figure 2.1 The active site structure of camphor-bound cytochrome P450cam: the heme (salmon), camphor (gray) and some selected residues including distal V247 (green) in P450cam are shown. The figures were generated from the crystal data (PDB code 2CPP) using PYMOL (22).

Additionally, redox potential measurements of the protein were performed to show the effect of the amino acid substitution on the redox property of the heme iron.

2.3 EXPERIMENTAL PROCEDURES

2.3.1 Materials

The PfuUltra High-Fidelity DNA polymerase used for site-directed mutagenesis was from Stratagene and the primers for the mutation were synthesized by Eurofins MWG Operon (Huntsville, AL). Dithiothreitol (DTT), carbon monoxide, hydrogen peroxide, 2, 2'-Azino-bis (3-Ethylbenzthiazoline-6-Sulfonic Acid), and δ - aminolevulinic acid were purchased from Sigma-Aldrich (St. Louis, MO). Yeast extract, tryptone, glycerol, sodium chloride, sodium bromide, sodium acetate, sodium dithionite, potassium chloride, potassium phosphate, potassium cyanide, potassium hydroxide, EDTA, Tris-HCl, isopropyl- β -D-thiogalactopyranoside (IPTG), Ribonuclease A, Deoxyribonuclease I, phenylmethylsulfonyl fluoride (PMSF), lysozyme, hemin, DL-tyrosine and DL-camphor were obtained from Fisher Scientific (Pittsburgh, PA). DEAE sepharose fast flow and Sephadex G-75 were purchased from GE Healthcare (Piscataway, NJ). All chemicals were used without further purification. Choloferoxidase (CPO) from *Caldariomyces fumago* was prepared in our own lab with R_z value over 1.40.

2.3.2 Bacterial strains, plasmids and DNA manipulations

The bacterial strains used were *E. coli* NovaBlue and *E. coli* Rosetta II (DE3) from Novagen (Gibbstown, NJ). The plasmid pUS200, constructed by Unger *et al.*, contains a 1578-bp fragment of *P. putida* (ATCC 17453) P450_{cam} plasmid fragment inserted into the PstI and HindIII sites of pEMBL8+ (24). To increase the protein yield, the P450_{cam} gene was constructed into a T7-based expression vector, pET-30a (+) from Novagen, at the sites of NdeI and HindIII by polymerase chain reactions and ligation reactions. Bacteria were grown in Luria-broth supplemented with antibiotic (kanamycin, 100 µg/ml) for the DNA manipulation. Site-directed mutagenesis was performed by using this T7-based expression vector, pET-30a (+). The V247H mutant of P450_{cam} was prepared with the 5'-sense oligonucleotide 5'- CTG TTA CTG CAT GGC GGC CTG GAT-3' coding for **LLLHGGLD**. The reconstituted plasmids of both wild type and V247H mutant were transformed into *E. coli* strain NovaBlue and verified by DNA sequencing.

2.3.3 Protein Expression and Purification

The wild type P450_{cam} and mutant V247H were expressed in *Escherichia coli* strain Rosetta II (DE3). Cells were grown on terrific broth supplemented with 100mg/L of kanamycin at 37 °C and induced with 1mM IPTG and 1mM camphor at OD₆₀₀ around 0.8, followed by further growth at 30°C for another 18h prior to harvesting cells. As for the mutant, the addition of δ -aminolevulinic acid to the growth media is necessitated to facilitate holoenzyme production.

Cells were lysed at 4°C in 50 mM Tris-HCl buffer at pH 7.4 containing 50 mM KCl, 0.5 mM DTT, 1 mM camphor, 1 mM EDTA, 200 μ M PMSF, 40 U/ml Dnase I, 3 U/ml Rnase A, and lysozyme. Following sonication and centrifugation, the lysate were concentrated by Amicon cell with 30,000 Da cut-off ultrafiltration membrane. The protein solution was applied onto a fast flow DEAE Sepharose column (50 ml) equilibrated with 50 mM Tris-HCl buffer (pH 7.4). After initial elution, the column was eluted with a linear 0-0.5 M KCl gradient in the same buffer. The red fractions containing the \sim 45 kDa proteins were pooled for further purification by size exclusion chromatography. Sephadex G-75 matrix (500 ml) was used for the gel filtration and the buffer used was 100 mM potassium phosphate containing 1mM camphor at pH 7.4. Substrate-free WT P450cam and its mutant were prepared by dialyzing the protein samples against phosphate buffer without camphor, followed by centrifugation with a microconcentrator (Centricon-30). Unless otherwise specified, all the steps in the protein purification were performed at 4 °C.

The R_z values of pure wild-type P450cam and V247H mutant were over 1.4 and 1.3 respectively. The protein concentration was determined using the Soret extinction coefficient determined by the *pyridine hemochrome method* following the standard protocol (25, 26). The extinction coefficients for the camphor bound WT at 392 nm and mutant enzyme at 416 nm were 102 and 115 mM⁻¹cm⁻¹ respectively. These values were found to be 115 and 116 mM⁻¹cm⁻¹ for the camphor-free forms of the WT and mutant enzyme at 418 nm.

2.3.4 Spectroscopic characterization

Optical characterization of the wild type P450_{cam} and its mutant was performed at room temperature on a Cary 300 spectrophotometer (Varian). The ferrous proteins were prepared by the addition of an excess amount of sodium dithionite and CO adducts were obtained by CO gas bubbling. The buffer used for the absorption measurements was 100mM potassium phosphate buffer with 1mM camphor at pH 7.4.

CD spectra were measured on a JASCO J-815 spectrometer at room temperature. The secondary-structure spectral region (200-260 nm) of the spectra was recorded in a quartz cuvette of 1 mm path length using about 2 μ M enzyme. As for the tertiary-structure spectral region (260-650 nm), it was recorded using about 20 μ M enzyme in a quartz cuvette of 1cm path length with or without camphor.

For resonance Raman data collection, the wild-type P450 and V247H mutant were prepared in a septum-sealed, cylindrical quartz cell. Samples were reduced to the ferrous form by first flushing the sample with argon and then injecting a molar excess of buffered sodium dithionite solution. The rotating sample cell was irradiated with 4 mW of 413.1 nm laser light using a mixed krypton/argon ion laser (Spectra Physics, Beamlok 2060). The spectral acquisition time was 5 min. The scattered light was collected at right angles to the incident beam and focused onto the entrance slit (125 μ m) of a 0.8 m spectrograph, where it was dispersed by a 600 groove/mm grating and detected by a liquid-N₂-cooled CCD camera (Horiba-JY). Spectral calibration was performed against the lines of

mercury. UV-vis spectra of each sample were collected before and after each RR measurement to ensure the sample integrity.

Proton nuclear magnetic resonance (^1H NMR) spectra for the cyanide-bound proteins were recorded at 298 K on a Bruker Avance 600 (Ultrashield) spectrometer operating at a proton frequency of 599.97 MHz. Protein samples for NMR experiments were prepared in D_2O buffer solutions containing 100 mM potassium phosphate at pH 7.4, by at least four isotope exchanges of the protein solution in H_2O with D_2O buffer. The isotope exchanges were carried out in a microconcentrator (Centricon-30) at 4 °C. All NMR samples contained more than 2 mM protein and the cyanide adducts of the protein were prepared by the addition of a 10-fold to 20-fold molar excess of cyanide from a freshly made 1M stock solution of KCN in 99.9% D_2O . The residual solvent signal was suppressed with presaturation during relaxation delay. Chemical shift values were referenced to the residual HDO signal at 4.76 ppm.

Phase-sensitive NOESY spectra for the cyanide-bound derivatives of P450cam and its V247H mutant were acquired with mixing times ranging from 1.5 to 25 ms. Typical NOESY spectra were collected with 256 experiments in the F1 dimension using the hypercomplex method (27). In general, 1600-2000 scans were accumulated for each F1 experiment, which was acquired with 4096 complex points in the F2 dimension over a spectral width of 27 or 60 kHz. The residual solvent signal in all NOESY experiments was suppressed using a 200-ms presaturation with a weak decoupler power.

All the spectroscopic experiments were done with freshly prepared samples in 100mM potassium phosphate buffer (pH 7.4).

2.3.5 Redox measurements

The electrochemical measurements of wild type P450cam and V247H mutant were performed with a CHI 660 electrochemical analyzer (CH Instruments) at room temperature by using a conventional three electrode cell, with a glassy carbon (GC) electrode as the working electrode, platinum wire as counter electrode and Ag/AgCl electrode as the reference electrode. The carbon electrode has been modified with single-walled carbon nanotubes (SWCNT). The preparation of the SWCNTs was carried out as reported (28) and SWCNT suspension was cast onto the electrode and dried under infrared lamp. The SWCNT modified electrode is electrochemically activated by cyclical scanning between -1.0 and +1.5V at a scan rate of 1 V/sec for 2 minutes to improve the sensitivity of the electrode. The redox potentials of P450camV247H mutant and the wild type protein were obtained and normalized with the reference to NHE.

2.3.6 Peroxidase activity

The peroxidation activity of the V247H mutant was measured by using 2,2'-azino-bis-3-ethy-benzthiazoline-6-sulfonic acid (ABTS) as the electron donor and hydrogen peroxide as the sole oxidant (29). The reaction was initiated by the addition of H₂O₂ (3.3mM) into the reaction solution of enzyme (2μM) and ABTS (9.1 mM) in 100mM potassium buffer from pH 5.0 to pH 7.4. Wild type P450cam and

chloroperoxidase were also examined at pH 5.0. Chloroperoxidase from *Caldariomyces fumago* was prepared in our own lab, and the Rz value of the protein used in this assay was over 1.4. The peroxidase activity was monitored at 405 nm, and the initial rate of oxidized ABTS product formation was used to calculate the activity.

2.4 RESULTS

2.4.1 UV-visible Spectroscopy study

The UV-vis spectra for the ferric, ferrous, and ferrous-CO forms of V247H mutant were obtained to examine the coordination structure of the heme iron both in the absence and presence of camphor (Fig. 2.2A and 2.2B). The substrate-free V247H exhibited essentially identical spectra to that of the wild type enzyme. However, the camphor binding was perturbed in this mutant as compared to that in wild type according to the optical characterizations. Instead of having the Soret band shifted from 418 nm to 392 nm upon camphor binding, which is characteristic of the conversion of low-spin to high-spin Fe (III), the mutant only displayed a 2 nm blue shift from 418 nm to 416 nm. Therefore, the substrate-bound V247H mutant remained predominantly in the six-coordinate, low-spin ferric iron state, similarly as reported in the G248E mutant of cytochrome P450cam (30). The shape of the Soret band of camphor-bound V247H was also different from that of the camphor-free protein, with less symmetry and a less prominent δ -band

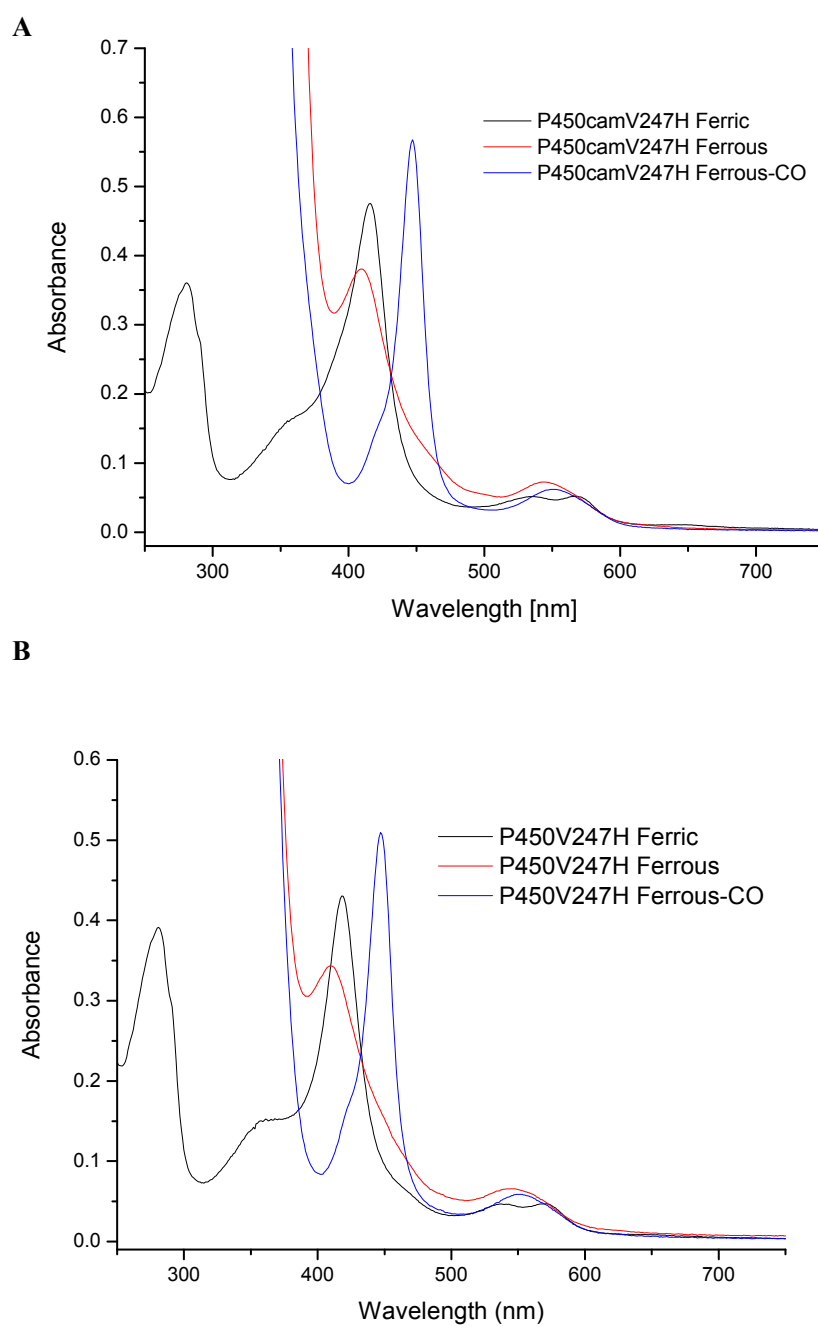


Figure 2.2. UV-vis spectra of P450camV247H in various oxidation states: **(A)** camphor-free and **(B)** camphor-bound forms in 100mM phosphate buffer (pH7.4) at room temperature.

feature at around 360nm, which is an indication of a sixth water ligand bound to the heme iron. Otherwise, there were only very small differences in the visible absorption bands (Table 2.1).

Table 2.1. Wavelength and extinction coefficients of absorption maxima for wild type and V247H mutant of cytochrome P450cam

Protein	Oxidation state	Soret (nm)	δ -band (nm)	Visible (nm)
WTP450 (camphor-free)	Fe ³⁺	418 (392)	360	535 , 569
	Fe ²⁺	408		540
	Fe ²⁺ -CO	446		550
V247H camphor-free	Fe ³⁺	418 (ϵ =116)	361	537 , 569
	Fe ²⁺	409		540
	Fe ²⁺ -CO	447		548
V247H camphor-bound	Fe ³⁺	416 (ϵ =115)	355	534, 569
	Fe ²⁺	409		542
	Fe ²⁺ -CO	447		550

It is worth mentioning that for both camphor-free and camphor-bound samples, the ferrous complexes displayed the Soret maximum initially at approximately 412nm upon reduction, but the addition of more sodium dithionite or mixing for a longer time period led to the Soret band shifting to 409nm. That could be an indication of the changed (most

likely increased) electron density on the thiolate in the reduced state (31). The CO-bound form of V247H showed a Soret maximum at 447nm, which supports the presence of an intact iron-sulfur coordination in this mutant (32). In addition, the ligand binding activity of the V247H showed very similar results compared with that of wild type. For example, the KCN binding of V247H mutant displayed about a 24 nm red shift of the Soret band to 440 nm (Fig. 2.3), almost identical to that of the WT P450cam (33).

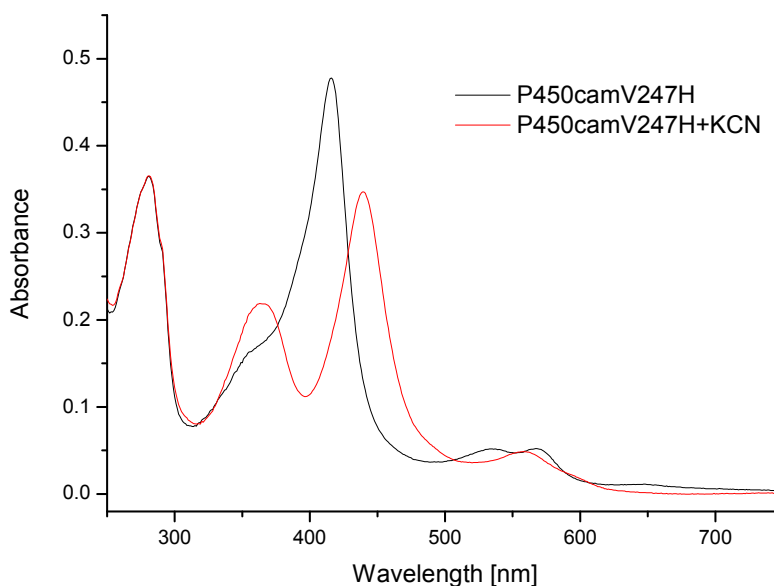


Figure 2.3. UV spectra of P450camV247H and its KCN bound complex. The enzyme concentration employed was $\sim 4\mu\text{M}$, and $10\mu\text{l}$ of 1M KCN was added to the enzyme.

2.4.2 Circular Dichroism spectroscopy study

Multi-wavelength CD studies of the wild type and V247H mutant P450cam were carried out to investigate the effect of the distal residue substitution on the conformational

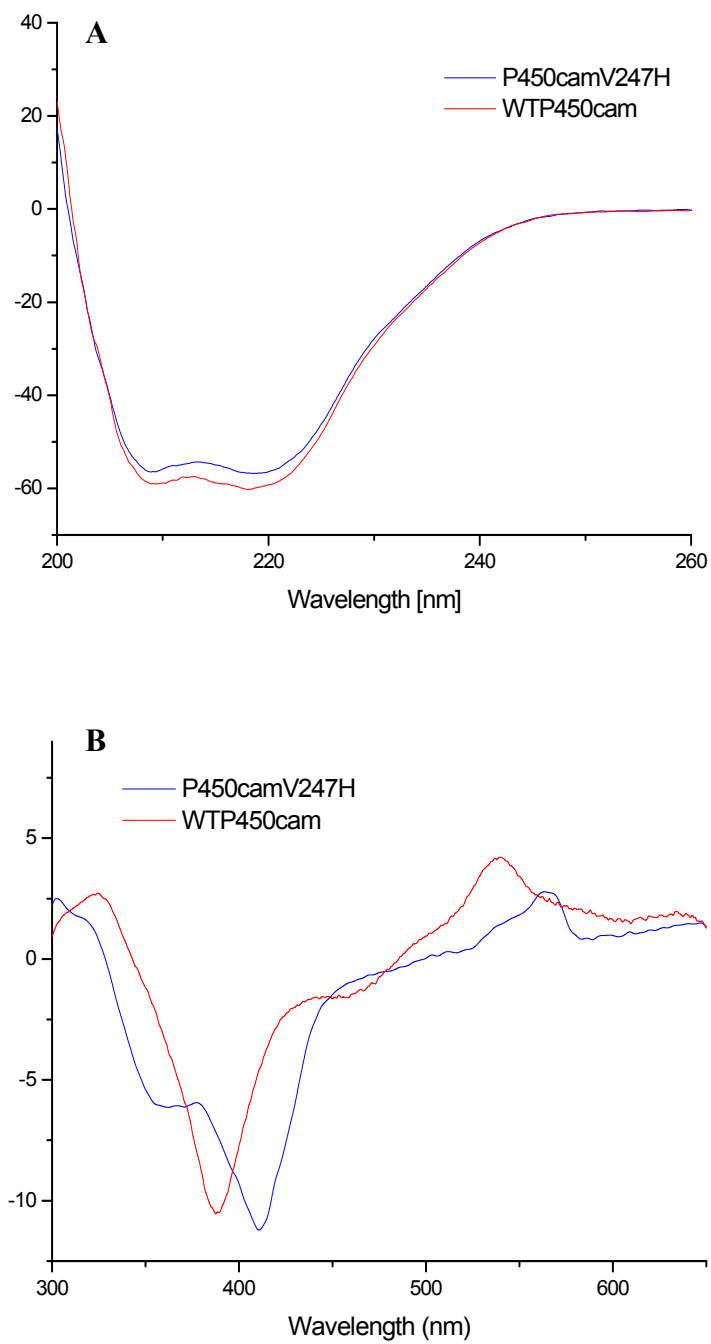


Figure 2.4. Far-UV CD (A) and visible CD (B) spectra of substrate-bound forms of the WT and V247H mutant of cytochrome P450cam.

properties of the enzyme. As shown in Fig. 2.4 A, the far-UV CD bands from 200-260 nm, which provide information on the secondary-structural features of the proteins, showed no significant difference between the wild type and the mutant, suggesting that the mutation of the valine residue had no detectable effect on the secondary structure of the protein. However, in the near-UV-visible CD region (300-650 nm), the camphor-bound V247H mutant displayed rather different spectra in its ferric form from those of the wild type (Fig. 2.4 B). This was consistent with the result of optical absorption measurement that exhibited similar properties with the substrate-free wild type protein.

2.4.3 Resonance Raman Spectroscopy study

To examine the heme environment and the iron spin and ligation state of wild type P450cam and V247H mutant, we obtained resonance Raman spectra in the absence and presence of camphor. For the camphor-free ferric species, both wild type and V247H mutant displayed a strong oxidation state marker band ν_4 at around 1370 cm^{-1} typical of ferric (Fe^{3+}) heme (Fig. 2.5A). The heme core-size marker bands ν_3 and ν_2 appeared at approximately 1500 and 1580 cm^{-1} , respectively for the camphor-free samples, indicating a six-coordinate (6C), low-spin (LS) heme iron (34-36). For the camphor-bound proteins, the V247H mutant showed a different pattern from the wild type. Whereas the wild type displayed the ν_3 and ν_2 bands at 1486 and 1568 cm^{-1} , indicative of five-coordinate (5C), high-spin (HS) heme iron component, the V247H displayed peaks at 1499 and 1581 cm^{-1} , consistent with a 6C-LS complex, similar to the camphor-free samples. The RR spectra of

ferrous P450cam and V247H with camphor bound showed a ν_4 band at 1344 cm^{-1} , consistent with thiolate proximal ligation (Fig. 2.5B) (37). The ν_3 and ν_2 band positions of these two samples at 1465 cm^{-1} and 1562 cm^{-1} confirmed that the ferrous forms of both wild type and mutant complexes were 5C-HS. However, the ferrous forms of substrate-free wild type and mutant proteins displayed a different spectral pattern from the camphor-bound forms. Most notably, the ν_4 band appeared at 1358 instead of 1344 cm^{-1} , indicating a loss of or modulation of the proximal thiolate ligation. However, for the wild type, there was a 1344 cm^{-1} shoulder of the ν_4 band, indicating that a weak population of thiolate proximal ligand was retained.

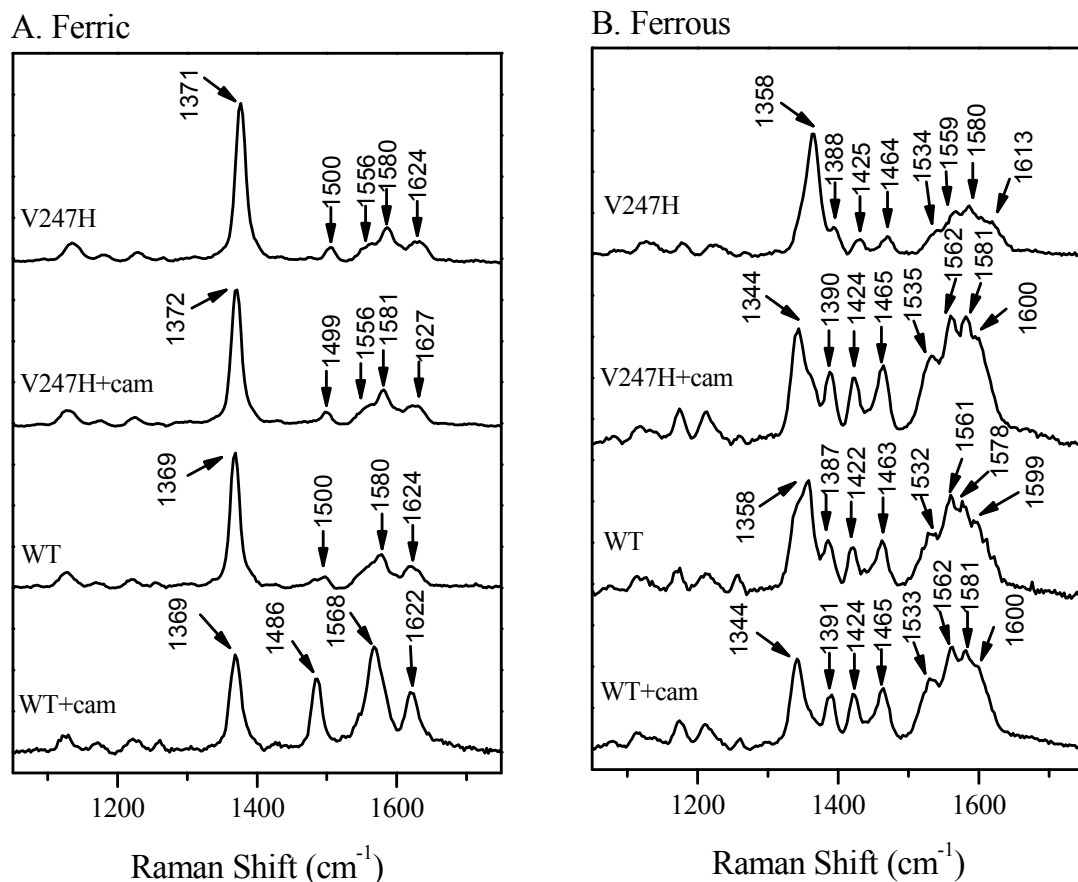


Figure 2.5. Resonance Raman spectra of (A) ferric and (B) ferrous wild-type P450 and P450V247H mutant with and without camphor binding. The excitation wavelength (λ_{ex}) was 413.1nm. The spectra of P450 and V247H samples in the presence and absence of 1mM camphor are shown.

2.4.4 NMR Spectroscopic study

Figure 2.6 showed the 1D proton NMR spectra of ferric low spin, cyanide-bound complexes of both wild type and V247H mutant of P450cam in the presence of camphor. The wild type P450cam exhibited almost identical results as reported in the literature, with two broad, fast relaxing, strongly hyperfine-shifted peaks at 33.1 ppm and -21.4 ppm respectively, indicative of the β protons from the coordinated Cys357 (38).

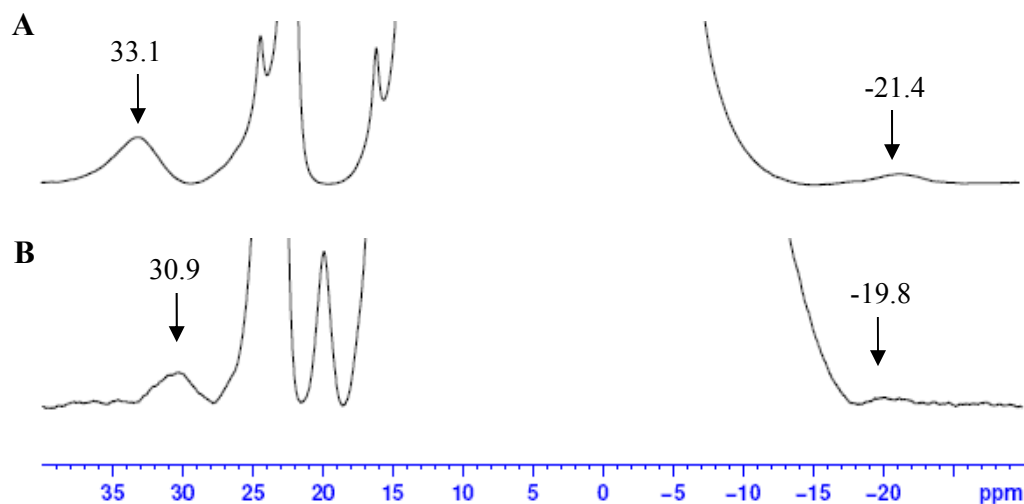


Figure 2.6 600-MHz ^1H Nuclear Magnetic Resonance spectra of the low spin cyanide complexes of (A) wild-type P450 and (B) V247H mutant. The spectra are collected at 298K in 0.1 M phosphate buffer at pH7.4.

Chloroperoxidase also shows a similar spectral pattern with that of P450cam with two hyperfine-shifted peaks at 38.3 and -20.7 ppm, the characteristic features of protons in close proximity to the heme iron from Cys29 (27). The P450cam V247H mutant (Fig. 2.6 (B)) displayed similar results, but with a slight shift compared with the wild type, which could be the result of conformational change caused by the substitution of the distal Val247. Nevertheless, the pair of peaks at 30.9 ppm and -19.8 ppm suggested the thiolate ligation in the V247H mutant was remained.

2.4.5 Electrochemistry study

Various reconstituted hemoproteins with modified heme or associated residues have been measured to analyze the factors that control their functions (39-41). However, the

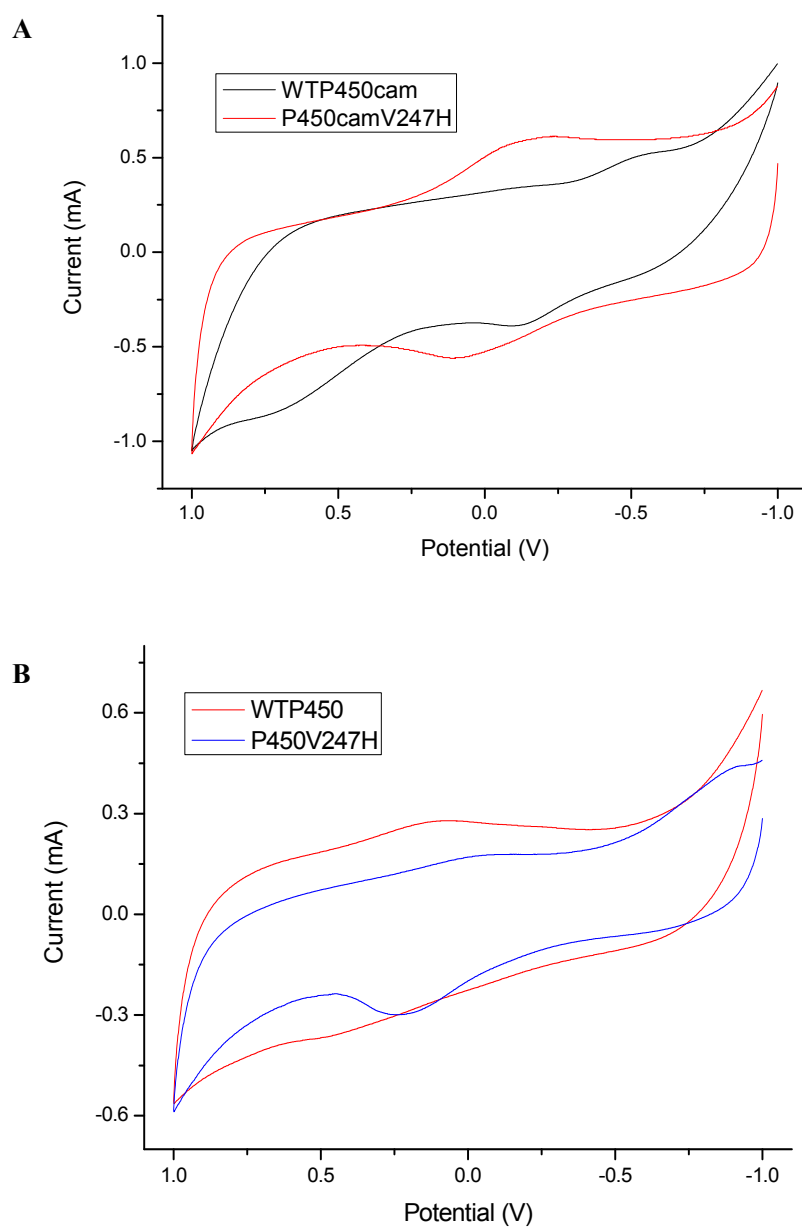


Figure 2.7 Cyclic voltammograms of WT P450cam and V247H mutant on a glass carbon electrode modified with SWNTs in the presence (A) and absence (B) of substrate camphor. Voltammograms were recorded between -1.0 and +1.5V at the scan rate of 1V/sec in 100mM phosphate buffer (pH7.4).

direct determination of the redox properties of heme proteins is often rendered difficult due to the strong adsorption of the protein onto electrode surface. The use of SWNT-coated carbon electrodes virtually eliminates this problem.

The reduction potentials for wild type P450cam were measured to be -304 and -135 mV in the absence and presence of camphor, respectively, both of which were in good agreement with the reported values (42). While the formal potential for the camphor-free V247H mutant was observed, to be much greater than the wild type, as high as +256 mV, upon substrate binding the value was decreased by about 50 mV to +206 mV (Fig. 2.7). This suggests that the substitution of the distal valine residue with a histidine induced a positive shift of the $\text{Fe}^{3+}/\text{Fe}^{2+}$ redox couple that might be attributed to the conformational change in the distal pocket.

2.4.6 ABTS assay

As shown in Fig. 2.8, the V247H mutant exhibited significant peroxidase activity compared with the wild type protein, and its reactivity was enhanced dramatically as pH increased. The highest peroxidation reactivity of the V247H mutant was observed at pH 7.4, which is the physiological optimum pH for P450cam. It displayed even higher peroxidase activity than CPO, and about 700-fold increase compared with the wild type P450cam at pH5.0.

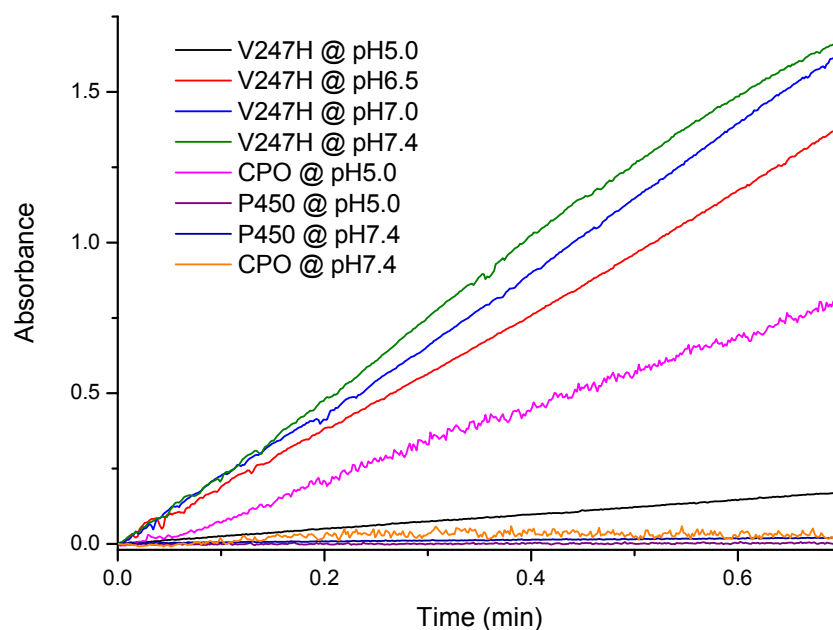
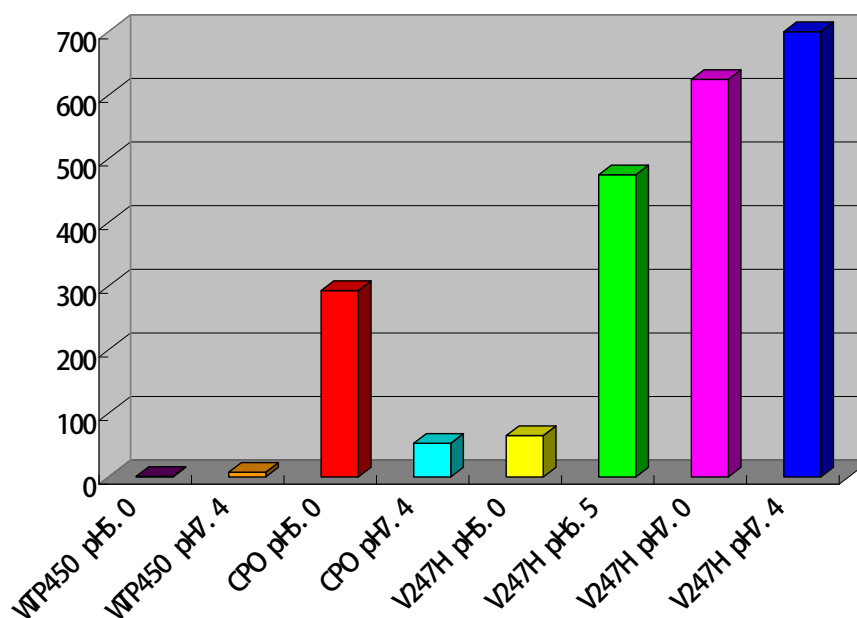
A**B**

Figure 2.8 ABTS assay of cytochrome P450cam, V247H mutant and CPO at different pH values. The peroxidase activity was monitored at 405nm in the presence of ABTS (9.1mM), enzyme (2 μ M), and H₂O₂ (3.3mM) in 100mM potassium phosphate buffer. The initial slope of the absorbance was used to calculate the peroxidase activity.

2.5 DISCUSSION

Though P450s are potentially significant enzymes for catalyzing the insertion of oxygen into unactivated C-H bonds, the practical application of cytochromes P450 as industrial biocatalysts has been greatly limited by the requirement of expensive cofactors and partner proteins. In this study, we converted the P450cam into an efficient peroxidase without the aid of any auxiliary elements by replacing the significant distal amino acid Val247 with a histidine residue. A distal His is found in many heme peroxidases and thus V247H mimics their distal environment.

The ABTS assay, which serves as a typical method to examine the peroxidase activity, was performed to test the mutant. We showed that after substitution of Val247 with a histidine, the mutant gained significantly higher peroxidase activity driven by H_2O_2 . Although in many heme peroxidases the distal histidine plays a key role in the formation of CpdI, a nearby arginine residue (also highly conserved) has also been suggested to cooperate with the histidine, thus playing an important role in assisting the catalytic cycle (17, 43, 44). Considering the possible contribution that a distal arginine might make to the peroxidase activity of V247H, we also replaced the nearby amino acid L244 in the distal helix with an arginine. However this double mutant L244R/V247H did not show higher peroxidase activity than the single mutant under the same conditions of study (data not shown). Previously, the proximal Cys357 was substituted with a

histidine to mimic heme peroxidases, but the V247H/C357H mutant did not exhibit better “peroxidase” activity compared with V247H alone (45).

The V247H mutant of P450cam was characterized by various spectroscopic techniques. UV-vis spectra showed that the resting state of V247H mutant without camphor is a six-coordinate, low spin ferric heme complex, similar to wild type P450cam, which has cysteinate and H₂O serving as the axial ligands. However, in addition to the wild type, V247H remained 6C-LS with addition of camphor. This suggests that the camphor-bound V247H mutant still remains predominantly in the six-coordinated, low-spin ferric iron state. This indicates that the camphor enters or binds to the heme prosthetic group differently due to the possible conformational changes caused by the replacement of Val247. The substituted bulkier histidine residue might sterically hinder the entrance of the substrate by having the imidazole group oriented in the direction of the heme iron. This was further confirmed with the CD spectroscopic study. Nevertheless, the characteristic Soret band of the ferrous-CO complex of V247H appeared at around 450nm, suggesting that the V247H mutant maintains the proximal heme-thiolate coordination. The reduced form of the mutant possesses a Soret maximum at 412nm upon initial reduction, which probably implies increased electron density on the thiolate in the reduced state (46).

Resonance Raman spectroscopy has proven to be a powerful probe to investigate the heme environment, especially the coordination, spin state and axial ligations of the heme.

In this study, both substrate-free and substrate-bound wild type and mutant proteins were examined (Fig. 3.4). Overall the spectra of P450cam with camphor in different oxidation states agree well with previous RR results (47, 48). The RR results of the ferric forms of the mutant protein in the presence and absence of camphor are also consistent with the UV-Vis absorption data discussed earlier.

The ν_4 band in the RR spectrum of 5C-Fe²⁺ heme complexes is a useful diagnostic marker of the identity of the proximal ligand. RR studies of a wide variety of heme proteins over the years have established that 5C-Fe²⁺ heme complexes with histidine (imidazole) as proximal ligand produce a ν_4 band in the 1350-1360 cm⁻¹ region whereas those with a cysteine (thiolate) proximal ligand display a ν_4 band in the 1340-1348 cm⁻¹ region (37, 49). The ferrous forms of camphor-bound wild type P450cam and V247H mutant display a ν_4 band in the range for 5C thiolate proximal ligation. Although the UV absorption spectrum of the ferrous-CO complex of camphor-free V247H indicated that the thiolate proximal ligand is preserved, the RR spectrum of the ferrous form does not indicate the same based on the previously established signatures. Thus, the ν_4 band is located at 1358 cm⁻¹, significantly higher than the expected 1340-1348cm⁻¹ range for proximal thiolate ligation (37). A ν_4 peak at 1358 cm⁻¹ was also observed for the camphor-free wild type protein, although in this case a shoulder was observed at ~1344 cm⁻¹. Evidently, in the absence of camphor, the proximal thiolate ligand is altered either by being fully replaced by a histidine ligand, or by being protonated or elongated.

Replacement of the cysteine ligand by a histidine appears unlikely because the CD data did not indicate any significant conformational changes upon camphor binding (Fig. 3.4 (A)). Also, we substituted all of the histidine residues present in the distal helix with either glycine or alanine and this species exhibited the same RR spectroscopic features (see Chapter III). Therefore it is likely that the proximal cysteine in the present case is protonated rather than replaced by another proximal residue. Indeed, Sabat et al. recently showed that protonation of the proximal cysteine ligand in iNOS leads to similar RR spectroscopic features as has been traditionally ascribed to a proximal histidine ligand (50).

The electrochemistry of this mutant together with wild type P450cam has shown that the distal environment can regulate the redox potential of the heme iron. For heme-containing oxygenases and peroxidases, the “push-pull” mechanism has been proposed where the generation of Cpd I is facilitated by an anionic proximal ligand and/or positive polar distal residues (51). In peroxidases like horseradish peroxidase or cytochrome *c* peroxidase, the “push” effect is provided by the proximal histidine and “pull” effect is mainly provided by the distal histidine that serves as a general acid–base catalyst to generate and stabilize the Cpd I (16, 52). For P450cam, since it lacks the distal residue that could promote the heterolytic O–O bond cleavage, the strong “push” effect from the proximal thiolate axial ligand is proposed to be responsive for the O–O bond heterolysis. It has also been suggested that the total charge near the heme could be

important for the heme redox potential. In the V247H mutant of P450cam, the redox potential was greatly increased, over 300 mV higher compared with that of the wild type. The increased redox potential of the V247H mutant clearly indicated the enhanced “pull” effect because of the introduction of the distal histidine residue which would increase the total charge near the heme prosthetic group and facilitate the generation of Cpd I.

In summary, we have shown that the substitution of Val247 in the distal helix with a hydrophilic histidine residue, which is highly conserved in many heme peroxidases, has successfully converted P450cam into an efficient self-sufficient H₂O₂-driven peroxidase, with the thiolate ligation intact in the proximal side.

2.6 REFERENCES

1. Guengerich, F. P. (1991) Reactions and Significance of Cytochrome P-450 Enzymes, *Journal of Biological Chemistry* 266, 10019-10022.
2. Ortiz de Montellano, P. R. (2005) *Cytochrome P450: structure, mechanism, and biochemistry*, 3 ed., Kluwer Academic/Plenum Publishers, New York.
3. Sigel, A., Sigel, H., and Sigel, R. K.O. (2007) The ubiquitous roles of cytochrome P450 proteins in *Metal Ions in Life Sciences* (Sigel, A., Sigel, H., and Sigel, R. K.O. , Ed.), Wiley, Chichester.
4. Sono, M. R., M. P.; Coulter, E. D.; and Dawson, J. H. (1996) Heme-Containing Oxygenases, *Chemical Reviews* 96, 2841-2847.
5. Denisov, I. G., Makris, T. M., Sligar, S. G., and Schlichting, I. (2005) Structure and chemistry of P450, *Chem. Review* 105, 2253-2277.

6. Dawson, J. H. (1988) Probing structure-function relations in heme-containing oxygenases and peroxidases, *Science* 240, 433-439.
7. Newcomb, M., Zhang, R., Chandrasena, R. E. P., Halgrimson, J. A., Horner, J. H., Makris, T. M., and Sligar, S. G. (2006) Cytochrome P450 Compound I, *J. Am. Chem. Soc.* 128, 4580-4581.
8. Joo, H., Lin, Z. L., and Arnold, F. H. (1999) Laboratory evolution of peroxide-mediated cytochrome P450 hydroxylation, *Nature* 399, 670-673.
9. Nordblom, G. D., White, R. E. and Coon, M. J. (1976) Studies on hydroperoxide-dependent substrate hydroxylation by purified liver microsomal cytochrome P450, *Arch. Biochem. Biophys.* 175, 524-533.
10. Hrycay, E. G., Gustafsson, J.-A., Ingelman-Sundberg, M. and Ernster, L. (1975) Sodium periodate, sodium chlorite, organic hydroperoxides and hydrogen peroxide as hydroxylating agents in steroid hydroxylation reactions catalyzed by partially purified cytochrome P450, *Biochem. Biophys. Res. Commun.* 66, 209-216.
11. Cirino, P. C., and Arnold, F. H. (2003) A self-sufficient peroxide-driven hydroxylation biocatalyst, *Angew. Chem. Int. Ed.* 42, 3299-3301.
12. Shoji, O., Fujishiro, T., Nakajima, H., Kim, M., Nagano, S., Shiro, Y., Watanabe, Y. (2007) Hydrogen Peroxide-Dependent Monooxygenations by Tricking the Substrate Recognition of Cytochrome P450BS β , *Angew. Chem. Int. Ed.* 46, 3656-3659.
13. Cirino, P. C., and Arnold, F. H. (2002) Regioselectivity and activity of cytochrome P450 BM-3 and mutant F87A in reactions driven by hydrogen peroxide, *Advanced Synthesis & Catalysis* 344, 932-937.
14. Poulos, T. L., and Kraut, J. (1980) The Stereochemistry of Peroxidase Catalysis, *J. Biol. Chem.* 255, 8199-8205.
15. Davydov, R. M., Ledenev, A.N. (1981) Activation mechanism of molecular oxygen by cytochrome P-450, *Biofizika* 26, 1096.

16. Tanaka, M., Ishimori, K., Mukai, M., Kitagawa, T., and Morishima, I. (1997) Catalytic activities and structural properties of horseradish peroxidase distal His42->Glu or Gln mutant, *Biochemistry* 36, 9889-9898.
17. Howes, B. D., RodriguezLopez, J. N., Smith, A. T., and Smulevich, G. (1997) Mutation of distal residues of horseradish peroxidase: Influence on substrate binding and cavity properties, *Biochemistry* 36, 1532-1543.
18. Newmyer, S. L., and Demontellano, P. R. O. (1995) Horseradish-peroxidase His-42 -> Ala, His-42 ->Val, and Phe-41 ->Ala mutants - Histidine Catalysis and Control of Substrate Access to the Heme Iron, *J. Biol. Chem.* 270, 19430-19438.
19. Erman, J. E., Vitello, L. B., Miller, M. A., Shaw, A., Brown, K. A., and Kraut, J. (1993) Histidine 52 is a critical residue for rapid formation of cytochrome c peroxidase compound I, *Biochemistry* 32, 9798-9806.
20. Poulos, T. L., and Kraut, J. (1980) THE STEREOCHEMISTRY OF PEROXIDASE CATALYSIS, *J. Biol. Chem.* 255, 8199-8205.
21. Matsunaga, I., and Shir, Y. (2004) Peroxide-utilizing biocatalysts: structural and functional diversity of heme-containing enzymes, *Current Opinion in Chemical Biology* 8, 127-132.
22. Poulos, T. L., Finzel, B. C., and Howard, A. J. (1987) HIGH-RESOLUTION CRYSTAL-STRUCTURE OF CYTOCHROME-P450CAM, *Journal of Molecular Biology* 195, 687-700.
23. Poulos, T. L., Finzel, B. C., Gunsalus, I. C., Wagner, G. C., and Kraut, J. (1985) THE 2.6-Å CRYSTAL-STRUCTURE OF PSEUDOMONAS-PUTIDA CYTOCHROME-P-450, *Journal of Biological Chemistry* 260, 6122-6130.
24. Unger, B. P., Gunsalus, I. C., Sligar, S. G. (1986) Nucleotide-sequence of the Pseudomonas-putida Cytochrome P450-cam Gene and Its Expression in Escherichia-coli, *J. Biol. Chem.* 261, 1158-1163.
25. Paul, K. G., Theorell, H., Akesson, A. (1953) The Molar Light Absorption of Pyridine Ferroprotoporphyrin (Pyridine Haemochromogen), *Acta Chem. Scand.* 7, 1284-1287.

26. Berry, E. A., and Trumpower, B. L. (1987) Simultaneous Determination of Hemes-a, Hemes-b, and Hemes-c from Pridine Hemochrome Spectra, *Analytical Biochemistry* 161, 1-15.
27. Wang, X., Tachikawa, H., Yi, X., Manoj, K. M., and Hager, L. P. (2003) Two-dimensional NMR Study of the Heme Active Site Structure of Chloroperoxidase, *J. Biol. Chem.* 278, 7765-7774.
28. Alwarappan, S., Prabhulkar, S., Durygin, A., and Li, C. . (2009) The effect of electrochemical pretreatment on the sensing performance of single walled carbon nanotubes, *J. Nanosci. Nanotech.* 9, 2991-2996.
29. Yi, X. W., Mroczko, M., Manoj, K. M., Wang, X. T., and Hager, L. P. (1999) Replacement of the proximal heme thiolate ligand in chloroperoxidase with a histidine residue, *Proc. Natl. Acad. Sci. U.S.A.* 96, 12412-12417.
30. Limburg, J., LeBrun, L. A., and de Montellano, P. R. O. (2005) The P450(cam) G248E mutant covalently binds its prosthetic heme group, *Biochemistry* 44, 4091-4099.
31. Suzuki, N., Higuchi, T., Urano, Y., Kikuchi, K., Uekusa, H., Ohashi, Y., Uchida, T., Kitagawa, T., and Nagano, T. (1999) Novel Iron Porphyrin-Alkanethiolate Complex with Intramolecular NH...S Hydrogen Bond: Synthesis, Spectroscopy, and Reactivity, *J. Am. Chem. Soc.* 121, 11571-11572.
32. Gunsalus, I. C., Wagner, G. C. (1978) Bacterial P-450cam methylene monooxygenase components: Cytochrome m, putidaredoxin, and putidaredoxin reductase, *Methods Enzymol.* 52, 166-188.
33. Dawson, J. H., Andersson, L. A. and Sono, M. (1982) Spectroscopic Investigations of Ferric Cytochrome P-450-CAM Ligand Complexes, *J. Biol. Chem.* 257, 3606-3617.
34. Spiro, T. G., Stong, J. D., and Stein, P. (1979) Porphyrin core expansion and doming in heme proteins. New evidence from resonance Raman spectra of six-coordinate high-spin iron(III) hemes, *J. Am. Chem. Soc.* 101, 2648-2655.
35. Andersson, L. A., Mylrajan, M., Sullivan, E. P., Jr., and Strauss, S. H. . (1989) *J. Biol. Chem.* 264, 19099-19102.

36. Lou, B. S., Snyder, J. K., Marshall, P., Wang, J. S., Wu, G., Kulmacz, R. J., Tsai, A. L., and Wang, J. (2000) *Biochemistry* 39, 12424-12434.
37. Anzenbacher, P., Evangelista-Kirkup, R., Schenkman, J., Spiro, T. G. (1989) Influence of Thiolate Ligation on the Heme Electronic-Structure in Microsomal Cytochrome-P450 and Model Compounds - Resonance Raman-Spectroscopic Evidence, *Inorganic Chemistry* 28, 4491-4495.
38. Wakasugi, K., Ishimori, K., and Morishima, I. (1996) NMR studies of recombinant cytochrome P450cam mutants, *Biochimie* 78, 763-770.
39. Li, C., Taniguchi, I., Mulchandani, A. . (2009) Redox properties of engineered ruthenium myoglobin, *Bioelectrochemistry* 75, 182-188.
40. Li, C., Nishiyama, K. and Taniguchi, I. (2000) Electrochemical and spectroelectrochemical studies on cobalt myoglobin, *Electrochim. Acta.* 45, 2883-2888.
41. Li, C. Z., Taniguchi, I., Mulchandani, A. (2009) Redox properties of engineered ruthenium myoglobin, *Bioelectrochemistry* 75, 182-188.
42. Yoshioka, S., Takahashi, S., Ishimori, K., Morishima, I. (2000) Roles of the axial push effect in cytochrome P450cam studied with the site-directed mutagenesis at the heme proximal site, *J. Inorg. Biochem.* 81, 141-151.
43. Schiodt, C. B., Veitch, N. C., and Welinder, K. G. (2007) Roles of distal arginine in activity and stability of *Coprinus cinereus* peroxidase elucidated by kinetic and NMR analysis of the Arg51Gln, -Asn, -Leu, and -Lys mutants, *Journal of Inorganic Biochemistry* 101, 336-347.
44. Bujons, J., Dikiy, A., Ferrer, J. C., Banci, L., and Mauk, A. G. (1997) Charge reversal of a critical active-site residue of cytochrome-c peroxidase - Characterization of the Arg48->Glu variant, *European Journal of Biochemistry* 243, 72-84.
45. Auclair, K., Moenne-Loccoz, P., Ortiz de Montellano, P. R. (2001) Roles of the Proximal Heme Thiolate Ligand in Cytochrome P450cam, *J. Am. Chem. Soc.* 123, 4877-4885.

46. Yoshioka, S., Tosha, T., Takahashi, S., Ishimori, K., Hori, H., and Morishima, I. (2002) Roles of the Proximal Hydrogen Bonding Network in Cytochrome P450cam-Catalyzed Oxygenation, *J. Am. Chem. Soc.* *124*, 14571-14579.
47. Champion, P. M., Gunsalus, I. C., and Wagner, G. C. (1978) Resonance Raman Investigations of Cytochrome P450cam from *Pseudomonas-putida*, *J. Am. Chem. Soc.* *100*, 3743-3751.
48. Wells, A. V., Li, P. S., Champion, P. M., Martinis, S. A., and Sligar, S. G. (1992) Resonance Raman Investigations of *Escherichia-coli* Expressed *Pseudomonas-putida* Cytochrome-P450 and Cytochrome P420, *Biochemistry* *31*, 4384-4393.
49. Wang, J., Caughey, W. S., Rousseau, D. L. (1996) Resonance Raman Scattering: a Probe of Heme Protein-bound Nitric Oxide., in *Methods in Nitric Oxide Research* (Feelisch, M., Stamler, J., Ed.), pp 427-454, J. Wiley, Chichester ; New York.
50. Sabat, J., Stuehr, D. J., Yeh, S. R., and Rousseau, D. L. (2009) Characterization of the Proximal Ligand in the P420 Form of Inducible Nitric Oxide Synthase, *Journal of the American Chemical Society* *131*, 12186-12192.
51. Takahashi, S., Wang, J., Rousseau, D. L., Ishikawa, K., Yoshida, T., Host, J. R., and Ikeda-Saito, M. (1994) Heme-Heme Oxygenase Complex, *J. Biol. Chem.* *269*, 1010-1014.
52. Newmyer, S. L., and Ortiz de Montellano, P. R. (1996) Rescue of the Catalytic Activity of an H42A Mutant of Horseradish Peroxidase by Exogenous Imidazoles, *J. Biol. Chem.* *271*, 14891-14896.

CHAPTER III. ENGINEERING CYTOCHROME P450cam INTO P420 WITH CATALYTIC ACTIVITIES

3.1 SUMMARY

In an effort to engineer cytochrome P450cam into a self-sufficient biocatalyst, key structural components within the heme active site of P450cam and chloroperoxidase (CPO) were evaluated and the P450cam L246K mutant was constructed. L246K works as a self-sufficient peroxidase demonstrating the importance of polarity of the distal heme environment in regulating the catalytic property of P450cam. The similar UV-vis and resonance Raman (RR) spectra of ferric L246K and substrate-free ferric P450cam support a hexacoordinate, low-spin heme with thiolate ligation in this form of the mutant. Surprisingly, the reduced L246K and its CO complex display spectral properties similar to those of the inactivated species of P450cam (P420), suggesting the proximal ligand of L246K was changed or modified during reduction and CO binding. Contrary to what has been generally thought, formation of a myoglobin-like heme structure in L246K via histidine coordination is ruled out by the expression of a P450cam mutant (L246K-3H, H352G/H355G/H361A) where all three histidines located in the vicinity of the proximal ligand helix were replaced by glycine or alanine. On the basis of the spectral similarities and functional differences among L246K, the native P450cam, and the inactive P420, it is proposed that upon reduction and CO binding, the proximal cysteine ligand of P420 becomes protonated due to harsh conditions employed in its preparation while the proximal ligand of L246K retains the parent protein's thiolate character but with a longer Fe-S bond due to conformational changes induced by the mutation.

3.2 INTRODUCTION

The cytochromes P450 are a ubiquitous class of heme-containing monooxygenases named for their characteristic optical absorption maximum near 450 nm upon reduction in the presence of carbon monoxide (1). They catalyze a variety of difficult chemical transformations with high specificity and selectivity under physiological conditions, making them attractive candidates for large-scale production of fine chemicals and pharmaceuticals that are difficult to synthesize with standard organic chemistry (2-4).

Cytochrome P450cam (CYP101) from *Pseudomonas putida* catalyzes the hydroxylation of camphor and has been extensively studied as the prototype of P450 monooxygenases because of its solubility, availability and extensive mechanistic and structural characterizations. It was the first to be characterized by crystallographic techniques among P450 enzymes (5). Previous study has shown that the resting state of P450cam is a predominately low spin Fe (III) porphyrin with water cluster occupying the sixth coordination position, upon substrate binding the water is replaced by the substrate camphor and the complex becomes high spin followed by reduction to Fe (II) and subsequent binding of O₂ (6).

The P450s and chloroperoxidase (CPO) from *Caldariomyces fumago* are distinct from most heme proteins in possessing a deprotonated cysteine residue at the proximal side serving as the axial ligand to the heme iron (Fig. 3.1) (7-9). The role of axial-thiolate ligation in P450s has been widely studied and the thiolate ligand is suggested to serve as

a strong internal electron donor, facilitating the heterolytic cleavage of the dioxygen bond to generate the activated iron (IV)-oxo species known as Cpd I (10, 11). Also the presence of the cysteinate thiolate proximal heme iron ligand is believed to be responsible for the red-shift of the Soret absorption band at 450nm. Although P450s and CPO share similar metal binding sites, their heme environments are quite different in terms of polarity (12). The active site of P450 is highly hydrophobic in nature with the lack of obvious acid-base catalytic residues in close proximity to the oxygen binding pocket, while CPO has evolved a more polar distal heme pocket analogous to that of the hydro-peroxidases (13). Another dissimilarity between P450cam and CPO is that CPO only needs hydrogen peroxide to be catalytically active, while P450cam requires dioxygen, cofactor NADH and two electron-transfer proteins—putidaredoxin reductase and putidaredoxin which are known as the “physiological partners” (14). These requirements for activity are believed to be the major factors that hinder the application of P450s in biotechnological processes. The goal of this study is to understand the structure-functional relationships in hemoproteins and to investigate the feasibility of converting P450cam to an active catalyst without cofactors and explore the correlation and possible conversion between P450s and peroxidases (such as CPO).

Most P450 enzymes would undergo a universal denaturing transition to a stable but inactive species known as P420s because the absorption maximum of the resulting Fe^{II} -CO complex is at 420 nm rather than at 450 nm as is characteristic of P450 (15).

Cytochrome P420 could be formed from all known types of P450 by numerous chemical and physical techniques, such as incubation in organic solvents (16), exposure to high temperature, pressure (17, 18), neutral salts (19), or to very low and high pH buffer (20). P420 can sometimes, depending on how it is prepared, be converted back to P450 by incubation with thiols, spermine, dimethyl sulfoxide, polyols, and native substrates (16, 22-25). Therefore, knowledge about the structural relationship between the inactive P420 and the native P450 is of paramount importance to our understanding of the catalytic activity and the nature of the putative transient intermediates involved in the catalytic cycle of P450 enzymes. Furthermore, the structural alterations that occur during the conversion of P450 to P420 will not only shed light on the conformational modification in many hemoprotein variants with thiolate axial ligands, but also greatly help us in the rational design of self sufficient P450 mutants with enhanced activity and stability.

In fact, there are some other P420 forms of the heme-thiolate proteins besides P450. As a member of P450 family, inducible nitric oxide synthase (iNOS) possesses a negatively charged thiolate ligand from a deprotonated cysteine residue proximal to the heme iron (26). Like other P450 proteins, the reduced iNOS exhibits the absorption Soret band at around 450nm upon CO binding (iNOSP450), which can spontaneously convert to an inactive species like “P420” (iNOSP420) with the Soret band at around 420nm (27-30). The spectroscopic studies have shown that the iNOSP420 species is inactivated by protonation of the proximal thiolate ligand to a neutral thiol, instead of by ligand

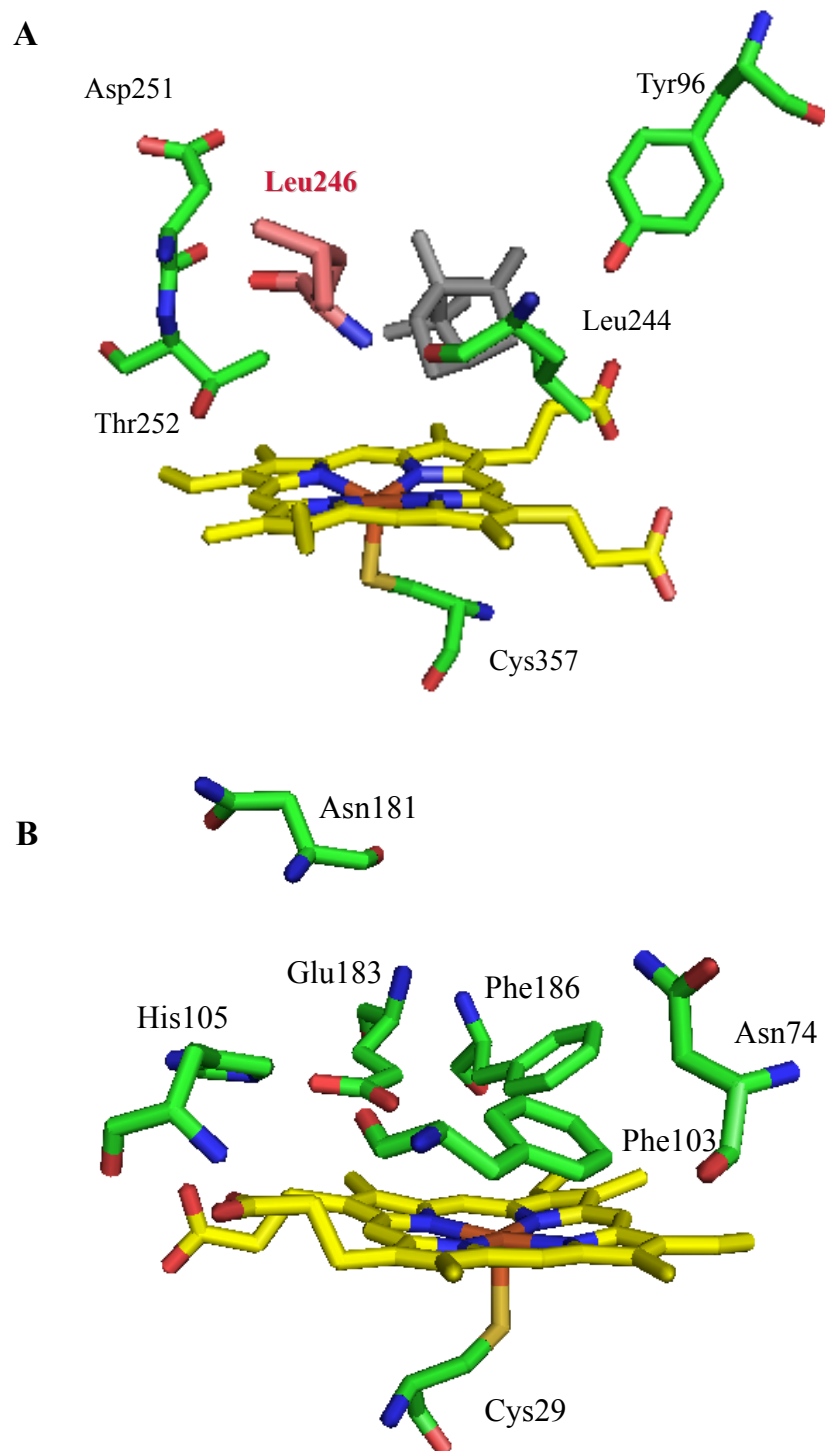


Figure 3.1 Heme environmental structure of ferric cytochrome P450cam (A) and chloroperoxidase (CPO: B): the heme (yellow), camphor (gray) and some selected residues including distal Leu246 (salmon) in P450cam are shown. The figures were generated from the crystal data (PDB code 2CPP and 1CPO) using PYMOL (5, 21).

switching (e.g. to a histidine) (31). The iNOSP450 to iNOSP420 transition is controlled by the conformational state of the enzyme. In addition chloroperoxidase, under alkaline conditions, could also undergo a denaturing transition to an inactive species that has a spectrum essentially identical to that of cytochrome P420, and is named C420 (32). Although the conversion of CPO to C420 can be stopped at any point by lowering the pH, it is not likely to convert C420 back to native CPO by adjusting the complex to lower pH values or by adding natural sulfhydryl compounds such as mercaptides (33). The heme iron oxidation state has been suggested to influence the transition to C420 which triggers the conformational change. In ferric C420, the proximal ligand C29 appears at least partially retained in a thiolate/imidazole coordination sphere. However the ferrous C420 loses the thiolate ligand and has a bis-histidine coordination structure instead. Upon CO binding, one of the axial histidine ligands remains trans to the carbon monoxide (32).

Although many physical and chemical methods have been employed to investigate the structural features of P420 and its counterparts in iNOS and CPO, the structural relationship between P450 and P420 remains controversial (22, 34-36). Postulation concerning the structure of P420 has been focused on the nature of the proximal heme iron ligand. In particular, it has been suggested that a conformational change results in replacement of the thiolate ligand by histidine or exogenous ligand, yielding a myoglobin (Mb)-like heme coordination structure (36-38). Alternatively, theoretical calculations and recent studies with Mb H93G cavity mutant have indicated that the proximal thiolate may

be protonated, resulting in a weaker thiol ligand (39, 40), or that the Fe-S bond might be weakened by lengthening (41). Unfortunately, there is little experimental evidence in the literature to distinguish these hypotheses (35, 42). Therefore, it is desirable to make a P450 variant that does not need harsh physical and chemical treatment but displays P420-like spectral features.

In an effort to engineer P450cam into a self sufficient catalyst, we designed several mutants focused on modulating the polarity of the distal heme environment. As predicted by the structural comparison of P450 with most heme peroxidases, introducing polar residues to the heme distal environment indeed improved the catalytic efficiency of P450 dramatically. First, multiple mutations were carried out in P450cam to replace the hydrophobic amino acids in the distal side of the heme group with polar amino acids. The P450 variant was named as P450H with the substitutions of L244K, L245K, L246K, L250K, T252H, V253A and V254R. The spectroscopic studies of P450H showed P420-like properties in its ferrous and ferrous-CO complexes. To elucidate which one or ones of the nonpolar residues in the distal pocket induced such transition, single mutation and multiple mutations were performed. It turned out that the L246K mutant of P450 was the first example that demonstrated typical spectral features of P420s but acted as a self-sufficient catalyst. Through the process, the introduction of polar residues to the heme distal environment indeed improved the catalytic efficiency of P450 dramatically. More significantly, structural and biochemical studies of this P420-P450 hybrid allowed

us to discern the nature of the proximal heme iron ligand in the active P450 and the inactive P420 species.

3.3 EXPERIMENTAL PROCEDURES

3.3.1 Site-directed mutagenesis and protein expression.

The pUS200 plasmid used in this work, containing a 1578-bp CAM plasmid fragment of *Pseudomonas putida* (ATCC 17453), was subcloned into the PstI and HindIII sites of vector pEMBL8+. To increase the protein yield, the P450_{cam} gene was constructed into pET-30a (+), a high copy number vector, at the sites of NdeI and HindIII by polymerase chain reactions and ligation reactions. The L246K mutant of P450_{cam} was prepared with the 5'-sense oligonucleotide 5'- ATG TGT GGC CTG TTA AAG GTC GGC coding for MCGLLKVG. The L246K 3H mutant was obtained based on the L246K mutant with the 5'-sense oligonucleotide 5'- TTT GGC GGT GGC AGC GGT CTG TGC CTT GGC CAG GCA CTG GCC coding for FGHGSHLCLGQHLA. The primers used for P450H, and other mutants were listed in Appendix C. The reconstructed plasmids containing wild type P450_{cam} and its P450H, L246K and L246K 3H mutants were transformed into *E. coli* strain NovaBlue and verified by DNA sequencing. Then the proteins were expressed in *E. coli* strain Rosetta II (DE3). Cells were grown on terrific broth supplemented with 100mg/L of kanamycin at 37 °C and induced with 1mM IPTG and 1mM camphor at OD₆₀₀ around 0.8, followed by further growth at 30°C for another

18h prior to harvesting cells. As for the mutants, the addition of δ -aminolevulinic acid to the growth media is necessitated to facilitate holoenzyme production. The cells were then harvested and frozen at -80°C.

3.3.2 Protein purification

Cells were lysed at 4°C in 50mM Tris-HCl buffer at pH 7.4 containing 50 mM KCl, 0.5 mM DTT, 1 mM camphor (buffer A), 1 mM EDTA, 200 μ M PMSF, 40 U/ml Dnase I, 3 U/ml Rnase A, and lysozyme. Following sonication and centrifugation, the lysed cells were concentrated by Amicon cell with 30,000 Da cut-off ultrafiltration membrane. The protein solution was first applied on a fast flow DEAE Sepharose column. After initial elution, the column was eluted with a linear 0-0.5 M KCl gradient in the same buffer. As for the L246K and L246K 3H mutants, they were expressed as apo-proteins. So the fractions containing the ~45 kDa proteins were pooled for heme reconstitution. Hemin was added to the apo-protein dropwise and stirred overnight (43). After heme reconstitution, the protein was again applied on the fast flow DEAE Sepharose column. The reddish fractions of correct molecular weight were pooled and concentrated using a Centriprep with an YM30 membrane for further purification by size exclusion chromatography. The buffer applied on the gel filtration was 0.1 M potassium phosphate buffer at pH7.4.

P420 was prepared as reported by adding 30% acetone and incubate at room temperature for 30 minutes (16). Unless otherwise specified, all the steps in the protein purification were performed at 4 °C.

3.3.3 Electronic absorption spectroscopy

The UV-visible spectra of the P450cam mutants were recorded on a Varian Cary 300 Bio UV-visible spectrophotometer at room temperature. The ferrous proteins were prepared by the addition of excess amount of sodium dithionite and CO adducts were obtained by CO gas bubbling. The buffer used for the absorption measurements was 100mM potassium phosphate buffer at pH7.4.

3.3.4 Resonance Raman spectroscopy

For the resonance Raman data collection, the wild-type P450 and its mutant samples with concentration about 50 μ M were prepared in a septum-sealed, cylindrical quartz cell. Samples were reduced to the ferrous form by first flushing the sample with argon and then injecting a molar excess of buffered sodium dithionite solution. The rotating sample cell was irradiated with 4mW of 413.1nm laser light using a mixed krypton/argon ion laser. The spectral acquisition time was 5 min. The scattered light was collected at right angles to the incident beam and focused onto the entrance slit (125 μ m) of a 0.8m spectrograph, where it was dispersed by a 600 groove/mm grating and detected by a liquid-N₂-cooled CCD camera (Horiba-JY). Spectral calibration was performed against

the lines of mercury. UV-vis spectra of each sample were collected before and after each RR measurement to ensure the sample integrity.

3.3.5 Peroxidase activity

2, 2'-azino-bis (3-ethylbenzthiazoline-6-sulfonic acid) (ABTS) was used as the substrate for the enzymatic assay of peroxidase activity of wild type P450cam, P450H, CPO, P420 and the P450cam L246K mutant protein. 9.1mM ABTS substrate solution was prepared in 50mM phosphate buffer at pH5.0. Hydrogen peroxide was added to initiate the reaction, and the increase of the absorbance was monitored at 405nm for 2 min. The spectrophotometer cell holder was equipped with a magnetic stirrer and the incubation mixture was stirred throughout the reaction.

3.4 RESULTS AND DISCUSSION

3.4.1 Optical properties and catalytic activity of P450H

The P450H mutant of cytochrome P450cam, in which seven hydrophobic amino acids were replaced by polar residues, showed very different electronic absorption properties with those of the wild type in all oxidation states (Fig. 3.2). Especially, the ferrous-CO complex of the P450H mutant displayed the absorption maximum at 420nm instead of 450nm which is characteristic of P450. The blue shift of the spectrum could be caused by the change of polarity in the distal pocket and some distinct conformational alteration in the active site. To examine whether the P450H mutant with increased

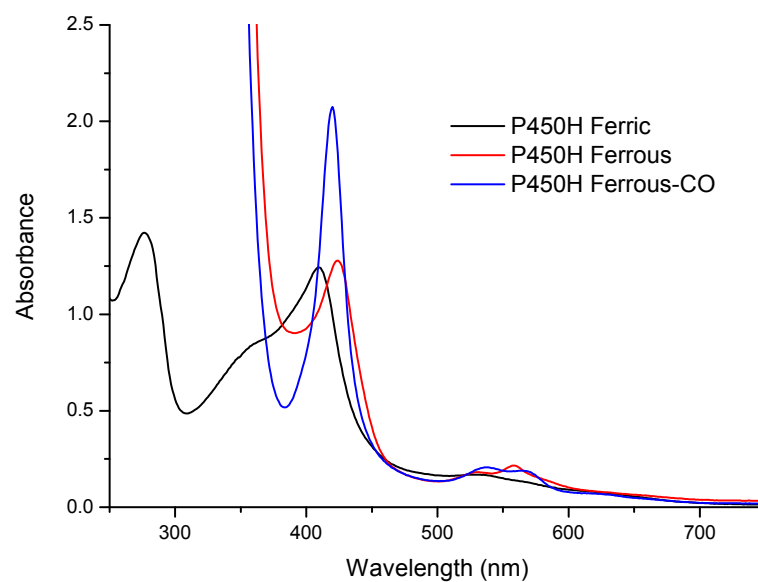


Figure 3.2 UV-visible spectra of P450H in various oxidation states.

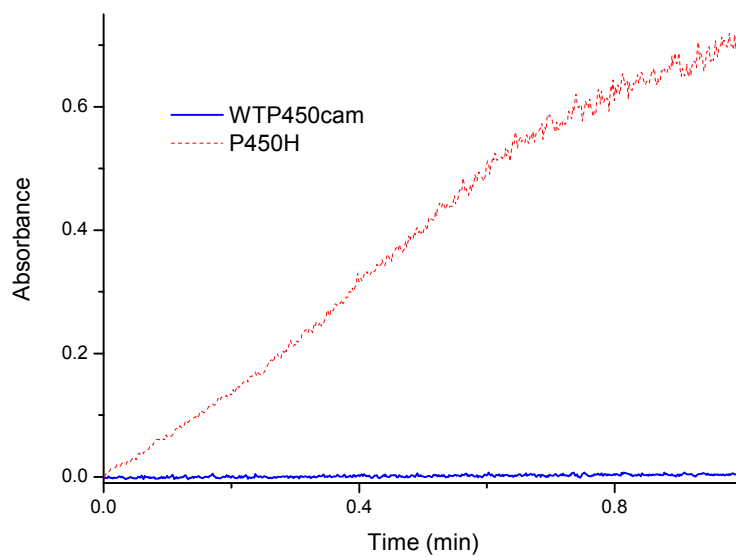


Figure 3.3 Peroxidase activities of wild type P450cam and its P450H mutant determined by monitoring the oxidation of ABTS at 405nm in the presence of H_2O_2 (3.3mM), ABTS (9.1mM), and enzyme (2 μM).

polarity in distal side gained some peroxidase activities, a peroxidase assay using ABTS as the substrate was performed that showed greatly increased activity of P450H compared with that of wild type protein (Fig. 3.3). These results suggested the modified distal environment of P450cam induced some marked changes both structurally and functionally.

3.4.2 UV-visible spectroscopic studies of P450L246K

To examine specifically which one or which ones of the seven substituted residues in the distal pocket caused the dramatic change, single mutation and multiple mutations were carried out. It turned out that the single mutant L246K exhibited quite similar properties with those of P450H. The identity of the mutant proteins was verified by SDS-PAGE. Changing L246, a non-polar residue located on the distal heme of the protein, to lysine, a basic and polar residue resulted in a mutant typical of ferric low spin, six-coordinate heme proteins as demonstrated by the electronic absorption spectra of the mutant (Fig. 3.4). The absorption maxima of the spectra in Figure 3.4 are essentially identical to those of the substrate-free wild-type P450cam and P420cam (Table 3.1), suggesting that the proximal heme iron ligand, Cys357, in wild-type P450cam was retained in the L246K mutant (34, 44). However, the electronic absorption spectra of the ferrous and the ferrous-CO complex of the L246K mutant displayed absorption maximum at 423 and 419 nm, rather than at 408 and 450 nm, respectively, expected for

most heme thiolate proteins. It has been generally believed that these spectral features are characteristics of hemoproteins with proximal histidine ligand (45).

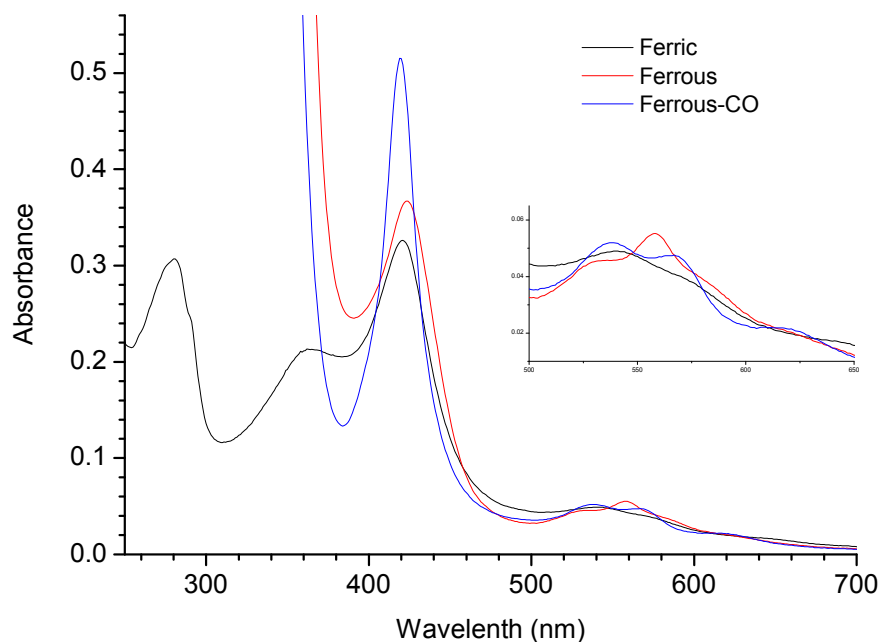


Figure 3.4 UV-vis spectra of P450camL246K in various oxidation states. The *inset* shows a magnification of the spectra in the α/β band region. The enzyme concentration employed was 4 μ M.

However, histidine ligation in this case has been ruled out due to the following two considerations. First, there is no histidine in the distal pocket of P450cam (9). Second, the ferrous and ferrous-CO forms of the P450 L246K-3H mutant (H352G/H355G/H361A) where all three histidines that locate in the vicinity of the proximal helix have been replaced by glycine or alanine, display virtually identical optical absorption features to those of P420 and L246K (Table 3.1). Therefore, it is proposed that the observed absorption maximum at 420 nm in L246K and L246K-3H mutants as well as in P420 is

due to milder changes such as protonation of the proximal ligand or lengthening of the Fe-S bond caused by conformational changes induced by mutation or conditions used in the preparation of P420 rather than more drastic changes such as ligand switching.

Table 3.1 Wavelength and extinction coefficients of absorption maxima for WT P450_{cam}, P420_{cam}, P450_{cam}L246K and P450_{cam}L246K 3H

Protein		Soret (nm)	δ -band (nm)	Visible (nm)
WT P450cam	Fe ³⁺	417	360	535, 569
	Fe ²⁺	408		540
	Fe ²⁺ -CO	446		550
P420cam (22)	Fe ³⁺	422	367	541, 566, 651
	Fe ²⁺	424		530, 558
	Fe ²⁺ -CO	420		540, 572
P450camL246K	Fe ³⁺	421	362	540
	Fe ²⁺	423		532, 558
	Fe ²⁺ -CO	419		539, 567, 620
P450camL246K 3H	Fe ³⁺	411	360	535, 569
	Fe ²⁺	423		531, 558
	Fe ²⁺ -CO	420		540, 569, 621

Indeed, thiol-ligated ferrous heme-CO adducts of both synthetic heme model compounds and biomimetic protein models display Soret absorption maximum at 420 nm (39, 46). Alternatively, it has been reported that lengthening of the Fe-S bond by 0.2 Å could induce the optical spectral transition of ferrous-CO complex of heme thiolate proteins from ~450 nm to ~420 nm (34, 41). Alternatively, protonation of the native proximal thiolate ligand to a neutral thiol could be responsible for the P420-like spectral

pattern of both L246K and L246K-3H mutants. In fact, neutral thiol-ligated ferrous heme-CO adducts of both synthetic heme model compounds and biomimetic protein models displayed absorption maximum at 420 nm (39, 46, 47).

3.4.3 Resonance Raman spectroscopic study

The resonance Raman (RR) spectra of heme proteins are characterized in the high frequency region by strong porphyrin in-plane vibrational bands, which are diagnostic of the oxidation-, spin-, and coordination-state of the heme iron (48-50). To further examine the heme environment of L246K and L246K-3H mutants together with wild type P450cam and P420, we obtained resonance Raman spectra in various oxidation states. The RR spectra of all the ferric protein samples displayed a strong oxidation state marker band ν_4 at around 1370 cm^{-1} that is typical for ferric (Fe^{3+}) heme (Fig. 3.5 A). The camphor-bound P450cam heme core-size marker bands ν_3 and ν_2 appeared at 1486 cm^{-1} and 1568 cm^{-1} , respectively, indicating a five-coordinate (5C), high-spin (HS) heme iron (51-53). While for all other samples, the spectra displayed the ν_3 and ν_2 bands at around 1500 cm^{-1} and 1580 cm^{-1} , suggesting a six-coordinate (6C), low-spin (LS) heme iron component. Overall the camphor-free, camphor-bound P450cam and P420 RR spectra agree well with previous RR studies (54, 55). The spectra of both ferric L246K and L246K-3H closely resemble that of ferric P420, with mainly 6C-LS heme iron in each case (Fig. 3.5 A).

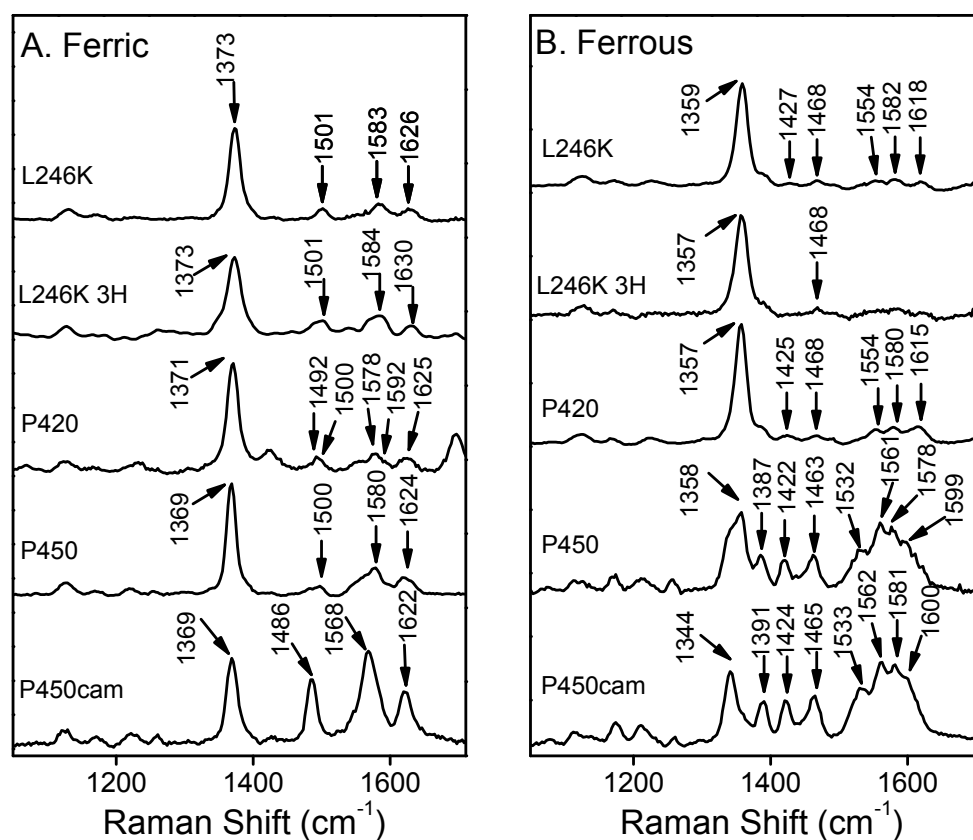


Figure 3.5 Resonance Raman spectra of (A) ferric and (B) ferrous wild-type P450 (in the presence and absence of 1mM camphor), P420, P450L246K mutant and P450L246K 3H mutant. The excitation wavelength (λ_{ex}) was 413.1nm.

The ν_4 band in the RR spectrum for 5C-Fe²⁺ heme complexes is a useful diagnostic marker of the identity of the proximal ligand. RR studies of a wide variety of heme proteins have shown that 5C-Fe²⁺ heme complexes with histidine (imidazole) as proximal ligand produce a ν_4 band in the 1350-1360 cm⁻¹ region whereas those with a cysteine (thiolate) proximal ligand display a ν_4 band in the 1340-1348 cm⁻¹ region (56, 57). The RR spectrum of ferrous P450cam shows a ν_4 band at 1344 cm⁻¹ that is consistent with thiolate proximal ligation (Fig. 3.5B). The ν_3 and ν_2 band at 1465 cm⁻¹ and 1562 cm⁻¹

confirm that the ferrous P450cam complex is 5C-HS. The RR spectrum of ferrous P420 also indicates a mainly 5C-HS complex but in contrast to P450cam the ν_4 band occurs at 1357 cm^{-1} , which is consistent with proximal histidine ligation (Fig. 3.5B). The RR spectra of ferrous L246K and L246K-3H mutants are almost identical to that of P420, thus ruling out the possibility that the high value for the position of the ν_4 band is associated with proximal histidine ligation in this case.

An alternative possibility is that for ferrous P420, L246K and L246K 3H mutants the proximal ligand is the protonated cysteine (neutral thiol) form (58). Assignment of the

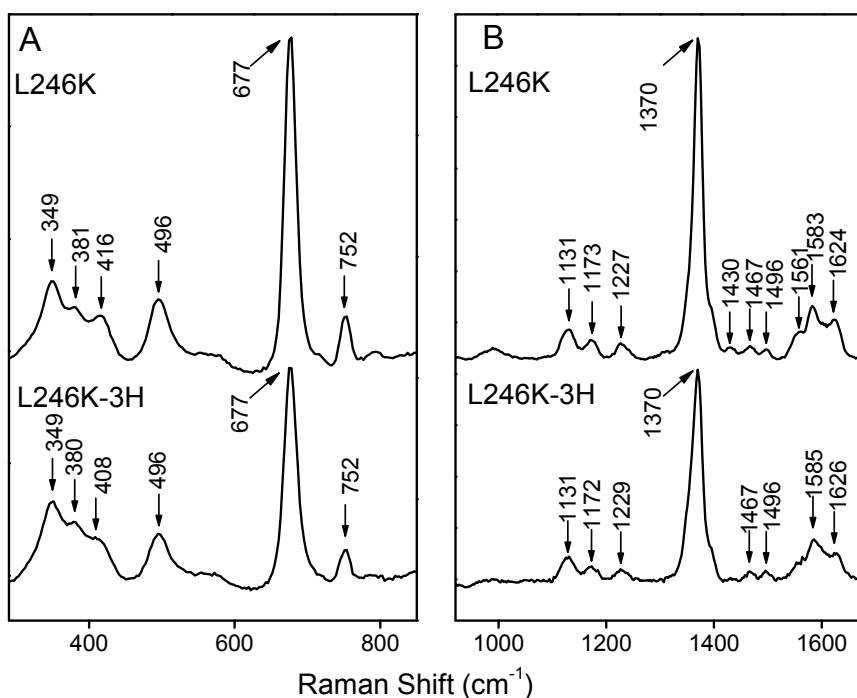


Figure 3.6 Resonance Raman spectra of Fe^{II} -CO complexes of P450camL246K and L246K-3H mutants in both low frequency region (A) and high frequency region (B).

Fe–CO and C–O stretching modes of the Fe^{II}–CO complexes is useful because they are influenced by the nature of proximal ligand and the polarity of the distal pocket environment (59, 60). The RR spectra of the Fe^{II}–CO complex of L246K mutant in the high-frequency region displayed a characteristic six-coordinate low-spin pattern, with peaks at around 1,370 cm⁻¹ (v4), 1,496 cm⁻¹ (v3), and 1,583 cm⁻¹ (v2) (Fig. 3.6 B). The L246K-3H showed almost identical six-coordinate features, indicating that it shared very similar heme environment with L246K. The $\nu_{\text{Fe-CO}}$ bands for both of them were both of them were seen at 496 cm⁻¹. Confirmation of these assignments was provided by the observed shifts in the presence of ¹³C¹⁸O (Fig. 3.7 A). In addition, $\nu_{\text{C-O}}$ for L246K was at approximately 1960 cm⁻¹ in the ¹²C¹⁶O–¹³C¹⁸O difference spectrum (Fig. 3.7 B). Relating the frequencies of $\nu_{\text{Fe-CO}}$ and $\nu_{\text{C-O}}$ can provide valuable information about the proximal

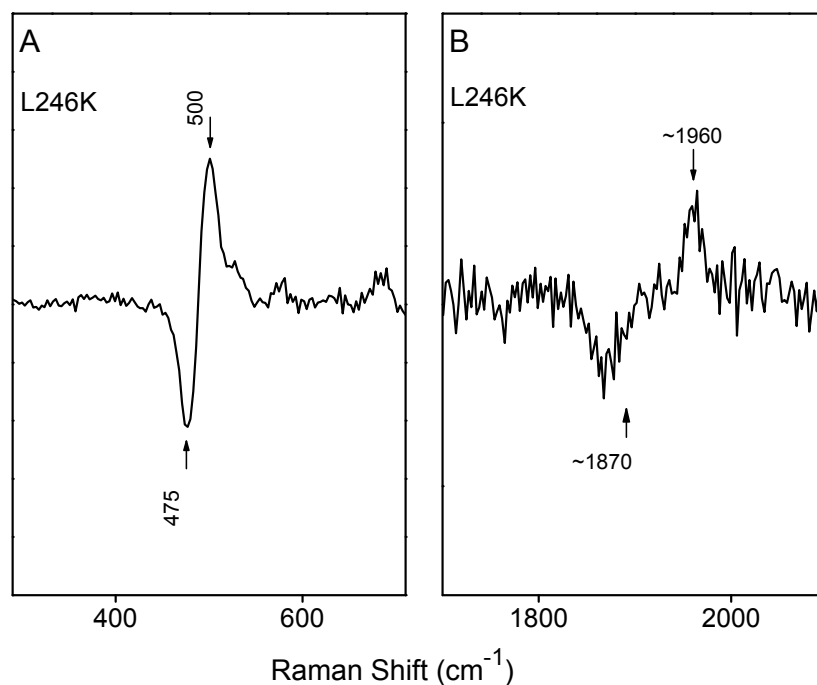


Figure 3.7 $\text{Fe}^{2+}\text{-CO} - \text{Fe}^{2+} - ^{13}\text{C}^{18}\text{O}$ difference spectra P450camL246K in both low frequency region (A) and high frequency region (B).

ligand identity and polarity of the distal environment of hemoproteins (61-63). Plots of $\nu_{\text{Fe-CO}}$ versus $\nu_{\text{C-O}}$ for a wide variety of heme-CO complexes are shown in Figure 3.8. The observed 500 and 1960 cm^{-1} pairing frequency for the CO complex of L246K mutant placed it in the region of histidine proximal ligand and a hydrophobic distal environment compared with myoglobin and peroxidases. Since the proximal histidine ligand has been ruled out in the L246K mutant, the RR results of the CO complex could be indicative of a protonated thiolate proximal ligation or an elongated iron-thiolate ligand.

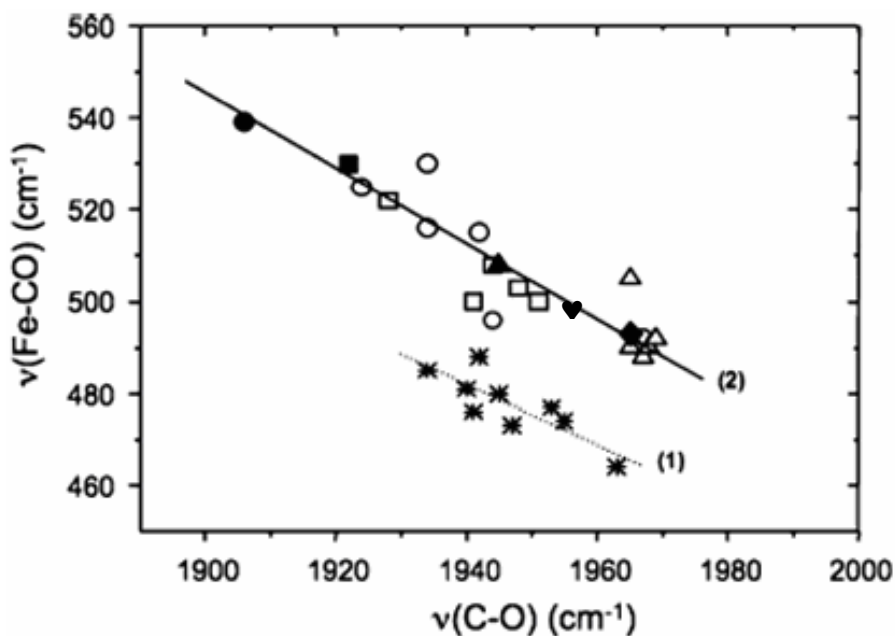


Figure 3.8 Correlation of Fe–CO and C–O stretching frequencies for different heme proteins and porphyrin derivatives. Lines 1 and 2 are for complexes in which the proximal ligand is thiolate and histidine, respectively. The open circles, open squares, and open triangles correspond to data are obtained for mutant and pH-variant forms of horseradish peroxidase (\circ), cytochrome c peroxidase (\square), and myoglobin (Δ), respectively. The corresponding filled symbols represent data are obtained from the wild-type proteins. The filled heart corresponds to P450L246K data measured in this work. This figure is adapted from (61-63).

3.4.4 Catalytic activity of P450L246K

While it still remains challenging to distinguish between a protonated neutral thiol and an elongated thiolate ligand in heme proteins that display abnormal spectroscopic properties, it is generally agreed that the deprotonation of the proximal cysteine to cysteinate that provides the necessary “push” effect throughout the reaction cycle is indispensable for the catalytic activity of all known heme thiolate proteins.(1, 7-9, 47, 64) Therefore, an activity assay should provide a convenient measure for the identification of

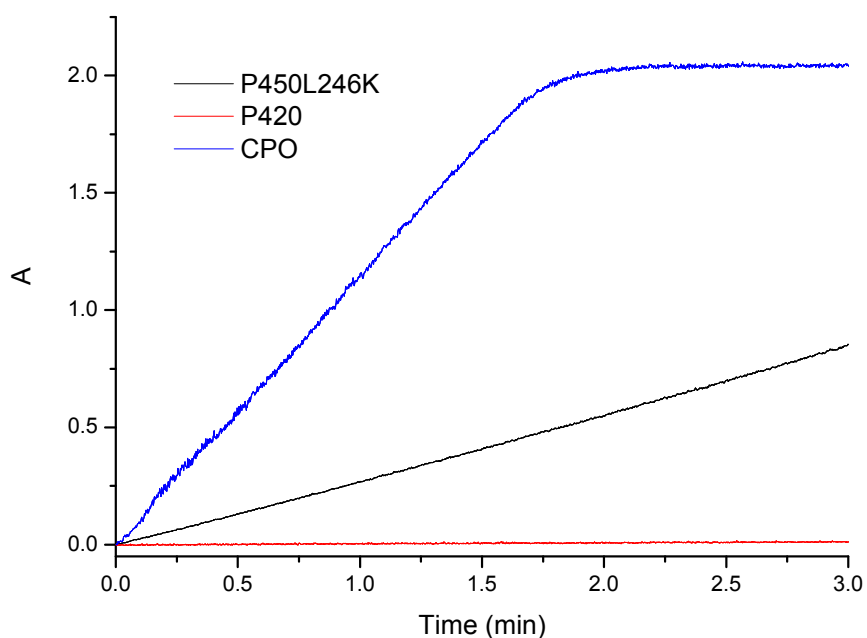


Figure 3.9 Peroxidase activity of P450camL246K mutant, P420 and CPO determined by monitoring the oxidation of ABTS at 405nm in the presence of H₂O₂ (3.3mM), ABTS (9.1mM), and enzyme (2μM).

the nature of the proximal ligand in these proteins. Although both P420 and L246K display essentially identical UV-vis spectral patterns, the proximal ligand to the heme iron may not necessarily be the same. The fact that P420 is devoid of any catalytic activity suggests a protonated cysteine as the proximal heme ligand in this inactivated form of P450. However, the ABTS assay of L246K has shown that the mutant is able to act as an efficient peroxygenase (Fig. 3.9), with comparable peroxidase activity with CPO, via the peroxide shunt pathway. That implies that a deprotonated cysteinate ligates weakly to the heme iron of the mutant with a lengthened Fe-S bond. The ability of L246K to oxidize ABTS, a standard peroxidase substrate, in the presence of H₂O₂ alone

strongly supports the importance of polarity of heme distal environment in regulating the chemistry of heme proteins as predicted by structural comparison of CPO and P450cam.

In conclusion, our study shows that it is possible to engineer P450cam into a self-sufficient biocatalyst by changing the polarity of the distal heme environment of the protein. Our results provide strong evidence that the inactivated form of P450 (P420) uses a protonated cysteine as its proximal heme iron ligand while L246K keeps the parent protein's thiolate ligand but with a longer Fe-S bond due to conformational changes induced by the mutation. It is therefore concluded that proteins with identical spectral signatures do not necessarily share the same heme environment.

3.5 REFERENCES

1. Ortiz de Montellano, P. R., (Ed.) (2005) *Cytochrome P450: Structure, Mechanism, and Biochemistry*, 3rd ed., Kluwer Academic/Plenum Publishers, New York.
2. Sono, M., Roach, M. P., Coulter, E. D., and Dawson, J. H. (1996) Heme-Containing Oxygenases, *Chem. Rev.* 96, 2841-2888.
3. Rabe, K., Gandubert, V., Spengler, M., Erkelenz, M., and Niemeyer, C. (2008) Engineering and assaying of cytochrome P450 biocatalysts, *Anal. Bioanal. Chem.* 392, 1059-1073.
4. Bernhardt, R. (2006) Cytochromes P450 as versatile biocatalysts, *J. Biotechnol.* 124, 128-145.
5. Poulos, T. L., Finzel, B. C., and Howard, A. J. (1987) High-Resolution Crystal-Structure of Cytochrome-P450cam, *Journal of Molecular Biology* 195, 687-700.

6. Sigel, A., Sigel, H., and Sigel, R. K.O. (2007) The ubiquitous roles of cytochrome P450 proteins in *Metal Ions in Life Sciences* (Sigel, A., Sigel, H., and Sigel, R. K.O. , Ed.), Wiley, Chichester.
7. Dawson, J. H., Holm, R. H., Trudell, J. R., Barth, G., Linder, R. E., Bunnenberg, E., Djerassi, C., and Tang, S. C. (1976) Magnetic circular dichroism studies. 43. Oxidized cytochrome P-450. Magnetic circular dichroism evidence for thiolate ligation in the substrate-bound form. Implications for the catalytic mechanism, *J. Am. Chem. Soc.* 98, 3707-3709.
8. Tarr, G. E., Black, S. D., Fujita, V. S., and Coon, M. J. (1983) Complete amino acid sequence and predicted membrane topology of phenobarbital-induced cytochrome P-450 (isozyme 2) from rabbit liver microsomes, *Proc. Natl. Acad. Sci. U. S. A.* 80, 6552-6556.
9. Poulos, T. L., Finzel, B. C., Gunsalus, I. C., Wagner, G. C., and Kraut, J. (1985) The 2.6-A crystal structure of *Pseudomonas putida* cytochrome P-450, *J. Biol. Chem.* 260, 16122-16130.
10. Sono, M. R., M. P.; Coulter, E. D.; and Dawson, J. H. (1996) Heme-Containing Oxygenases, *Chemical Reviews* 96, 2841-2847.
11. Behan, R. K., Stone, K. L., Hoffart, L. M., Krebs, C., and Green, M. T. (2006) Evidence for protonated ferryls in compound II of cytochromes P450, *J. Am. Chem. Soc.* 128, 11471-11474.
12. Dawson, J. H., and Sono, M. (1987) Cytochrome P-450 and Chloroperoxidase: Thiolate-Ligated Heme Enzymes. Spectroscopic Determination of Their Active Site Structures and Mechanistic Implications of Thiolate Ligation, *Chemical Reviews* 87, 1255-1276.
13. Dawson, J. H. (1988) Probing structure-function relations in hemecontaining oxygenases and preoxidases, *Science* 240, 433-439.
14. Katagiri, M., Ganguli, B. N., and Gunsalus, I. C. (1968) A Soluble Cytochrome P-450 Functional in Methylene Hydroxylation, *J. Biol. Chem.* 243, 3543-3546.
15. Omura, T., Sato, R. (1964) The Carbon Monoxide-binding Pigment of Liver Microsomes: I. EVIDENCE FOR ITS HEMOPROTEIN NATURE, *J. Biol. Chem.* 239, 2370-2378.

16. Yu, C.-A., Gunsalus, I. C. (1974) Cytochrome P-450cam: II. Interconversion with P-420, *J. Biol. Chem.* 249, 102-106.
17. Hui Bon Hoa, G., Di Primo, C., Dondaine, I., Sligar, S. G., Gunsalus, I. C., Douzou, P. (1989) Conformational Changes of Cytochromes P-450cam, and P-450lin Induced by High Pressure, *Biochemistry* 28, 651-656.
18. FISHER, M. T., SCARLATA, S. F., SLIGAR, S. G. (1985) High-Pressure investigations of Cytochrome P-450 Spin and Substrate Binding Equilibria, *Arch. Biochem. Biophys.* 240, 456-463.
19. Imai, Y., Sato, R. (1967) Conversion of P-450 to P-420 by Neutral Salts and some other Reagents, *Eur. J. Biochem.* 1, 419-426.
20. O'Keefe, D. H., Ebel, R. E., Peterson, J. A., Maxwell, J. C., Caughey, W. S. (1978) An infrared spectroscopic study of carbon monoxide bonding to ferrous cytochrome P-450, *Biochemistry* 17, 5845-5852.
21. Sundaramoorthy, M., Turner, J., and Poulos, T. L. (1995) The crystal structure of chloroperoxidase: A heme peroxidase-cytochrome P450 functional hybrid, *Structure* 3, 1367-1377.
22. Martinis, S. A., Blanke, S. R., Hager, L. P., Sligar, S. G., Hoa, G. H. B., Rux, J. J., and Dawson, J. H. (1996) Probing the heme iron coordination structure of pressure-induced cytochrome P420cam, *Biochemistry* 35, 14530-14536.
23. Hui Bon Hoa, G., Di Primo, C., Dondaine, I., Sligar, S. G., Gunsalus, I. C., and Douzou, P. (1989) Conformational changes of cytochromes P-450cam and P-450lin induced by high pressure, *Biochemistry* 28, 651-656.
24. Hui Bon Hoa, G., Di Primo, C., Geze, M., Douzou, P., Kornblatt, J. A., and Sligar, S. G. (1990) The formation of cytochrome P-450 from cytochrome P-420 is promoted by spermine, *Biochemistry* 29, 6810-6815.
25. Ichikawa, Y., and Yamano, T. (1967) Reconversion of detergent- and sulfhydryl reagent-produced P-420 to P-450 by polyols and glutathione, *Biochim. Biophys. Acta* 131, 490-497.
26. Stern, J. O., Peisach, J. J. (1974) A Model Compound Study of the CO-Adduct of Cytochrome P-450, *J. Biol. Chem.* 249, 7495-7498.

27. Sono, M., Stuehr, D. J., Ikeda-Saito, M., Dawson, J. H. (1995) Identification of Nitric Oxide Synthase as a Thiolate-ligated Heme Protein Using Magnetic Circular Dichroism Spectroscopy: COMPARISON WITH CYTOCHROME P-450-CAM AND CHLOROPEROXIDASE, *J. Biol. Chem.* 270, 19943-19948.
28. Dunford, A. J., McLean, K. J., Sabri, M., Seward, H. E., Heyes, D. J., Scrutton, N. S., Munro, A. W. . (2007) Rapid P450 Heme Iron Reduction by Laser Photoexcitation of Mycobacterium tuberculosis CYP121 and CYP51B1: ANALYSIS OF CO COMPLEXATION REACTIONS AND REVERSIBILITY OF THE P450/P420 EQUILIBRIUM, *J. Biol. Chem.* 282, 24816-24824.
29. Hui Bon Hoa, G., McLean, M. A., Sligar, S. G. (2002) High pressure, a tool for exploring heme protein active sites, *Biochim. Biophys. Acta* 1595, 297-308.
30. White, K. A., Marletta, M. A. (1992) Nitric oxide synthase is a cytochrome P-450 type hemoprotein, *Biochemistry* 31, 6627-6631.
31. Sabat, J., Stuehr, D. J., Yeh, S. R., and Rousseau, D. L. (2009) Characterization of the Proximal Ligand in the P420 Form of Inducible Nitric Oxide Synthase, *Journal of the American Chemical Society* 131, 12186-12192.
32. Blanke, S. R., Martinis, S. A., Sligar, S. G., Hager, L. P., Rux, J. J., Dawson, J. H. (1996) Probing the Heme Iron Coordination Structure of Alkaline Chloroperoxidase, *Biochemistry* 35, 14537-14543.
33. Hollengerg, P. F., Hager, L. P. (1973) The P450-nature of the carbon monoxide complex of ferrous chloroperoxidase, *J. Biol. Chem.* 248, 2630-2633.
34. Martinis, S. A., Blanke, S. R., Hager, L. P., Sligar, S. G., Hui Bon Hoa, G., Rux, J. J., and Dawson, J. H. (1996) Probing the Heme Iron Coordination Structure of Pressure-Induced Cytochrome P420cam, *Biochemistry* 35, 14530-14536.
35. Jiang, Y., Trnka, M. J., Medzihradsky, K. F., Ouellet, H., Wang, Y., and Ortiz de Montellano, P. R. (2009) Covalent heme attachment to the protein in human heme oxygenase-1 with selenocysteine replacing the His25 proximal iron ligand, *J. Inorg. Biochem.* 103, 316-325.

36. Vetter, S., Terentis, A., Osborne, R., Dawson, J., and Goodin, D. (2009) Replacement of the axial histidine heme ligand with cysteine in nitrophorin 1: spectroscopic and crystallographic characterization, *J. Biol. Inorg. Chem.* *14*, 179-191.
37. Dawson, J. H., Trudell, J. R., Linder, R. E., Barth, G., Bunnenberg, E., and Djerassi, C. (1978) Magnetic circular dichroism of purified forms of rabbit liver cytochromes P-450 and P-420, *Biochemistry* *17*, 33-42.
38. Wells, A. V., Li, P., Champion, P. M., Martinis, S. A., and Sligar, S. G. (1992) Resonance Raman investigations of Escherichia coli-expressed Pseudomonas putida cytochrome P450 and P420, *Biochemistry* *31*, 4384-4393.
39. Perera, R., Sono, M., Sigman, J. A., Pfister, T. D., Lu, Y., and Dawson, J. H. (2003) Neutral thiol as a proximal ligand to ferrous heme iron: Implications for heme proteins that lose cysteine thiolate ligation on reduction, *Proc. Natl. Acad. Sci. U. S. A.* *100*, 3641-3646.
40. Hanson, L. K., Eaton, W. A., Sligar, S. G., Gunsalus, I. C., Gouterman, M., and Connell, C. R. (1976) Origin of the anomalous Soret spectra of carboxycytochrome P-450, *J. Am. Chem. Soc.* *98*, 2672-2674.
41. Jung, C. (1985) Quantum chemical explanation of the "hyper" spectrum of the carbon monoxide complex of cytochrome P-450, *Chem. Phys. Lett.* *113*, 589-596.
42. Liu, Y., Moenne-Loccoz, P., Hildebrand, D. P., Wilks, A., Loehr, T. M., Mauk, A. G., and Ortiz de Montellano, P. R. (1999) Replacement of the Proximal Histidine Iron Ligand by a Cysteine or Tyrosine Converts Heme Oxygenase to an Oxidase, *Biochemistry* *38*, 3733-3743.
43. Wagner, G. C., Perez, M., Toscano, W. A. Jr., and Gunsalus, I. C. (1981) Apoprotein Formation and Heme Reconstitution of Cytochrome P-450cam, *J. Biol. Chem.* *256*, 6262-6265.
44. Dawson, J. H., Andersson, L. A., and Sono, M. (1982) Spectroscopic investigations of ferric cytochrome P-450-CAM ligand complexes. Identification of the ligand trans to cysteinate in the native enzyme, *J. Biol. Chem.* *257*, 3606-3617.

45. Omura, T. (2005) Heme-thiolate proteins, *Biochem. Biophys. Res. Commun.* 338, 404-409.
46. Collman, J. P., Sorrell, T. N., Dawson, J. H., Trudell, J. R., Bunnenberg, E., and Djerassi, C. (1976) Magnetic circular dichroism of ferrous carbonyl adducts of cytochromes P-450 and P-420 and their synthetic models: further evidence for mercaptide as the fifth ligand to iron, *Proc. Natl. Acad. Sci. U. S. A.* 73, 6-10.
47. Sabat, J., Stuehr, D. J., Yeh, S.-R., and Rousseau, D. L. (2009) Characterization of the Proximal Ligand in the P420 Form of Inducible Nitric Oxide Synthase, *J. Am. Chem. Soc.* 131, 12186-12192.
48. Andersson, L. A., Mylrajan, M., Sullivan, E. P., and Strauss, S. H. (1989) Modeling low-pH hemoproteins, *J. Biol. Chem.* 264, 19099-19102.
49. Hu, S. Z., Morris, I. K., Singh, J. P., Smith, K. M., and Spiro, T. G. (1993) Complete Assignment of Cytochrome-C Resonance Raman-Spectra Via Enzymatic Reconstitution with Isotopically Labeled Hemes, *J. Am. Chem. Soc.* 115, 12446-12458.
50. Hu, S. Z., Smith, K. M. and Spiro, T. G. . (1996) Assignment of protoheme Resonance Raman spectrum by heme labeling in myoglobin, *J. Am. Chem. Soc.* 118, 12638-12646.
51. Andersson, L. A., Mylrajan, M., Sullivan, E. P., Jr., and Strauss, S. H. (1989) Modeling low-pH hemoproteins, *J Biol Chem* 264, 19099-19102.
52. Lou, B. S., Snyder, J. K., Marshall, P., Wang, J. S., Wu, G., Kulmacz, R. J., Tsai, A. L., and Wang, J. (2000) Resonance Raman studies indicate a unique heme active site in prostaglandin H synthase, *Biochemistry* 39, 12424-12434.
53. Spiro, T. G., Stong, J. D., and Stein, P. (1979) Porphyrin Core Expansion and Doming in Heme-Proteins - New Evidence from Resonance Raman-Spectra of 6-Coordinate High-Spin Iron(III) Hemes, *Journal of the American Chemical Society* 101, 2648-2655.
54. Wells, A. V., Li, P., Champion, P. M., Martinis, S. A., and Sligar, S. G. (1992) Resonance Raman investigations of Escherichia coli-expressed Pseudomonas putida cytochrome P450 and P420, *Biochemistry* 31, 4384-4393.

55. Champion, P. M., Gunsalus, I. C., and Wagner, G. C. (1978) Resonance Raman Investigations of Cytochrome P450cam from *Pseudomonas-Putida*, *Journal of the American Chemical Society* 100, 3743-3751.
56. Anzenbacher, P., Evangelista-Kirkup, R., Schenkman, J., and Spiro, T. G. (1989) Influence of thiolate ligation on the heme electronic structure in microsomal cytochrome P-450 and model compounds: resonance Raman spectroscopic evidence, *Inorg. Chem. FIELD Full Journal Title:Inorganic Chemistry* 28, 4491-4495.
57. Wang, J., Caughey, W. S., and Rousseau, D. L. (1996) Resonance Raman Scattering: a Probe of Heme Protein-bound Nitric Oxide, in *Methods in Nitric Oxide Research* (Feelisch, M., and Stamler, J., Eds.), pp 427-454, J. Wiley, Chichester ; New York.
58. Perera, R., Sono, M., Sigman, J. A., Pfister, T. D., Lu, Y., and Dawson, J. H. (2003) Neutral thiol as a proximal ligand to ferrous heme iron: implications for heme proteins that lose cysteine thiolate ligation on reduction, *Proc Natl Acad Sci U S A* 100, 3641-3646.
59. Spiro, T. G., Kozlowski, P. (2001) *Acc. Chem. Res.* 34, 137-144.
60. Vogel, K. M., Kozlowski, P.M., Zgierski, M.Z., Spiro T.G. (2000) *Inorg. Chim. Acta.* 297, 11-17.
61. Li, T., Quillin, M.L., Phillips, G.N., Olson, J.S. (1994) Structural Determinants of the Stretching Frequency of CO Bound to Myoglobin, *Biochemistry* 33, 1433-1446.
62. Feis, A., Rodriguez-Lopez, J.N., Thorneley, R.N.F., Smulevich, G. (1998) The Distal Cavity Structure of Carbonyl Horseradish Peroxidase As Probed by the Resonance Raman Spectra of His 42 Leu and Arg 38 Leu Mutants, *Biochemistry* 37, 13575-13581.
63. Terentis, A. C., Thomas, S. R., Takikawa, O., Littlejohn, T. K., Truscott, R. J. W., Armstrong, R. S., Yeh, S. R., and Stocker, R. (2002) The heme environment of recombinant human indoleamine 2,3-dioxygenase - Structural properties and substrate-ligand interactions, *Journal of Biological Chemistry* 277, 15788-15794.

64. Schlichting, I., Berendzen, J., Chu, K., Stock, A. M., Maves, S. A., Benson, D. E., Sweet, R. M., Ringe, D., Petsko, G. A., and Sligar, S. G. (2000) The Catalytic Pathway of Cytochrome P450cam at Atomic Resolution, *Science* 287, 1615-1622.

CHAPTER IV. SPECTROSCOPIC STUDY OF A NOVEL HEME IRON LIGAND SET IN ENGINEERED CYTOCHROME P450CAM

4.1 SUMMARY

Substitution of glycine-248, the distal residue closest to the heme iron of cytochrome P450cam, with a histidine leads to the formation of a mutant protein with a novel Cys-Fe-His ligand set. This is one of the rarest cases of His ligation in heme-thiolate proteins, and represents the first example observed for P450cam. The G248H mutant shows very unique electronic absorption properties. The ferric form of G248H displays a characteristic Soret band at 425 nm, while its ferrous-CO complex shows the distinctive absorption maximum at approximately 450 nm indicative of the intact Cys thiolate ligation. Surprisingly, this mutant does not bind any substrates or exogenous ligands and is inert toward pH changes, suggesting the replacement of the distal water molecule with the introduced His residue as the endogenous ligand. Resonance Raman and circular dichroism spectroscopy results also support this model. The spectrum of the ferric form of G248H displayed a six-coordinate low spin pattern. The spectrum of ferrous mutant showed a mixture of six-coordinate low spin and five-coordinate high spin, indicating that the distal His-Fe bond is weakened in the ferrous form. The results have also provided evidence about the nature of proximal

ligation of the P420 species, in which the nearby histidine is not a possible alternative for the heme iron ligand.

4.2 INTRODUCTION

Cytochromes P450, a superfamily of heme *b*-containing monooxygenases distributed in all domains of life, are involved in a wide range of physiologically and biotechnologically significant transformations, including steroid synthesis, drug metabolism, xenobiotic detoxification, and molecular signaling (1-4). The P450 enzymes typically activate dioxygen and insert one oxygen atom into a wide variety of organic substrates. The catalytic versatility makes these enzymes of great interest to the biochemical and potentially industrial applications. The most distinctive structural feature of cytochromes P450 is the coordination of a deprotonated cysteine to the heme iron as the proximal ligand, while many other hemoproteins possess a histidine at the proximal side. The strong electron-releasing character of the thiolate ligand has been reported to serve as the “push” effect to facilitate the heterolytic O-O bond cleavage to generate the activated intermediate Cpd I (iron-(IV)-oxo species) (5). With a few exceptions, the diverse reactions catalyzed by P450s all requires an external source of reducing equivalents like NAD(P)H and auxiliary proteins to transfer electrons to P450. The requirement of expensive cofactors and the complication caused by additional proteins is the limitation to the application of P450s as oxygenases. Some P450s are capable of

accepting hydrogen peroxide or organic peroxy compound as an oxidant to catalyze oxygen insertion through the so-called “peroxide-shunt” pathway in the absence of electron transport proteins and the NAD(P)H cofactor (6-11). However, P450s are typically not efficient in their utilization of hydrogen peroxide, the natural substrate for peroxidases, as the source of oxygen atom in the monooxygenation reactions.

Cytochrome P450cam from *Pseudomonas putida* is one of the most well studied members in the superfamily which catalyzes the region- and stereospecific hydroxylation of its natural substrate *d*-camphor to 5-exo-hydroxy-camphor (12). A great deal of effort has been made to suitably engineer this enzyme by directed evolution and active site modification for the oxygenation of significant unnatural substrates. It is still quite important to understand the roles of the active-site components in the reactivity, stability, specificity and substrate recognition of this enzyme after its discovery for over 50 years.

To explore the possibility of converting the cytochrome P450cam into an efficient self-sufficient heme peroxidase, we attempted to modify the heme distal side elements which play crucial mechanistic roles and regulate the enzyme functions. In most heme peroxidases, the distal histidine is highly conserved in the active site and has been considered to serve as a general acid-base catalyst necessary for the formation of Cpd I by donating a proton to the Fe^{3+} -OOH moiety to promote the heterolytic cleavage of the O-O bond in the peroxidase reaction cycles (13-16). It has been proposed that a functional nitrogen (such as the nitrogen of His42 in HRP and His52 in CcP), located at a

suitable distance from the heme iron, could behave as an acid-base catalyst in hemoproteins (13, 17).

Therefore, in order to probe the roles of the nonpolar amino acids in the distal helix and to make an efficient peroxxygenase, we tried to substitute a distal residue with a hydrophilic histidine. Given the proximity of the Gly248 residue to the heme group in P450cam, it is a rational to choose this residue as the target for our purpose (Fig. 4.1). The Gly248 residue, serving as a hydrogen bond partner with the side chain of Thr252 and resulting in an I-helix kink (18, 19), is conserved as a small residue (Gly or Ala) in many P450s. In the previous study of P450 variants with the Gly or Ala substituted by a carboxylate residue (Glu), the carboxylate group was reported to coordinate with the heme iron, resulting in a six-coordinate ferric resting state in both P450cam and P450BM3 (20-22). Thus, Gly248 in P450cam has been chosen as a good candidate to explore the consequences of functional alteration of the heme distal pocket on P450 structure and catalysis. Surprisingly, the results of the G248H variant did not show any catalytic activities at all because of the novel ligate set generated with the mutation. It is demonstrated to contain a similar heme coordination with the P450BM3 A264H mutant that was reported to possess a unique Cys-Fe-His heme ligand set (23). However, the G248H mutant of P450cam was rather different from its parallel model in the P450BM3 variant, especially the heme coordination in its ferrous and ferrous-CO complexes. It is shown for the first time that thiolate ligation remains intact without being displaced by

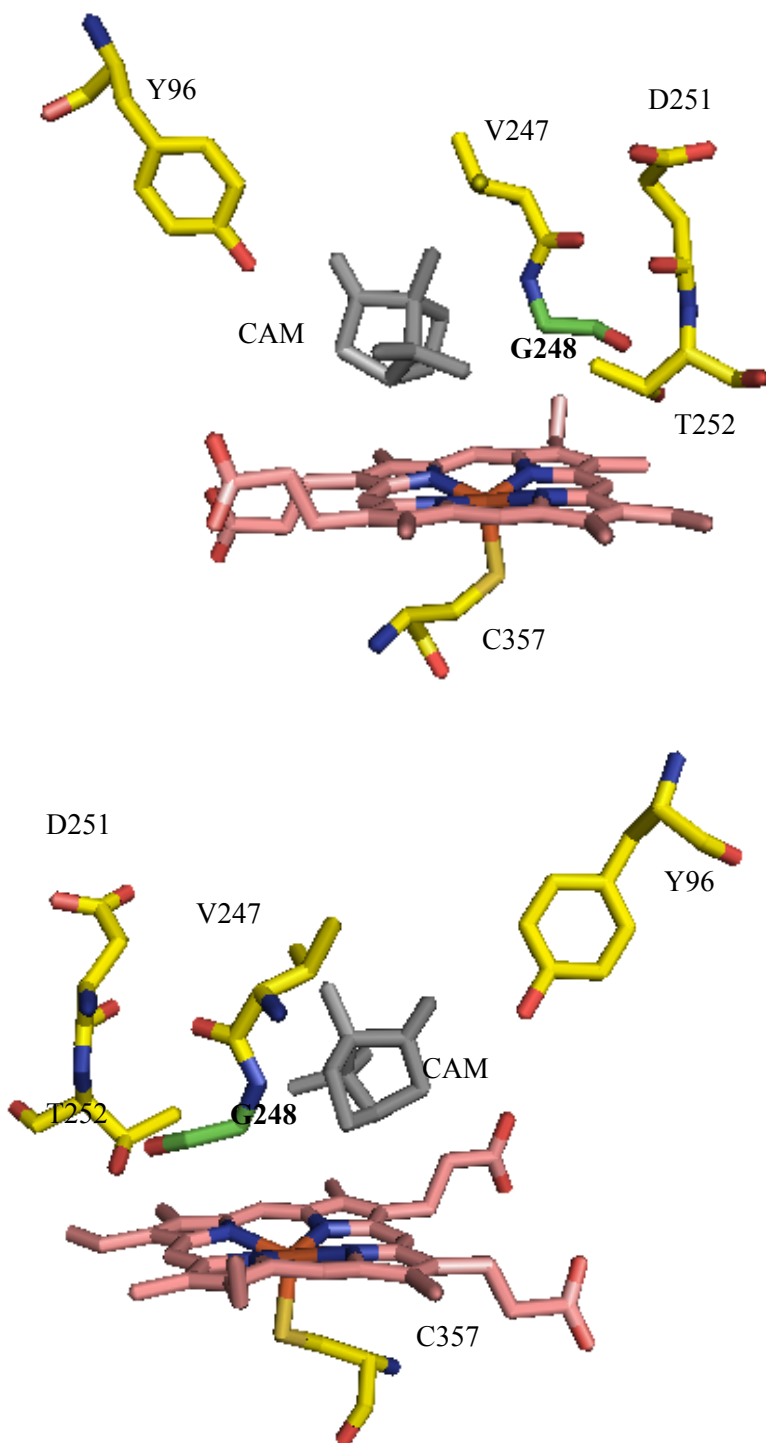


Figure 4.1 The active site structure of camphor-bound cytochrome P450cam showing the position of some important residues including G248. The figures were generated from the crystal data (PDB code 2CPP) using PYMOL (18).

another coordination group or deprotonated in various oxidation states either in modified heme-thiolate proteins or in other hemoproteins with engineered proximal thiolate ligation.

In this study various spectroscopic methods, such as electronic absorption, resonance Raman, and circular dichroism have been applied to investigate the heme coordination and ligation state of the heme active site in the G248H mutant. It has always been difficult to identify a ligand *trans* to thiolate in the absence of structural detail, but here we successfully presented sufficient spectroscopic results that identify axial ligand *trans* to the cysteinate in this distinctive mutant of P450cam.

4.3 EXPERIMENTAL PROCEDURES

4.3.1 Site-directed Mutagenesis

Site-directed mutagenesis was performed by using this T7-based expression vector, pET-30a (+). The G248H mutant of P450_{cam} was prepared with the 5'-sense oligonucleotide 5'- TTA CTG GTC CAT GGC CTG GAT ACG-3' coding for **LLVHGLDT**. The reconstituted plasmids of both wild type and G248H mutant were transformed into *E. coli* strain NovaBlue and verified by DNA sequencing.

4.3.2 Protein Expression and Purification

The wild type P450cam and mutant G248H were expressed in *Escherichia coli* strain Rosetta II (DE3). Cells were grown on terrific broth supplemented with 100mg/L

of kanamycin at 37 °C and induced with 1mM IPTG and 1 mM camphor at OD₆₀₀ around 0.8, followed by further growth at 30 °C for another 18 h prior to harvesting cells. As for the mutant, the addition of δ -aminolevulinic acid to the growth media is necessitated to facilitate holoenzyme production.

Cells were then lysed at 4 °C in 50 mM Tris-HCl buffer at pH 7.4 containing 50 mM KCl, 0.5 mM DTT, 1 mM camphor (buffer A), 1 mM EDTA, 200 μ M PMSF, 40 U/ml Dnase I, 3 U/ml Rnase A, and lysozyme. Following sonication and centrifugation, the lysed cells were concentrated by Amicon cell with 30,000 Da cut-off ultrafiltration membrane. The protein solution was applied on a fast flow DEAE Sepharose column (50ml) equilibrated with buffer A. After initial elution, the column was developed with a linear 0-0.5 M KCl gradient in the same buffer. The red fractions containing the ~45 kDa proteins were pooled for further purification by size exclusion chromatography. Sephadex G-75 matrix (500 ml) was used for the gel filtration and the buffer applied was 100 mM potassium phosphate buffer containing 1 mM camphor at pH 7.4. Substrate-free WTP450cam and its mutant were prepared in the same way except for no camphor was added during the expression and purification procedures. Unless otherwise specified, all the steps in the protein purification were performed at 4 °C.

4.3.3 Spectroscopic characterization

Optical characterization of the wild type P450_{cam} and its mutant was performed at room temperature on a Cary 300 spectrophotometer (Varian). The ferrous proteins were prepared by the addition of excess amount of sodium dithionite and CO adducts were

obtained by CO gas bubbling. The buffer used for the absorption measurements was 100 mM potassium phosphate buffer with 1 mM camphor at pH 7.4.

CD spectra were measured on a JASCO J-815 spectrometer at room temperature. The secondary-structure region (200-260 nm) of the spectra was recorded in a quartz cuvette of 1 mm path length using about 2 μ M enzyme. As for the tertiary-structure region (260-650 nm), they were recorded using about 20 μ M enzyme in a quartz cuvette of 1 cm path length with and without camphor.

For the resonance Raman data collection, the wild-type P450 and G248H mutant samples (about 30 μ M) were prepared in a septum-sealed, cylindrical quartz cell. Samples were reduced to the ferrous form by first flushing the sample with argon and then injecting a molar excess of buffered sodium dithionite solution. The rotating sample cell was irradiated with 4 mW of 413.1 nm laser light using a mixed krypton/argon ion laser (Spectra Physics, Beamlok 2060). The spectral acquisition time was 5 min. The scattered light was collected at right angles to the incident beam and focused onto the entrance slit (125 μ m) of a 0.8 m spectrograph, where it was dispersed by a 600 groove/mm grating and detected by a liquid-N₂-cooled CCD camera (Horiba-JY). Spectral calibration was performed against the lines of mercury. UV-vis spectra of each sample were collected before and after each RR measurement to ensure the sample integrity.

4.3.4 Redox potential measurements

The electrochemical measurements of the G248H mutant were performed with a CHI 660 electrochemical analyzer (CH Instruments) at room temperature by using a conventional three electrode cell, with a glassy carbon (GC) electrode as the working electrode, platinum wire as counter electrode and Ag/AgCl electrode as the reference electrode. The carbon electrode has been modified with single-walled carbon nanotubes (SWCNT). The SWCNT modified electrode is electrochemically activated by cyclical scanning between -1.0 and +1.5 V at a scan rate of 1 V/sec for 2 minutes to improve the sensitivity of the electrode. The redox potentials of P450cam G248H mutant was obtained and normalized with the reference to NHE.

4.4 RESULTS

4.4.1 Protein expression and purification

The G248H mutant of P450cam was expressed as a holoprotein with the facilitation of heme precursor. The R_z values of pure wild-type P450cam and G248H mutant were both over 1.4. The protein concentration was determined using the Soret extinction coefficient determined by the *pyridine hemochrome method* following the standard protocol (24, 25). The extinction coefficients for camphor-bound and camphor-free forms of the mutant were found to be 113 and 125 $\text{mM}^{-1}\text{cm}^{-1}$, respectively, comparing with 102 and 115 $\text{mM}^{-1}\text{cm}^{-1}$ of the wild type protein.

4.4.2 UV-vis spectroscopy

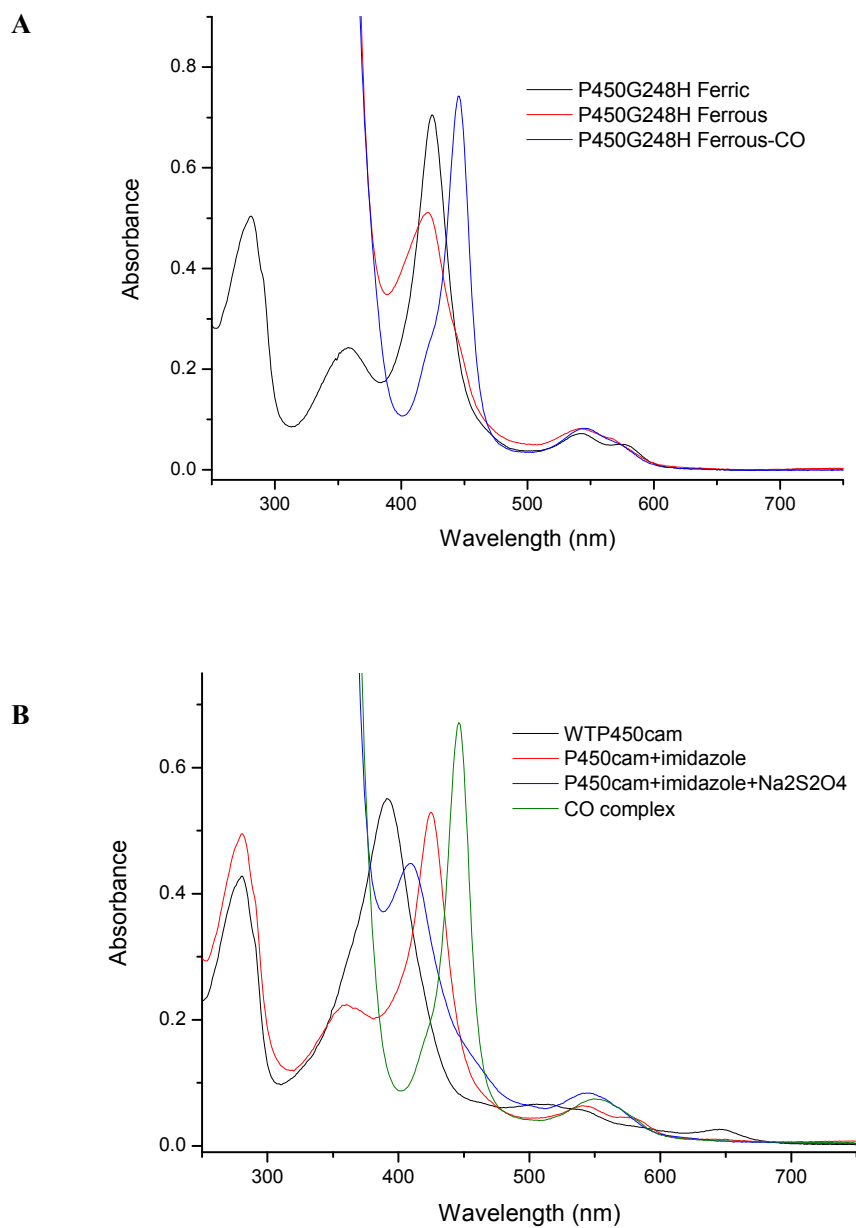


Figure 4.2 UV-vis spectra of ferric, ferrous and ferrous-CO complexes of P450camG248H: (A) camphor-free; (B) camphor-bound in 100mM phosphate buffer (pH7.4) at room temperature.

The UV-vis spectra of wild type P450cam and G248H mutant were recorded in all ferric, ferrous and ferrous carbon monoxide bound forms (Table 4.1). In contrast to the substrate-free wild type protein in its oxidized state that has the Soret maximum at 417 nm, the G248H mutant exhibited a Soret band at 425 nm, red shifted by 8 nm (Fig. 4.2). Notably, the ferric form of the mutant displayed an almost identical spectral pattern with that of the wild type protein complexed with imidazole (26) and that of the P450BM3 A264H mutant (23), indicating that the substitution of the Gly248 with a histidine residue similar to those proteins in these proteins. Furthermore, the UV-vis spectrum of ferric P450camG248H did not show any change upon any ligand or substrate binding, and is independent of pH change as well. However, the ferrous form of the mutant was quite different from the wild type and its imidazole complex. Instead of showing the Soret band at around 408nm upon reduction, the G248H mutant had its Soret band maximum at 421 nm. The ferrous-CO complex of the G248H mutant retained the characteristic Soret band at around 450nm like the wild type P450cam, which suggested that despite the introduction of a sterically larger group and also a stronger ligand, the thiolate ligation to the heme iron in the proximal side was preserved.

Another distinct UV-vis spectral difference between the mutant and wild type lies in the spectra of their camphor-bound forms. In wild type P450cam, the Soret band shifts from 417 nm to 392 nm upon substrate binding, indicating the conversion of low-spin to high-spin Fe (III). But the camphor binding was perturbed in the mutant since there was

no detectable change in its camphor-bound form. Thus, in the presence of camphor, the G248H mutant remained predominantly in the six-coordinate low-spin Fe (III) state.

Table 4.1 Wavelength and extinction coefficients of absorption maxima for wild type and G248H mutant of cytochrome P450cam

Protein	Oxidation state	Soret (nm)	δ -band (nm)	Visible (nm)
WTP450 (camphor-free)	Fe ³⁺	418 (ϵ =115)	360	535, 569
	Fe ²⁺	408		540
	Fe ²⁺ -CO	446		550
WTP450 + Imidazole (26)	Fe ³⁺	425 (ϵ =98)	360	541, 578
	Fe ²⁺	409		543
	Fe ²⁺ -CO	446		549
G248H (camphor-free)	Fe ³⁺	425 (ϵ =123)	359	542, 573
	Fe ²⁺	421		541, 568
	Fe ²⁺ -CO	446		545
G248H (camphor-bound)	Fe ³⁺	424 (ϵ =122)	359	542, 574
	Fe ²⁺	421		542, 569
	Fe ²⁺ -CO	446		546

4.4.3 Resonance Raman Spectroscopy

To further examine its heme environment and the iron spin and ligation state, we obtained RR spectra in various oxidation and coordination states of wild type and G248H mutant in the absence and presence of substrate camphor. The RR spectrum of ferric G248H with no camphor bound was very similar with to that of the wild type, displaying a strong oxidation state marker band ν_4 at around 1370 cm^{-1} that is typical of ferric (Fe^{3+}) heme (Fig. 4.3 A). The heme core-size marker bands ν_3 and ν_2 appeared at approximately 1500 and 1580 cm^{-1} , respectively for both camphor-free samples, indicating a six-coordinate (6C), low-spin (LS) heme iron (27-29). However for the camphor-bound proteins, the G248H mutant was markedly different from the wild type. The wild type displayed the ν_3 and ν_2 bands at 1486 cm^{-1} and 1568 cm^{-1} , respectively, typical of high-spin, five-coordinate (5C), heme iron component. On the contrary, the camphor-bound G248H was demonstrated to be a six-coordinate low-spin complex, as indicated by the appearance of the ν_3 and ν_2 bands at 1500 and 1586 cm^{-1} , almost identical to the camphor-free samples. This could be the result of an unusual axial ligation of the heme iron in the G248H mutant.

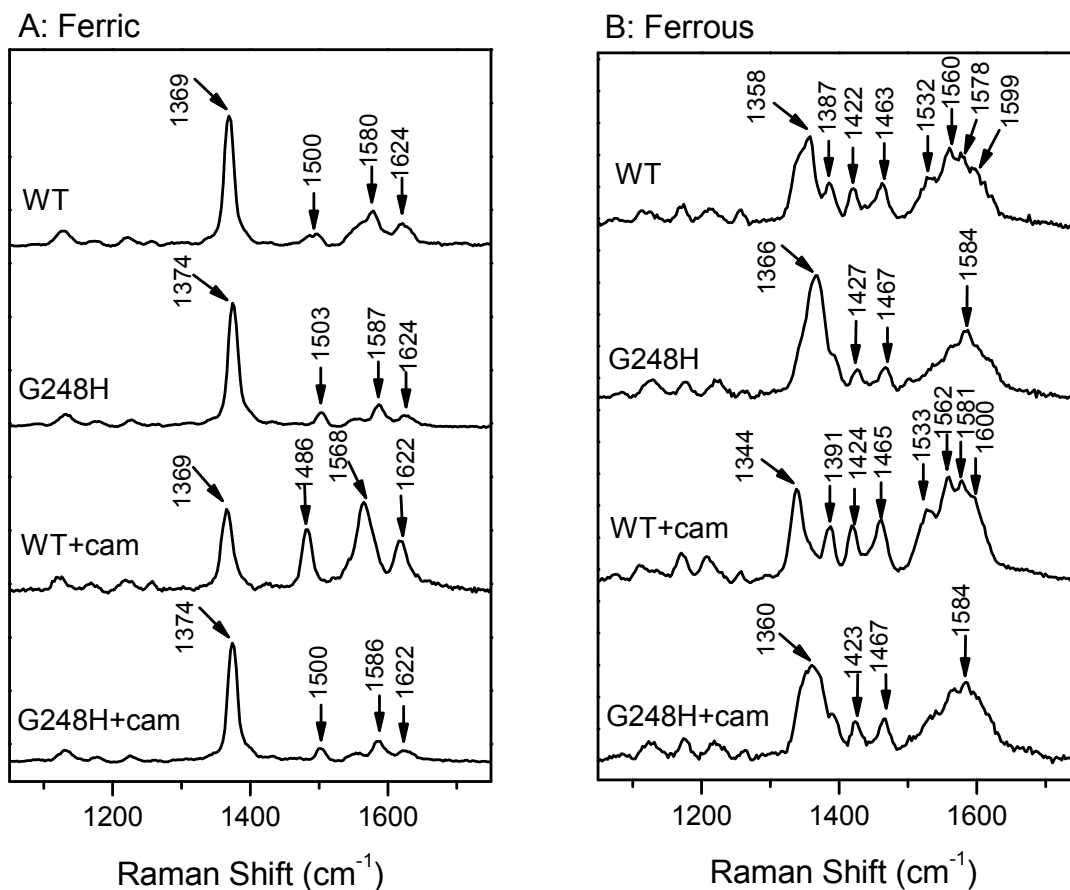


Figure 4.3 Resonance Raman spectra of (A) ferric and (B) ferrous wild-type P450 and P450G248H mutant with and without camphor binding. The excitation wavelength (λ_{ex}) was 413.1nm. The spectra of P450 and G248H samples in the presence and absence of 1mM camphor are shown.

In the ferrous form, the mutant also showed rather different spectral pattern from that of the wild type in the absence and presence of camphor. The RR spectrum of the camphor-free ferrous G248H had a significantly broadened ν_4 band at 1366 cm^{-1} that implied a six-coordinate complex and rather different from the wild type (Fig. 4.3 B).

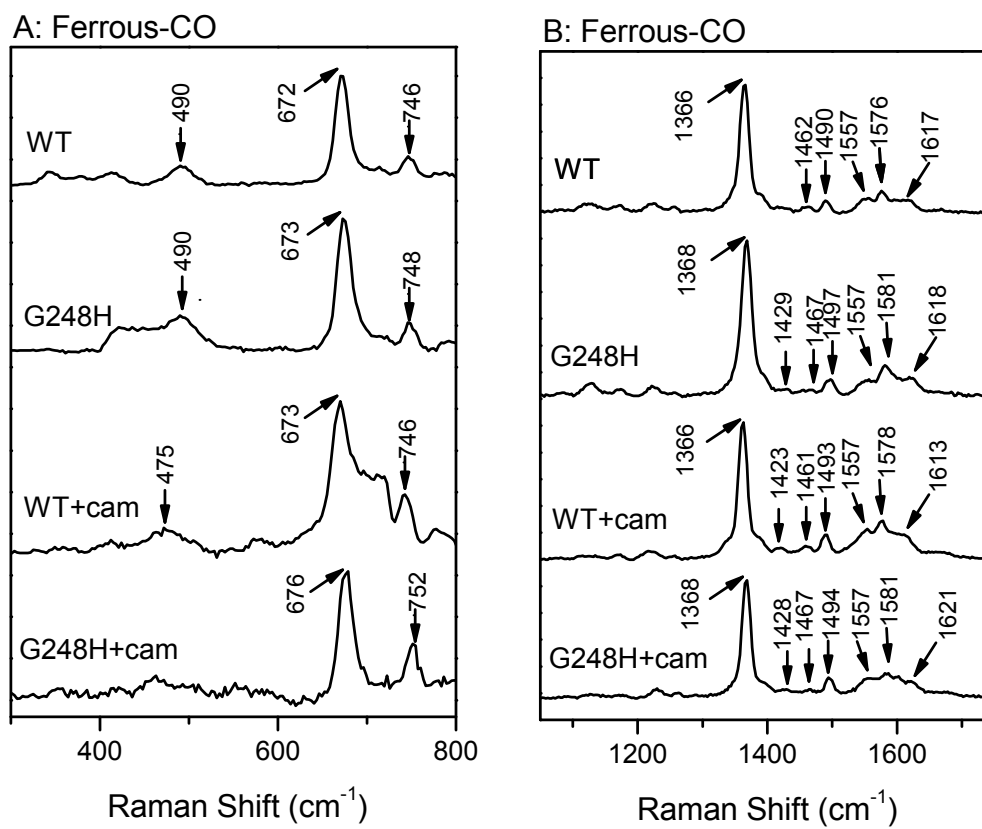


Figure 4.4 Resonance Raman spectra of ferrous-CO complexes of wild-type P450 and P450G248H mutant with and without camphor binding in both low frequency (A) and high frequency (B). The excitation wavelength (λ_{ex}) was 413.1nm. The spectra of P450 and G248H samples in the presence and absence of 1mM camphor are shown.

Typically the ν_4 band appears slightly higher ($\sim 1370 \text{ cm}^{-1}$) for six-coordinate ferrous complexes (e.g., CO and NO complexes), which suggested that in the case of G248H the sixth ligand was bonded rather weakly to the heme iron. Consistent with this, a very weak shoulder on the low frequency edge of the ν_4 band could be seen in the G248H RR spectrum that was the result of a small population of the five-coordinate thiolate complex. Compared with the camphor free protein, the camphor-bound mutant demonstrated a

similar spectral pattern except for the ν_4 band which shifted from 1366cm^{-1} to 1360cm^{-1} , possibly due to the interference of camphor in the His binding to the heme iron in some way.

Assignment of the Fe–CO and C–O stretching modes of the Fe^{II} –CO complexes is useful because they are influenced by the nature of proximal ligand (30, 31). The RR spectra of the Fe^{II} –CO complexes of the wild type and G248H mutant in the high-frequency region displayed a characteristic six-coordinate low-spin pattern, with peaks at about 1368 cm^{-1} (ν_4), 1495 cm^{-1} (ν_3), and 1580 cm^{-1} (ν_2), respectively (Fig. 4.4 B). The $\nu_{\text{Fe-CO}}$ bands showed some difference between the camphor-free and camphor-bound proteins. Especially for G248H with camphor, the CO stretch at around 500 cm^{-1} was missing which was possibly due to the preventive interference of the His ligand in the distal site, suggesting CO could only partially bind to the ferrous heme iron and there was still some portion of histidine ligated to the iron.

4.4.4 Circular dichroism spectroscopy

To investigate the effect of the mutation on the conformational change of the protein, multi-wavelength CD studies of the wild type and G248H mutant of P450cam were carried out. The far-UV CD spectra (190-260 nm) for both substrate-free and substrate-bound forms of G248H mutant heme domain exhibited no obvious change compared with that of the wild type, with minima at 219 and 209 nm respectively, indicating the secondary structure was not significantly altered by the substitution of

G248 with a histidine. Neither did the addition of camphor have any effect on the secondary structure of the protein in the predominantly α -helical heme domain.

However, in the near-UV-visible CD region (300-650 nm), the G248H mutant showed rather different spectra in its resting ferric form from that of the wild type. Furthermore, the substrate free and substrate bound forms of the mutant were markedly distinct from each other. In the absence of camphor, the Soret and δ bands in the heme CD spectrum of wild type P450cam appeared at 410 and 353 nm in negative ellipticity (Fig. 4.5A). The Soret band shifted to 388nm upon substrate binding, with the δ band disappearing (Fig. 4.5 B). Thus, the blue shift of the Soret band of P450cam mimicked the optical transition in the UV-vis spectrum to some extent. However, the near-UV-visible CD spectrum of the substrate-free G248H heme domain has its Soret band at 423 nm and the addition of substrate camphor triggered dramatic change in the Soret band, resulting in split peaks at 405 and 436 nm, respectively. This feature of the substrate-bound G248H mutant was more significantly different than that of the optical absorption spectra.

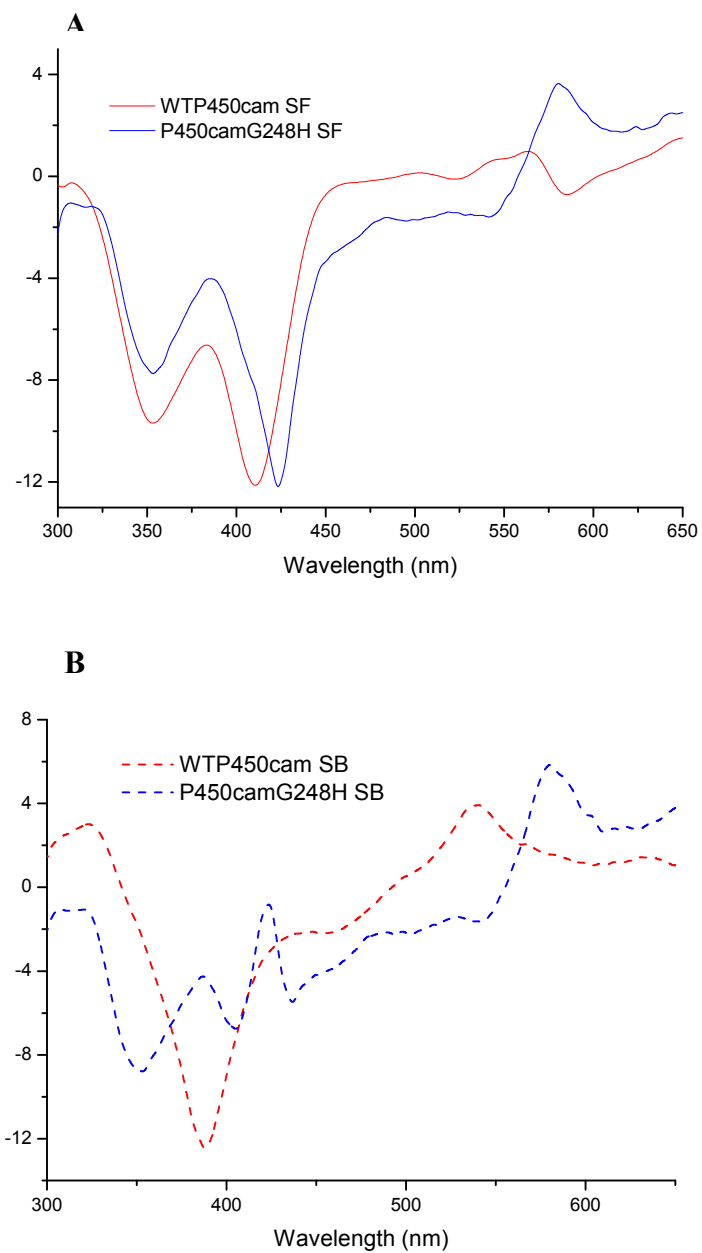


Figure 4.5 CD spectra of both substrate-free (A) and substrate-bound (B) forms of the WT and G248H mutant of cytochrome P450cam.

4.4.5 Electrochemical study

Derived from Figure 4.6, the redox potential for G248H mutant was measured to be about -92 mV, compared with -135 mV for wild type. There was some positive shift of the $\text{Fe}^{3+}/\text{Fe}^{2+}$ redox couple caused by the substitution of the distal glycine with a histidine residue. The redox potential change could be the result of the introduction of histidine into the distal heme pocket which increased the total charge near the heme group and made it easier to be reduced.

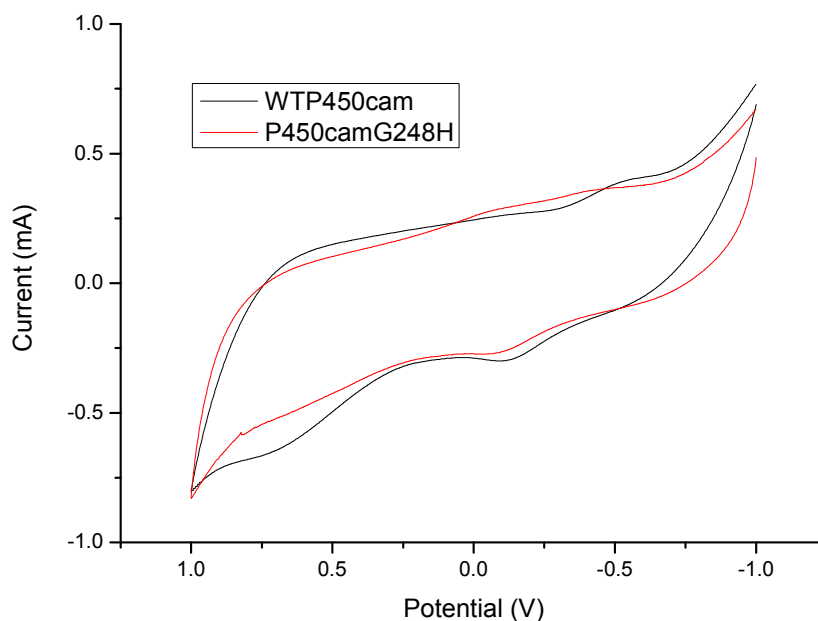


Figure 4.6 Cyclic voltammograms of P450cam and P450camG248H on a glass carbon electrode modified with SWNTs. Voltammograms were recorded between -1.0 and +1.5V at the scan rate of 1V/sec in 100mM phosphate buffer (pH7.4).

4.5 DISCUSSION AND CONCLUSION

This work has demonstrated an intriguing model of heme-thiolate protein with a histidine serving as the 6th axial ligand at the distal side of the heme group. Up to date, there are several proteins reported to possess such Cys-His coordination. In nature, this ligand set has only been seen in cystathionine β -synthase (32) and *Rhodovulum sulfidophilum* SoxAX enzyme (33). Also, a few hemoproteins have been engineered to introduce the distal histidine ligation or proximal cysteinate ligation in the heme pocket, such as the M80C variant of cytochrome *c* (34), A264H variant of cytochrome P450BM3 (23), and H39C mutant of cytochrome *b5* (35). But in all these cases, the proximal cysteinate ligation was only observed in the ferric but not the ferrous oxidation state. Upon reduction the proximal thiolate is either protonated or replaced by an alternative coordinating group except for the P450BM3 A264H mutant which was not even able to be completely reduced and form any significant amount of CO complex. We have presented here the first example of hemoprotein with a Cys-Fe-His ligand set which is preserved in various oxidation states.

In the electronic absorption spectroscopic studies, the UV-visible spectra of the G248H mutant of P450cam displayed features that are typical of six-coordinate, low-spin heme complexes in the absence of substrate. The Soret band of the camphor-free mutant was shown red shifted from 417 nm to 425 nm, similar to what was observed in the imidazole-coordinated wild type protein and cytochrome P450BM3 A264H mutant,

indicating the heme iron ligation is complete with distal water ligand replaced by histidine, a stronger field ligand. Interestingly the significant spin and coordination state changes that occur in wild type P450cam upon camphor binding were not observed in the mutant, and the UV spectra of G248H mutant in the absence and presence of camphor were virtually indistinguishable. This implied the substrate binding was perturbed in the variant, and camphor was not able to displace the axial heme ligand and alter the heme environment in the case of the wild type protein. Because of the complete axial ligation, it made the mutant unable to bind any ligands. This was confirmed by the resonance Raman spectroscopic spectra in which the ferric G248H variant showed LS, 6C with His and Cys as the distal and proximal ligand respectively, regardless of whether the substrate camphor is bound or not.

Comparing the ferrous form of the imidazole complex of wild type, the G248H mutant was different not only in its Soret band maximum but also in the Q band region. The mutant displayed two α and β bands in the ferrous form, which was strong evidence of six coordination of the heme iron. However as for the imidazole complex of wild type protein, it showed only one band like the wild type and many other hemoproteins, indicating the preference of a five-coordination heme upon reduction. Intriguingly, in the study of the P450BM3 A264H mutant, a parallel variant of G248H, the distal ligand remained firmly bound on reduction and CO was not able to displace the His264 ligand. In G248H mutant, its CO complex exhibited the characteristic Soret band at around

450nm as the wild type, strongly indicating the preserved thiolate ligation in its ferrous form. Also, the RR spectra displayed distinct features of the mutant in its ferrous and CO complexes. The ν_4 band of the ferrous G248H shifted to 1366 and 1360 cm^{-1} , respectively for the substrate-free and substrate-bound forms, which were not in the region of either 5C cysteine proximal ligation (1340-1348 cm^{-1}) or 5C histidine proximal ligation (1350-1358 cm^{-1}) (36, 37). This suggests that upon reduction, part of the histidine ligand was lost, resulting in a mixture of 5C and 6C coordination. Once CO was introduced, CO could partially bind to ferrous heme iron, but not dominantly.

According to the far-UV CD spectra, the secondary structure of the protein was not affected by the substitution of G248 with a histidine. However, there were indeed distinct changes in the tertiary structure around the heme pocket in the mutant compared with that of the wild type. The CD spectra showed markedly in different pattern in the presence and absence of camphor, especially in the substrate-bound form, which implied more significant conformational change. Except for the shift of Soret band, a set of split peaks was observed, indicative of strong six-coordinate ligation. Thus the binding of camphor makes the distal pocket more compact like the wild type and results in a stronger histidine ligation to the heme iron.

Taken together, the data of the various spectroscopic studies have demonstrated that the substitution of G248 with a histidine induces conformational change in the active site, yielding a histidine ligation to the heme iron and alteration of the access of the substrate

camphor to the heme prosthetic group. When the variant is reduced and CO is introduced, the proximal thiolate ligation remained intact while part of the distal histidine was displaced. This is quite different from other reported proteins with such Cys-Fe-His ligation set, whether it is naturally occurring or exogenously introduced. The thiolate ligand tends to be lost by protonation or displaced by another coordination group in the reduced form. This phenomenon has also been reported in many other hemoproteins with thiolate ligation in their ferric forms such as CO-sensing CooA protein (38), H93C mutant of myoglobin (Mb) (39), H175C mutant of cytochrome *c* peroxidase (40) and inactive forms of cytochrome P450 (P420) and chloroperoxidase (C420) (41, 42). Except for CooA, which has been reported that the proximal ferrous ligand switches from Cys75 to His77, other hemoproteins has been proposed to use neutral cysteine thiol as the possible ligand (43) or the proximal cysteinate ligand could be replaced by a nearby histidine residue.

For instance, in the study of heme iron coordination of C420, it was suggested that ferric C420 appeared to retain a thiolate proximal ligand but not in its ferrous form with the distal histidine serving as a potential ligand to the heme iron. It has also been proposed in the probe of ferrous P420 that histidine ligation might be involved. All the hypotheses imply that histidine serves as an axial ligand to heme iron more readily than cysteinate in the hemoproteins. However, our results failed to support these hypotheses. Our study unequivocally demonstrated that the endogenous thiolate ligand is retained in

all oxidation states in our G248H mutant. It is evident that with both His and Cys ligated to the heme iron at the ferric state, it is the His rather than the Cys that would fall off upon reduction and CO binding, suggesting the cysteinate ligation is more stable in this case, i.e. the iron-sulfur bond is stronger than the iron-nitrogen bond.

The crystal structural study of wild type P450cam complexed with imidazole has shown that the imidazole group was bound perpendicular to the plane of the heme (44). In the P450BM3 variant A264H, the angle between the plane of heme and imidazole ring of His-264 is almost exactly 90° and the imidazole is orientated at about 45° to the pyrrole nitrogens to minimize unfavorable interactions.(23) Therefore, we propose here that in the P450cam G248H mutant, the binding of the histidine ligand involves coordination of the imidazole group to the heme iron in a similar way to the two models mentioned above.

We conclude from the data presented in this work that the P450cam G248H mutant is the first model of complete axial coordination with cysteinate and histidine serving as the ligands to the heme iron, in which the thiolate ligation remains intact upon reduction and CO binding. We also propose that for hemoproteins with endogenous cysteine ligation, the thiolate ligand would not be easily displaced by another ligand provided by nearby residues or solvent and that cysteine serves as a stronger ligand than histidine. The study of this “locking” heme model could lead to the promising development of a diagnostic spectroscopic method for thiolate-ligated hemoproteins to recognize such

coordination when it occurs elsewhere in nature or in other pertinent engineered protein systems.

4.6 REFERENCES

1. Sigel, A., Sigel, H., and Sigel, R. K.O. (2007) The ubiquitous roles of cytochrome P450 proteins in *Metal Ions in Life Sciences* (Sigel, A., Sigel, H., and Sigel, R. K.O. , Ed.), Wiley, Chichester.
2. Guengerich, F. P. (1991) Reactions and Significance of Cytochrome P-450 Enzymes, *Journal of Biological Chemistry* 266, 10019-10022.
3. Ortiz de Montellano, P. R. (2005) *Cytochrome P450: structure, mechanism, and biochemistry*, 3 ed., Kluwer Academic/Plenum Publishers, New York.
4. Sono, M. R., M. P.; Coulter, E. D.; and Dawson, J. H. (1996) Heme-Containing Oxygenases, *Chemical Reviews* 96, 2841-2847.
5. Sono, M., Roach, M. P., Coulter, E. D., and Dawson, J.H. (1996) Heme-Containing Oxygenases, *Chemical Reviews* 96, 2841-2847.
6. Joo, H., Lin, Z. L., and Arnold, F. H. (1999) Laboratory evolution of peroxide-mediated cytochrome P450 hydroxylation, *Nature* 399, 670-673.
7. Nordblom, G. D., White, R. E. and Coon, M. J. (1976) Studies on hydroperoxide-dependent substrate hydroxylation by purified liver microsomal cytochrome P450, *Arch. Biochem. Biophys.* 175, 524-533.
8. Hrycay, E. G., Gustafsson, J.-A., Ingelman-Sundberg, M. and Ernster, L. (1975) Sodium periodate, sodium chlorite, organic hydroperoxides and hydrogen peroxide as hydroxylating agents in steroid hydroxylation reactions catalyzed by partially purified cytochrome P450, *Biochem. Biophys. Res. Commun.* 66, 209-216.
9. Cirino, P. C., and Arnold, F. H. (2003) A self-sufficient peroxide-driven hydroxylation biocatalyst, *Angew. Chem. Int. Ed.* 42, 3299-3301.

10. Shoji, O., Fujishiro, T., Nakajima, H., Kim, M., Nagano, S., Shiro, Y., Watanabe, Y. (2007) Hydrogen Peroxide-Dependent Monooxygenations by Tricking the Substrate Recognition of Cytochrome P450BS β , *Angew. Chem. Int. Ed.* 46, 3656-3659.
11. Cirino, P. C., and Arnold, F. H. (2002) Regioselectivity and activity of cytochrome P450 BM-3 and mutant F87A in reactions driven by hydrogen peroxide, *Advanced Synthesis & Catalysis* 344, 932-937.
12. Davydov, R. M., Ledenev, A.N. (1981) Activation mechanism of molecular oxygen by cytochrome P-450, *Biofizika* 26, 1096.
13. Tanaka, M., Ishimori, K., Mukai, M., Kitagawa, T., and Morishima, I. (1997) Catalytic activities and structural properties of horseradish peroxidase distal His42->Glu or Gln mutant, *Biochemistry* 36, 9889-9898.
14. Howes, B. D., RodriguezLopez, J. N., Smith, A. T., and Smulevich, G. (1997) Mutation of distal residues of horseradish peroxidase: Influence on substrate binding and cavity properties, *Biochemistry* 36, 1532-1543.
15. Newmyer, S. L., and Demontellano, P. R. O. (1995) Horseradish-peroxidase His-42 -> Ala, His-42 ->Val, and Phe-41 ->Ala mutants - Histidine Catalysis and Control of Substrate Access to the Heme Iron, *J. Biol. Chem.* 270, 19430-19438.
16. Erman, J. E., Vitello, L. B., Miller, M. A., Shaw, A., Brown, K. A., and Kraut, J. (1993) Histidine 52 is a critical residue for rapid formation of cytochrome c peroxidase compound I, *Biochemistry* 32, 9798-9806.
17. Poulos, T. L., and Kraut, J. (1980) THE STEREOCHEMISTRY OF PEROXIDASE CATALYSIS, *J. Biol. Chem.* 255, 8199-8205.
18. Poulos, T. L., Finzel, B. C., and Howard, A. J. (1987) High-Resolution Crystal-Structure of Cytochrome-P450cam, *Journal of Molecular Biology* 195, 687-700.
19. Schlichting, I., Berendzen, J., Chu, K., Stock, A. M., Maves, S. A., Benson, D. E., Sweet, B. M., Ringe, D., Petsko, G. A., and Sligar, S. G. (2000) The catalytic pathway of cytochrome P450cam at atomic resolution, *Science* 287, 1615-1622.

20. Limburg, J., LeBrun, L. A., and de Montellano, P. R. O. (2005) The P450(cam) G248E mutant covalently binds its prosthetic heme group, *Biochemistry* 44, 4091-4099.
21. Joyce, M. G., Girvan, H. M., Munro, A. W., and Leys, D. (2004) A single mutation in cytochrome P450BM3 induces the conformational rearrangement seen upon substrate binding in the wild-type enzyme, *J. Biol. Chem.* 279, 23287-23293.
22. Girvan, H. M., Marshall, K. R., Lawson, R. J., Leys, D., Joyce, M. G., Clarkson, J., Smith, W. E., Cheesman, M. R., and Munro, A. W. (2004) Flavocytochrome P450BM3 mutant A264E undergoes substrate-dependent formation of a novel heme iron ligand set, *J. Biol. Chem.* 279, 23274-23286.
23. Girvan, H. M., Seward, H. Ed., Toogood, H. S., Cheesman, M. R., Leys, D. and Munro, A. W. (2007) Structural and Spectroscopic Characterization of P450 BM3 Mutants with Unprecedented P450 Heme Iron Ligand Sets, *J. Biol. Chem.* 282, 564-572.
24. Paul, K. G., Theorell, H., Akesson, A. (1953) The Molar Light Absorption of Pyridine Ferroprotoporphyrin (Pyridine Haemochromogen), *Acta Chem. Scand.* 7, 1284-1287.
25. Berry, E. A., and Trumpower, B. L. (1987) Simultaneous Determination of Hemes-a, Hemes-b, and Hemes-c from Pyridine Hemochrome Spectra, *Analytical Biochemistry* 161, 1-15.
26. Dawson, J. H., Andersson, L. A. and Sono, M. (1982) Spectroscopic Investigations of Ferric Cytochrome P-450-CAM Ligand Complexes, *J. Biol. Chem.* 257, 3606-3617.
27. Spiro, T. G., Stong, J. D., and Stein, P. (1979) *J. Am. Chem. Soc.* 101, 2648-2655.
28. Andersson, L. A., Mylrajan, M., Sullivan, E. P., Jr., and Strauss, S. H. . (1989) *J. Biol. Chem.* 264, 19099-19102.
29. Lou, B. S., Snyder, J. K., Marshall, P., Wang, J. S., Wu, G., Kulmacz, R. J., Tsai, A. L., and Wang, J. (2000) *Biochemistry* 39, 12424-12434.
30. Spiro, T. G., Kozlowski, P. (2001) *Acc. Chem. Res.* 34, 137-144.

31. Vogel, K. M., Kozlowski, P.M., Zgierski, M.Z., Spiro T.G. (2000) *Inorg. Chim. Acta.* 297, 11-17.
32. Meier, M., Janosik, M., Kery, V., Kraus, J. P., and Burkhard, P. (2001) Structure of human cystathionine β -synthase: a unique pyridoxal 5'-phosphate-dependent heme protein., *EMBO Journal* 20, 3910-3916.
33. Cheesman, M. R., Little, P. J., and Berks, B. C. (2001) Novel Heme Ligation in a c-type Cytochrome Involved in Thiosulfate Oxidation:EPR and MCD of SoxAX from *Rhodovulum sulfidophilum*, *Biochemistry* 40, 10562-10569.
34. Raphael, A. L. a. G., H. B. (1991) Semisynthesis of Axial-Ligand (Position 80) Mutants of Cytochrome c, *J. Am. Chem. Soc.* 113, 1038-1040.
35. Wang, W.-H., Lu, J-X, Yao, P., Xie, Y., Huang, Z-X. (2003) The distinct heme coordination environments and heme-binding stabilities of His39Ser and His39Cys mutants of cytochrome b5, *Protein Eng.* 16, 1047-1054.
36. Anzenbacher, P., Evangelista-Kirkup, R., Schenkman, J., Spiro, T. G. (1989) Influence of Thiolate Ligation on the Heme Electronic-Structure in Microsomal Cytochrome-P450 and Model Compounds - Resonance Raman-Spectroscopic Evidence, *Inorganic Chemistry* 28, 4491-4495.
37. Wang, J., Caughey, W. S., Rousseau, D. L. (1996) Resonance Raman Scattering: a Probe of Heme Protein-bound Nitric Oxide., in *Methods in Nitric Oxide Research* (Feelisch, M., Stamler, J., Ed.), pp 427-454, J. Wiley, Chichester ; New York.
38. Nakajima, H., Nakagawa, E., Kobayashi, K., Tagawa, S., and Aono, S. (2001) Ligand-switching intermediates for the CO-sensing transcriptional activator CooA measured by pulse radiolysis, *Journal of Biological Chemistry* 276, 37895-37899.
39. Adachi, S., Nagano, S., Ishimori, K., Watanabe, Y., Morishima, I., Egawas, T., Kitagawa, T., Makino, R. (1993) Roles of Proximal Ligand in Heme Proteins: Replacement of Proximal Histidine of Human Myoglobin with Cysteine and Tyrosine by Site-Directed Mutagenesis as Models for P-450, Chloroperoxidase, and Catalase, *Biochemistry* 32, 241-252.

40. Sigman, J. A., Pond, A. E., Dawson, J. H., and Lu, Y. (1999) Engineering cytochrome c peroxidase into cytochrome P450: A proximal effect on heme-thiolate ligation, *Biochemistry* 38, 11122-11129.
41. Martinis, S. A., Blanke, S. R., Hager, L. P., Sligar, S. G., Hoa, G. H. B., Rux, J. J., and Dawson, J. H. (1996) Probing the heme iron coordination structure of pressure-induced cytochrome P420cam, *Biochemistry* 35, 14530-14536.
42. Blanke, S. R., Martinis, S. A., Sligar, S. G., Hager, L. P., Rux, J. J., Dawson, J. H. (1996) Probing the Heme Iron Coordination Structure of Alkaline Chloroperoxidase, *Biochemistry* 35, 14537-14543.
43. Perera, R., Sono, M., Sigman, J. A., Pfister, T. D., Lu, Y., and Dawson, J. H. (2003) Neutral thiol as a proximal ligand to ferrous heme iron: Implications for heme proteins that lose cysteine thiolate ligation on reduction, *Proc. Natl. Acad. Sci.* 100, 3641-3646.
44. Verras, A., Alian, A., and de Montellano, P. R. O. (2006) Cytochrome P450 active site plasticity: attenuation of imidazole binding in cytochrome P450(cam) by an L244A mutation, *Protein Engineering Design & Selection* 19, 491-496.

CHAPTER V. PROTEIN ENGINEERING OF MYOGLOBIN WITH THIOLATE PROXIMAL LIGATION

5.1 SUMMARY

Myoglobin has been used as a model in the investigations of protein folding, ligand binding and conformational transitions of heme-containing proteins. Many studies of heme-imidazole proteins including myoglobin have been carried out to replace the proximal axial histidine ligand with a cysteine residue to gain the heme-thiolate protein structural character. Although some of the protein variants achieved the iron-thiolate ligation in their ferric forms, the iron-thiolate ligand failed to retain upon reduction. Therefore, to explore the possibility of converting myoglobin to a heme-thiolate protein in all oxidation states, I tried to mimic the protein environment of both cytochrome P450cam and chloroperoxidase respectively in the proximal side of sperm whale myoglobin by replacing eight amino acids around the iron-histidine ligand. UV-visible spectroscopic studies were performed to examine the axial ligation in the wild type and mutant proteins of Mb. Neither the P450 mimic nor the CPO mimic showed the characteristic Soret absorption maxima around 450nm when reduced in the presence of carbon monoxide, suggesting the thiolate ligation was not reserved in the ferrous forms. Considering the possible interference of distal histidine as a competitive candidate ligand to the heme iron, the His64 was substituted with an alanine and glutamic acid based on

comparisons with the structure of P450 and CPO, respectively. The optical spectral properties showed no difference. It happened again in the further mutation by replacing the His 97 which is located in the proximal vicinity with an alanine.

5.2 INTRODUCTION

Myoglobin is a monomeric heme protein found mainly in muscle tissues where it acts as an intracellular primary storage site for oxygen by reversibly binding oxygen molecules (*1*). This protein has been the target of extensive biochemical and biophysical studies for many years because of its physiological importance, availability and simplicity compared with other bulky heme proteins. It serves as a prototype for elucidating the roles of critical active site residues in the interactions of hemoproteins with small molecules such as dioxygen, carbon monoxide, and cyanide (*2-5*). In myoglobin, there is a conserved histidine residue (His93) serving as the proximal axial ligand to the heme iron, anchoring the heme group in the globin, and a conserved histidine residue (His64) in the distal pocket, conferring a large measure of specificity for O₂ (*6*). Both of these histidine residues are important in terms of protein structure and function. Quite a few studies have been dedicated to examine their roles in the active site of myoglobins from various sources by site-directed mutagenesis in the last few decades (*7-11*).

Cysteine plays a key role as a metal ligand in metalloproteins, especially in heme-containing proteins. A distinctive feature of heme-thiolate proteins is a Soret absorption band at around 450 nm in the CO difference spectrum of the reduced forms. The anionic cysteinate that coordinates to the heme iron in heme-thiolate proteins has been claimed to serve as a strong electron donor to facilitate the heterolytic O-O bond cleavage and the formation of Cpd I, the highly active reaction intermediate responsible for the catalytic reactions (12, 13). To clarify the critical role of the anionic axial ligands of heme proteins on the O-O bond scission reaction and the contributions of proximal Cys ligation to the functional and catalytic properties of cytochrome P450 and CPO, the proximal histidine 93 of human myoglobins and horse heart myoglobin has been replaced with a cysteine residue (9, 10). The Mb H93C mutants resulted in altered axial ligations analogous to those of P-450 or CPO. The cysteine coordination to the ferric heme iron is confirmed by various biophysical methods, with the mutants showing almost identical spectroscopic properties to those of heme-thiolate proteins. The Mb H93C mutants were revealed to be in the ferric high-spin, five-coordinate state with the proximal cysteine ligated to the heme iron (9). Therefore, it is proved that the axial ligand of the heme iron is responsible for the spectroscopic features of hemoproteins, which has been indicated by various hemoproteins and their ligand-bound complexes.

For catalytic activities, the cysteine must be deprotonated to cysteinate throughout the reaction cycle as the iron changes oxidation state from ferric to ferrous and ferryl

states. The role of the anionic axial ligands on the O-O bond cleavage is examined by reactions utilizing peroxides. The results of Mb H93C mutants showed that the thiolate ligand enhanced the heterolytic O-O bond scission of the oxidant. This mutant also displayed about a 5-fold increase in epoxidation activity (9). Although the ferric forms of the mutants showed iron-cysteine ligation, upon reduction of the H93C variants with sodium dithionite under a CO atmosphere, the CO complexes displayed a similar spectrum to that of wild type Mb, the typical heme-imidazole protein, with the Soret band at around 420 nm instead of 450 nm. Thus, it is unlikely that the cysteine thiolate remains as the proximal ligand to the ferrous heme iron. The spectroscopic study of the mutants confirms that in Mb H93C the distal histidine is coordinated to the heme iron, despite the suggestion of a neutral thiol serving as the proximal ligand upon reduction (10, 14). On the basis of the H93C single mutant, several studies have been carried out to replace the distal histidine with a glycine, valine or isoleucine as well. The ferric state of these variants closely resembled the spectroscopic properties of the corresponding ferric cytochrome P450. However, the ferrous and ferrous-CO complexes of these variants remained virtually the same as for the H93C single mutant. According to these results, it is apparent that while simple mutagenesis modifications of the Mb active site can mimic the characteristics of ferric cytochrome P450 or CPO, the reproduction of the spectroscopic properties of their ferrous forms would require more subtle modifications though, which is the ultimate goal of this study.

Sperm whale myoglobin (Mb), a single-chain globin protein of 154 amino acids has been chosen because it represents one of the most extensively studied heme-containing proteins by biochemical, biophysical and spectroscopic techniques. It was the first protein whose crystal structure was determined to high resolution by x-ray crystallographic analysis in 1960 (15). Sperm whale myoglobin is composed of eight α helices (labeled A-H in Fig. 5.1) that form an amphipathic pocket with the heme prosthetic group bound between the helices. The heme iron is coordinated to the protein via a histidine ligand located in the F helix at the proximal site. The majority of other heme-protein contacts are hydrophobic except for the two solvent-exposed propionate side chains of the heme group that interact electrostatically with the protein residues around the prosthetic group.

Figure 5.2 illustrates the active site structure of sperm whale myoglobin with histidine residues in both proximal and distal sides along with several important amino acids in the proximal helix F from Leu89 to His97, with His 93 in the middle. To engineer sperm whale myoglobin into a heme-thiolate protein model in various oxidation states, all eight proximal residues around the axial ligand were replaced by the corresponding amino acids in P450cam and CPO, resulting in the P450 mimic of Mb (MbP) and CPO mimic of Mb (MbO). Furthermore, the distal histidine was substituted with an alanine and glutamic acid, respectively, for MbP and MbO. Finally, as the distal H97 that could be a potential competitive ligand to the heme iron in the ferrous forms of the Mb variants was also replaced. UV-visible spectroscopic studies have been carried out

to examine the optical properties and structural characteristics of the generated mutants of sperm whale myoglobin.

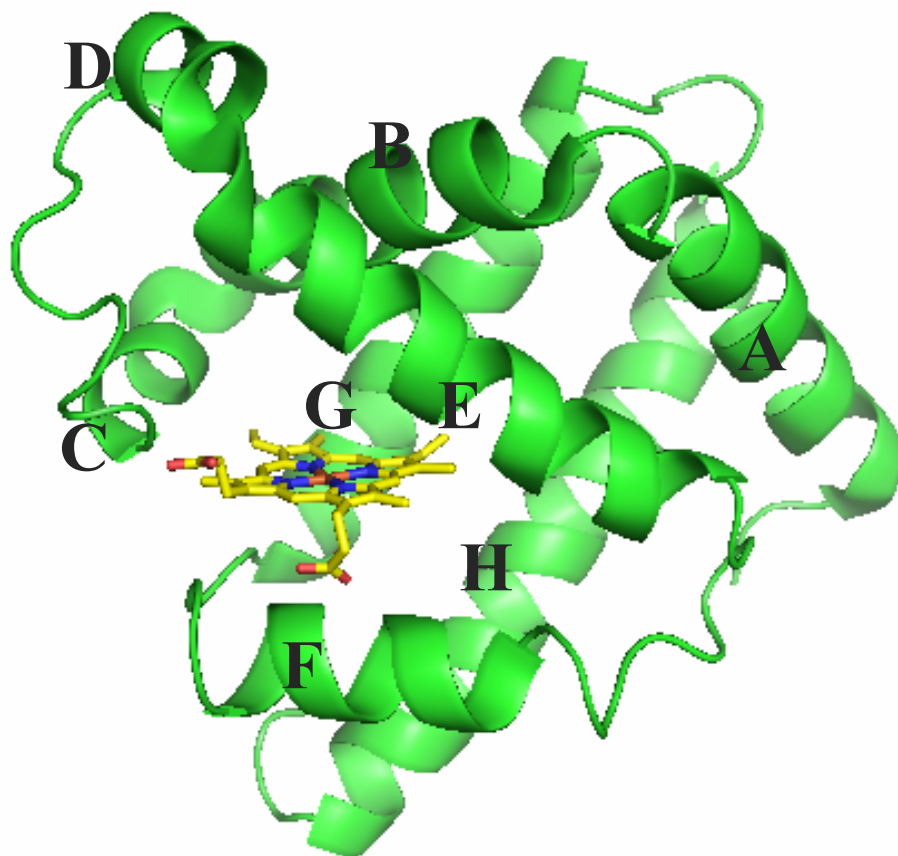


Figure 5.1 A ribbon diagram of the sperm whale myoglobin crystal structure showing the arrangement of eight α helices and the heme group (shown in yellow). This figure was generated from the crystal data (PDB code 1VXH) using PYMOL (6).

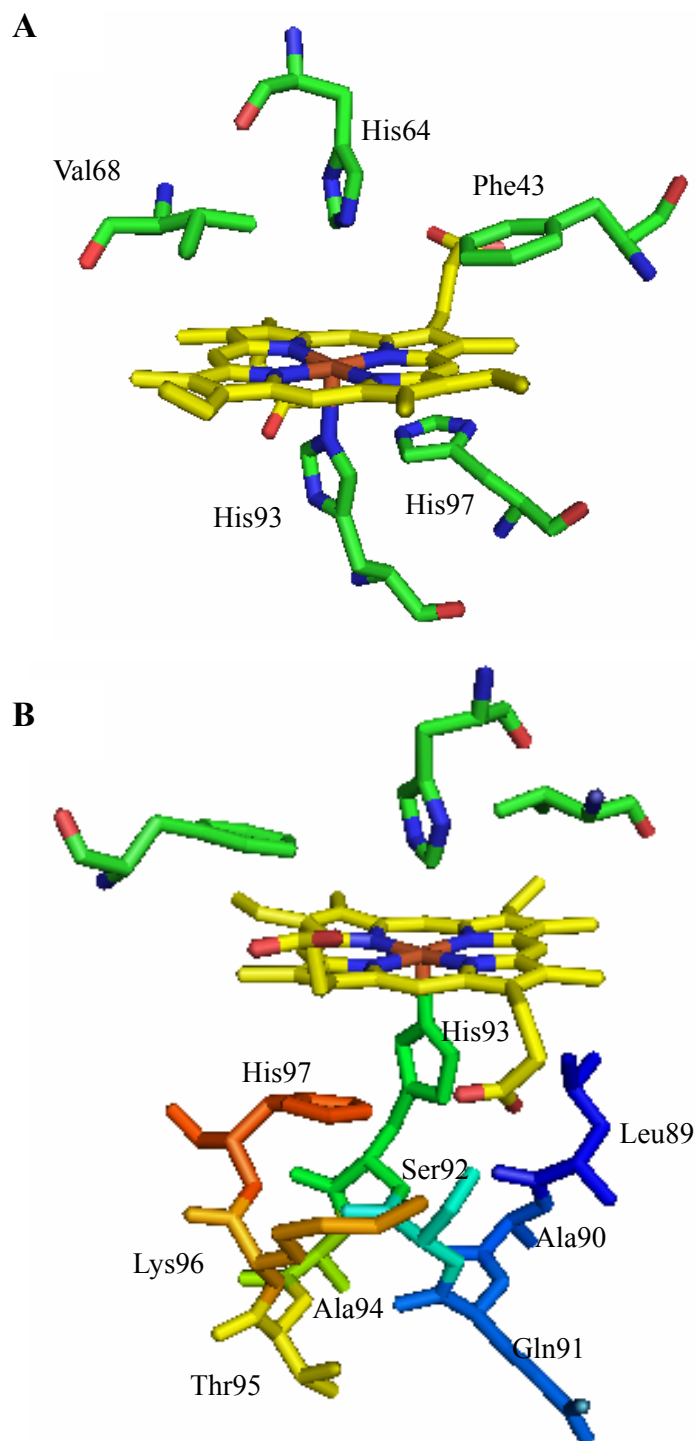


Figure 5.2 Crystal structure of sperm whale myoglobin active site with some important amino acids around heme group (yellow) viewed from different angles. In **(B)** the proximal amino acids were colored in rainbow. The figures were generated from the crystal data (PDB code 1VXH) using PYMOL (*1*).

5.3 EXPERIMENTAL PROCEDURES

5.3.1 Bacterial strains, plasmids and DNA manipulations

The bacterial strains used were *E. coli* NovaBlue and *E. coli* Rosetta II (DE3) from Novagen (Gibbstown, NJ). The used plasmid pMb122 containing wild type sperm whale myoglobin gene in a pUC19 vector is identical to pMb413a used by Springer *et al.* except for a correction in the coding sequence (N122D) due to a mistake in the original sequence (16). To increase the protein yield, the Mb gene was constructed into a T7-based expression vector, pET-30a (+) from Novagen, at the sites of NdeI and KpNI by polymerase chain reactions and ligation reactions. Bacteria were grown in Luria-broth supplemented with antibiotic (kanamycin 100 µg/ml) for DNA manipulation.

5.3.3 Site-directed mutagenesis and protein expression.

Table 5.1 Proximal sequence alignment of Mb and its P450 and CPO mimics

Protein	Proximal sequence								
WT Mb	L	A	Q	S	H93	A	T	K	
MbP (P450 mimic)	G	S	R	L	C93	L	G	Q	
MbO (CPO mimic)	S	R	A	P	C93	P	A	L	

The proximal sequence alignment of sperm whale Mb and its P450 and CPO mimics is listed in Table 5.1. The MbP mutant was prepared with the 5'-sense oligonucleotide 5'-GGT TCT CGT CTG TGC CTG GGT CAG CAT AAG ATC CCG ATC AA coding for GSRLCLGQHKIPI (P450mimic). The MbO mutant was obtained with the 5'-sense

oligonucleotide 5'- TCT CGT GCT CCT TGC CCA GCT CTG CAT AAG ATC CCG ATC AA coding for SRAPCPALHKIPI. Primers used for all other Mb variants are listed in appendix C. The reconstituted plasmids containing Mb and the mutants were transformed into *E. coli* strain NovaBlue and verified by DNA sequencing (MacroGen, MD). Proteins were expressed in *E. coli* strain Rosetta II (DE3). Cells were grown on Luria broth supplemented with 100 mg/L of kanamycin at 37 °C and induced with 1mM IPTG when OD₆₀₀ reaches around 1.2, followed by further growth for 4 hours prior to harvest. As for the mutants, the addition of δ -aminolevulinic acid to the growth media is necessitated to facilitate holoenzyme production. The cells were then harvested and frozen at -80 °C.

5.3.4 Protein purification

Cells were lysed at 4°C in 25 mM Tris-HCl buffer at pH 8.0 containing 0.5 mM DTT, 1 mM EDTA, 200 μ M PMSF, 40 U/ml Dnase I, 3 U/ml Rnase A, and lysozyme for overnight in a shaker. After freezing at -80°C for the second time, the cells were thawed again followed by centrifugation and concentration using an Amicon cell with 10,000 Da cut-off ultrafiltration membrane. The protein solution was first applied on a fast flow DEAE Sepharose column equilibrated with the 10mM Tris-HCl buffer at pH 8.2. After initial wash, proteins were eluted with a linear 0-0.5 M NaCl gradient in the same buffer. All Mb mutants were expressed as apo-proteins and converted to holoproteins via heme reconstitution. Typically, hemin was added to the apo-protein drop wise which was

mixing on a stirrer for overnight (17). After heme reconstitution, the protein sample was again applied onto a fast flow DEAE Sepharose column. The reddish fractions of correct molecular weight were pooled and concentrated using a Centriprep with an YM10 membrane for further purification by size exclusion chromatography. The buffer used for gel filtration was 0.1 M potassium phosphate buffer at pH 7.0. Unless otherwise specified, all steps in the protein purification procedure were performed at 4 °C.

5.3.5 Electronic absorption spectroscopy

The UV-visible spectra of the Mb and its mutants were recorded on a Varian Cary 300 Bio UV-visible spectrophotometer at room temperature. The ferrous proteins were prepared by the addition of excess amount of sodium dithionite and CO adducts were obtained by CO gas bubbling. The buffer used for the absorption measurements was 100 mM potassium phosphate buffer at pH 7.0.

5.4 RESULTS AND DISCUSSION

There are two major groups of hemoprotein found in living organisms, namely “heme-thiolate proteins” and “heme-imidazole proteins”. The difference between these two classes of proteins is that when carbon monoxide binds to the reduced forms, heme-thiolate proteins usually give a characteristic optical absorption spectrum with a prominent Soret peak at around 450 nm, whereas the corresponding absorption spectrum of heme-imidazolate proteins shows a Soret peak at around 420 nm. This work intended

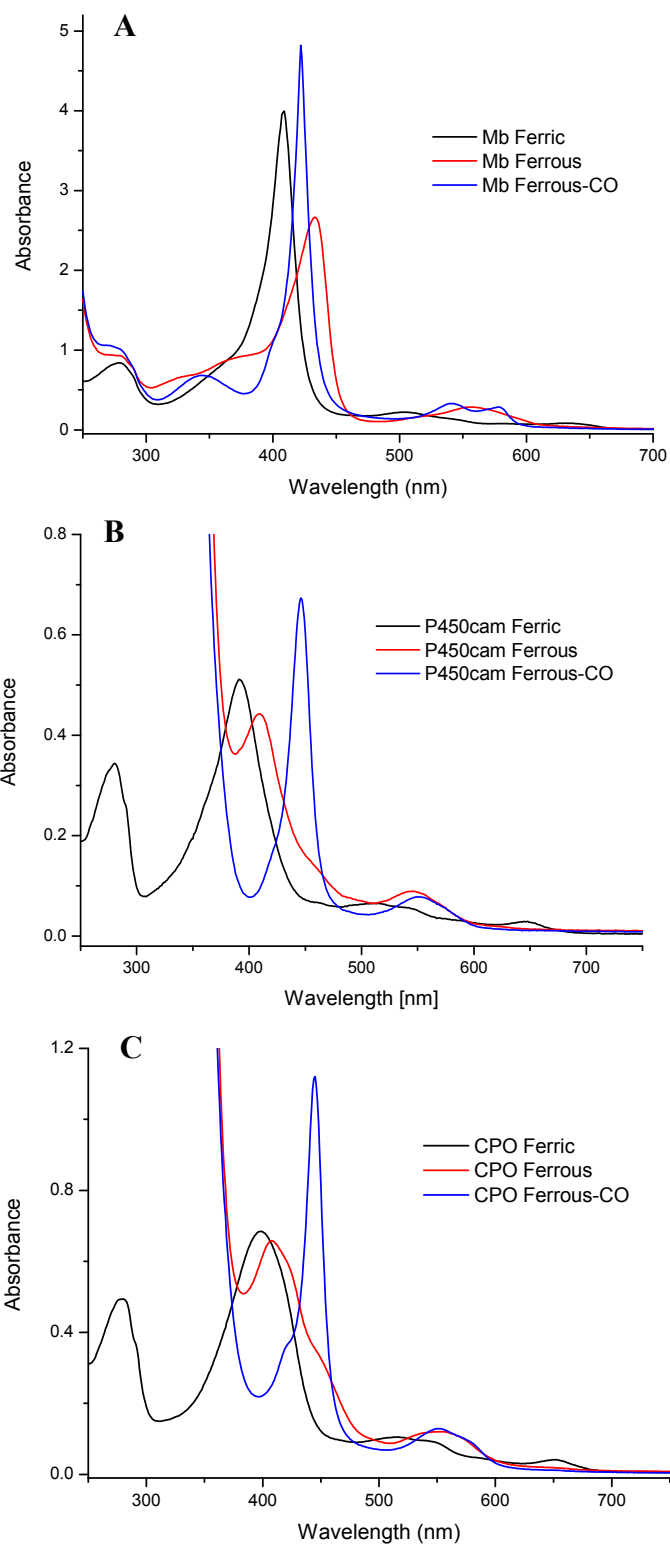


Figure 5.3. UV-visible spectra of wild type Mb (**A**), P450cam (**B**) and CPO (**C**) in various oxidation states

to investigate the role of proximal ligands in heme-thiolate proteins by changing the amino acids at the proximal side of sperm whale myoglobin, a typical heme-imidazole protein, to that of P450 or CPO.

First of all, wild type myoglobin, cytochrome P450cam and CPO were expressed and purified according to reported procedures (18-20). Figure 5.3 showed the UV-vis spectroscopic results of these proteins. In agreement with the literature, the ferrous-CO complexes of Mb displayed Soret absorption maximum at 420 nm, while P450cam and CPO exhibited the Soret band at 450 nm. By changing the proximal helix residues to mimic those of P450 and CPO, the resulted mutants were expected to show spectral properties similar to such heme-thiolate proteins.

5.4.1. Mb mutant: MbP/MbO

Eight amino acids, at the heme proximal side of sperm whale Mb, including His 93 have been replaced to mimic the protein environment of cytochrome P450cam and CPO, respectively. The mutants were named MbP and MbO. The primers were designed as one containing all the mutations at the end and the other one having the gene sequence at the opposite direction. The PCR and self-ligation reactions were performed which directly produced the mutated recombinant plasmid with the facilitation of T4 polynucleotide kinase. Both of the mutants were over expressed in *E. coli*. Since they showed quite similar results, only the electronic absorption spectra of the P450 mimic were included. As shown in Fig. 5.4, the UV-vis spectra of Mb exhibited very similar results with those

of wild type Mb with the Soret band of the ferrous heme-CO complex at 420nm, instead of 450nm expected for Fe-thiolate ligation. This indicated that the thiolate sulfur might not be ligated to the heme iron upon reduction and CO binding. There could be other possible factors governing the spectral properties of the mutant, for instance the influence of the distal histidine. Therefore, the distal histidine was replaced by a glycine and glutamic acid in the P450 and CPO mimics, respectively.

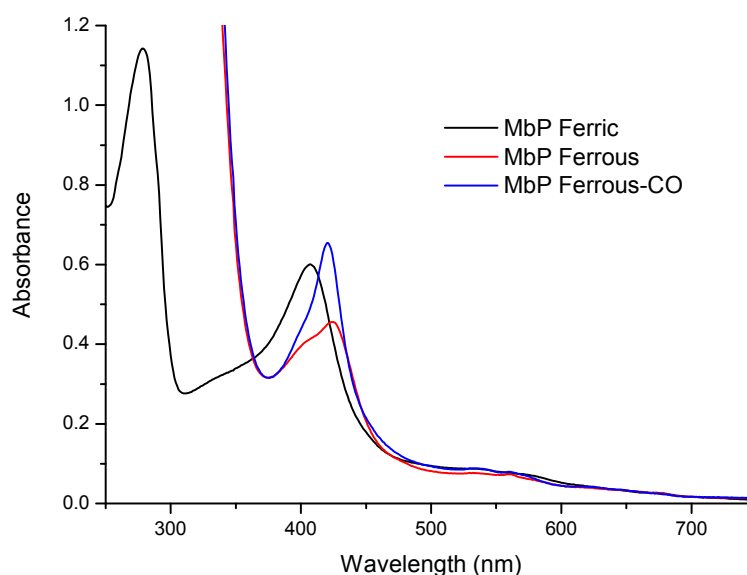


Figure 5.4 UV-visible spectra of MbP in various oxidation states.

5.4.2. Mb mutant: MbP H64G/MbO H64E

To investigate the possible interference of the distal histidine, MbP H64G and MbO H64E mutants were obtained. Fig. 5.5 shows the UV-vis results of the MbP H64G mutant. Unexpectedly, the Soret peak of the ferrous-CO complex of this Mb mutant remained at around 420 nm (Table 5.2). Thus, further modifications are needed to achieve a thiolate proximal ligand in the Mb variant at reduced state.

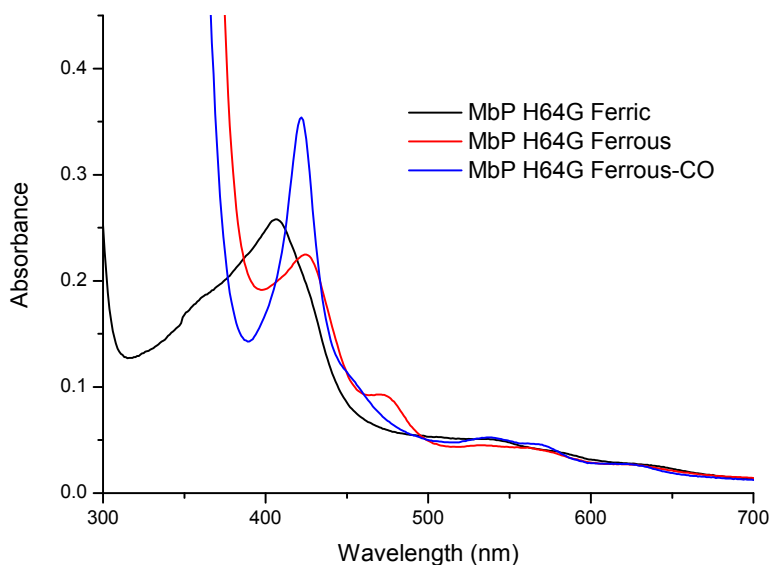


Figure 5.5 UV-visible spectra of MbP H64G in various oxidation states.

Table 5.2 Wavelength and extinction coefficients of absorption maxima for P450cam, Mb, MbP, and MbP H64G.

Protein	Oxidation state	Soret band (nm)	Visible bands (nm)
P450cam	Fe ³⁺	392 ($\epsilon=102$) (21)	535, 569
	Fe ²⁺	408	540
	Fe ²⁺ -CO	446	550
CPO	Fe ³⁺	398 ($\epsilon=91.2$) (22)	516, 550, 650
	Fe ²⁺	408	550
	Fe ²⁺ -CO	445	550
Mb	Fe ³⁺	408 ($\epsilon=184$) (11)	502, 631
	Fe ²⁺	433	556
	Fe ²⁺ -CO	422	541, 578
MbP	Fe ³⁺	407	534, 569
	Fe ²⁺	425	532, 559
	Fe ²⁺ -CO	421	533, 561, 619
MbP H64G	Fe ³⁺	407	537, 576
	Fe ²⁺	425	533, 561
	Fe ²⁺ -CO	422	538, 568, 620

5.4.3. Mb mutant: MbP H64G H97A/MbO H64E H97A

Considering that the proximal histidine 97 is located in the helix F closely to the heme iron and the iron-histidine ligand (His93) (Fig. 5.2), it could be a possible competitor to interference the altered thiolate ligation in the proximal side of MbP H64G mutant. Therefore, it was replaced by an alanine, which is a good helix promoter, for both the P450 and CPO mimics. Unfortunately, the UV-vis results showed nothing different from the MbP H64G mutant (data not shown). In conclusion, the attempt to engineer

myoglobin with a proximal thiolate ligand that can be retained in all oxidation states to achieve a P450-like variant was not successful. This difficulty was also reported by several previous studies, in which the proximal histidine was replaced by a cysteine but the thiolate ligation was lost upon reduction (23-26). It is apparent that the heme-thiolate proteins and heme-imidazole proteins have distinct structural and functional differences and it would take more than just mimicking the active site residues to convert one to another.

5.5 REFERENCES

1. Yang, F., and Phillips, G. N. (1996) Crystal structures of CO-, deoxy- and met-myoglobins at various pH values, *J. Mol. Biol.* 256, 762-774.
2. Brancaccio, A., Cutruzzolá, F., Allocatelli, C.T., Brunori, M., Smerdon, S.J., Wilkinson, A.J., Dou, Y., Keenan, D., Ikeda-Saito, M., and Brantley, R.E. (1994) Structural factors governing azide and cyanide binding to mammalian metmyoglobins, *J. Biol. Chem.* 269, 13843-13853.
3. Springer, B. A., Egeberg, K.D., Sligar, S.G., Rohlfs, R.J., Mathews, A.J., and Olson, J.S. (1989) Discrimination between oxygen and carbon monoxide and inhibition of autooxidation by myoglobin. Site-directed mutagenesis of the distal histidine, *J. Biol. Chem.* 264, 3057-3060.
4. Olson, J. S., and Phillips, J. N. (1996) Kinetic Pathways and Barriers for Ligand Binding to Myoglobin, *J. Biol. Chem.* 271, 17593-17596.
5. Dou, Y., Olson, J.S., Wilkinson, A.J., and Ikeda-Saito, M. (1996) Mechanism of Hydrogen Cyanide Binding to Myoglobin, *Biochemistry* 35, 7107-7113.
6. Springer, B. A., Sligar, S. G., Olson, J. S., Phillips, G. N. (1994) Mechanisms of ligand recognition in myoglobin, *Chem. Rev.* 94, 699-714.

7. Egeberg, K. D., Springer, B. A., Martinis, S. A., Sligar, S. G., Morikis, D., and Champion, P. M. (1990) Alteration of sperm whale myoglobin heme axial ligation by site-directed mutagenesis, *Biochemistry* 29, 9783-9791.
8. Matsui, T., Ozaki, S., and Watanabe, Y. (1999) Formation and catalytic roles of compound I in the hydrogen peroxide-dependent oxidations by His64 myoglobin mutants, *Journal of the American Chemical Society* 121, 9952-9957.
9. Adachi, S., Nagano, S., Ishimori, K., Watanabe, Y., Morishima, I., Egawa, T., Kitagawa, T., and Makino, R. (1993) Roles of Proximal Ligand in Heme-proteins-Replacement of Proximal Histidine of Human Myoglobin with Cysteine and Tyrosine by Site-directed Mutagenesis as Models for P-450, Chloroperoxidase, and Catalase, *Biochemistry* 32, 241-252.
10. Hildebrand, D. P., Ferrer, J. C., Tang, H.-L., Smith, M., Mauk, A. G. (1995) Trans Effects on Cysteine Ligation in the Proximal His93Cys Variant of Horse Heart Myoglobin, *Biochemistry* 34, 11598-11605.
11. Matsui, T., Nagano, S., Ishimori, K., Watanabe, Y., and Morishima, I. (1996) Preparation and reactions of myoglobin mutants bearing both proximal cysteine ligand and hydrophobic distal cavity: Protein models for the active site of P-450, *Biochemistry* 35, 13118-13124.
12. Ortiz de Montellano, P. R. (2005) *Cytochrome P450: structure, mechanism, and biochemistry*, 3 ed., Kluwer Academic/Plenum Publishers, New York.
13. Newcomb, M., Zhang, R., Chandrasena, R. E. P., Halgrimson, J. A., Horner, J. H., Makris, T. M., and Sligar, S. G. (2006) Cytochrome P450 Compound I, *Journal of the American Chemical Society* 128, 4580-4581.
14. Perera, R., Sono, M., Sigman, J. A., Pfister, T. D., Lu, Y., and Dawson, J. H. (2003) Neutral thiol as a proximal ligand to ferrous heme iron: Implications for heme proteins that lose cysteine thiolate ligation on reduction, *Proc. Natl. Acad. Sci.* 100, 3641-3646.
15. Kendrew, J. C., Dickerson, R. E., Strandberg, B. E., Hart, R. G., Davis, D. R., Phillips, D. C., and Shore, V. C. (1960) Structure of Myoglobin: A Three-Dimensional Fourier Synthesis at 2 Å Resolution, *Nature* 185, 422-427.

16. Phillips, G. N., Arduini, R. M., Springer, B. A., and Sligar, S. G. (1990) Crystal Structure of Myoglobin From a Synthetic Gene, *Proteins-Structure Function and Genetics* 7, 358-365.
17. Wagner, G. C., Perez, M., Toscano, W. A. Jr., and Gunsalus, I. C. (1981) Apoprotein Formation and Heme Reconstitution of Cytochrome P-450cam, *J. Biol. Chem.* 256, 6262-6265.
18. Springer, B. A., and Sligar, S. G. (1987) High-Level Expression of Sperm Whale Myoglobin in Escherichia-coli, *Proc. Natl. Acad. Sci. U. S. A.* 84, 8961-8965.
19. Morris, D. R., Hager, L. P. (1966) Chloroperoxidase: I. Isolation and Properties of the Crystalline Glycoprotein *J. Biol. Chem.* 241, 1763-1768.
20. Unger, B. P., Gunsalus, I. C., Sligar, S. G. (1986) Nucleotide-sequence of the Pseudomonas-putida Cytochrome P450-cam Gene and Its Expression in Escherichia-coli, *J. Biol. Chem.* 261, 1158-1163.
21. Yu, C.-A., Gunsalus, I. C., Katagiri, M., Suhara, K., and Takemori, S. (1974) Cytochrome P-450cam: I. Crystallization and Properties *J. Biol. Chem.* 249, 94-101.
22. Chiang, R., Makino, R., Spomer, W. E., Hager, L. P. (1975) Chloroperoxidase. P-450 type absorption in the absence of sulfhydryl groups, *Biochemistry* 14, 4166-4171.
23. Sigman, J. A., Pond, A. E., Dawson, J. H., and Lu, Y. (1999) Engineering cytochrome c peroxidase into cytochrome P450: A proximal effect on heme-thiolate ligation, *Biochemistry* 38, 11122-11129.
24. Liu, Y., Moenne-Loccoz, P., Hildebrand, D. P., Wilks, A., Loehr, T. M., Mauk, A. G., and Ortiz de Montellano, P. R. (1999) Replacement of the Proximal Histidine Iron Ligand by a Cysteine or Tyrosine Converts Heme Oxygenase to an Oxidase, *Biochemistry* 38, 3733-3743.
25. Raphael, A. L. a. G., H. B. (1991) Semisynthesis of Axial-Ligand (Position 80) Mutants of Cytochrome c, *J. Am. Chem. Soc.* 113, 1038-1040.

26. Wang, W., Lu, J., Yao, P., Xie, Y., and Huang, Z. (2003) The distinct heme coordination environments and heme-binding stabilities of His39Ser and His39Cys mutants of cytochrome b5, *Protein Engineering* 16, 1047-1054.

APPENDIX A

Sequences of P450cam and pET-30a (+) Vector

General information

The cytochrome P450cam protein includes 414 amino acids.

Figure A.1 lists the amino acid sequence of full-length, wild-type cytochrome P450cam.

Figure A.2 lists the complete nucleotide sequence of the 1578-bp PstI-HindIII fragment, including the wild-type cytochrome P450cam structural gene from *Pseudomonas putida*, 155 bp of 5' flanking sequence, and 175 bp of 3' DNA.

Figure A.3 lists the nucleotide sequence of vector pET-30a (+) from Novagen.

Figure A.4 displays a map of plasmid pET-30a (+)_P450cam, which is the pET-30a (+) vector with the P450cam gene cloned in.

Figure A.5 lists the nucleotide sequence of plasmid pET-30a (+)_P450cam containing vector pET-30a(+) and wild-type cytochrome P450cam gene cloned into NdeI (5'-end, nucleotide position 1596 in the pET-30a (+) vector sequence) and HindIII (3'-end, nucleotide position 173 in the pET-30a (+) vector sequence). The numbering is correspondent to that of Figure A.5.

Figure A.1 Amino acid sequence of full-length of WT cytochrome P450cam.

1 MTTETIQSNA NLAPLPPHVP EHLVFDFDMY NPSNLSAGVQ EAWAVLQESN
51 VPDLVWTRCN GGHWIATRQ LIREAYEDYR HFSSECPFIP REAGEAYDFI
101 PTSMDPPEQR QFRALANQVV GMPVVDKLEN RIQELACSLI ESLRPQGQCN
151 FTEDYAEPFP IRIFMLLAGL PEEDIPHLKY LTDQMTRPDG SMTFAEAKEA
201 LYDYLIPIIE QRRQKPGTDA ISIVANGQVN GRPITSDEAK RMCGLLLVGG
251 LDTVVNFLSF SMEFLAKSPE HRQELIERPE RIPAACEELL RRFSLVADGR
301 ILTSDYEFHG VQLKKGDQIL LPQMLSGLDE RENACPMHVD FSRQKVSHTT
351 FGHGSHLCLG QHLARREIIV TLKEWLTRIP DFSIAPGAQI QHKSGIVSGV
401 QALPLVWDPA TTKAV

Figure A.2 Nucleotide sequence of full-length WT cytochrome P450cam from *Pseudomonas putida* (5 bp upstream of PstI site, total 1578bp).

```
1 CTGCAGGATC GTTATCCGCT GGCCGATCTG ATCACCCAGC GTTTTTCCAT
51 CGACGAGGCC AGCAAGGCAC TTGAACTGGT CAAGGCAGGA GCACTGATCA
101 AACCCGTGAT CGACTCCACT CTTTAGCCAA CCCGCGTTCC AGGAGAACAA
151 CAACAATGAC GACTGAAACC ATACAAAGCA ACGCCAATCT TGCCCCTCTG
201 CCACCCCATG TGCCAGAGCA CCTGGTATTC GACTTCGACA TGTACAATCC
251 GTCGAATCTG TCTGCCGGCG TGCAGGAGGC CTGGGCAGTT CTGCAAGAAT
301 CAAACGTACC GGATCTGGTG TGGACTCGCT GCAACGGCGG AACTGGATC
351 GCCACTCGCG GCCAACTGAT CCGTGAGGCC TATGAAGATT ACCGCCACTT
401 TTCCAGCGAG TGCCCGTTCA TCCCTCGTGA AGCCGGCGAA GCCTACGACT
451 TCATTCCAC CTCGATGGAT CCGCCCGAGC AGCGCCAGTT TCGTGCGCTG
501 GCCAACCAAG TGGTTGGCAT GCCGGTGGTG GATAAGCTGG AGAACCGGAT
551 CCAGGAGCTG GCCTGCTCGC TGATCGAGAG CCTGCGCCCG CAAGGACAGT
601 GCAACTTCAC CGAGGACTAC GCCGAACCCT TCCCGATACG CATCTTCATG
651 CTGCTCGCAG GTCTACCGGA AGAAGATATC CCGCACTTGA AATACCTAAC
701 GGATCAGATG ACCCGTCCGG ATGGCAGCAT GACCTTCGCA GAGGCCAAGG
751 AGGCGCTCTA CGACTATCTG ATACCGATCA TCGAGCAACG CAGGCAGAAG
801 CCGGGAACCG ACGCTATCAG CATCGTTGCC AACGGCCAGG TCAATGGGCG
851 ACCGATCACC AGTGACGAAG CCAAGAGGAT GTGTGGCCTG TTAGTGGTCG
901 GCGGCCTGGA TACGGTGGTC AATTTCTCA GCTTCAGCAT GGAGTTCCTG
951 GCCAAAAGCC CGGAGCATCG CCAGGAGCTG ATCGAGCGTC CCGAGCGTAT
1001 TCCAGCCGCT TCGAGGAAC TACTCCGGCG CTTCTCGCTG GTTGCCGATG
1051 GCCGCATCCT CACCTCCGAT TACGAGTTTC ATGGCGTGCA ACTGAAGAAA
1101 GGTGACCAGA TCCTGCTACC GCAGATGCTG TCTGGCCTGG ATGAGCGCGA
1151 AAACGCCTGC CCGATGCACG TCGACTTCAG TCGCCAAAAG GTTTCACACA
1201 CCACCTTTGG CCACGGCAGC CATCTGTGCC TTGGCCAGCA CCTGGCCCGC
1251 CGGGAAATCA TCGTCACCCT CAAGGAATGG CTGACCAGGA TTCCTGACTT
1301 CTCCATTGCC CCGGGTGCCC AGATTCAGCA CAAGAGCGGC ATCGTCAGCG
1351 GCGTGCAGGC ACTCCCTCTG GTCTGGGATC CGGCGACTAC CAAAGCGGTA
1401 TAAACACATG GGAGTGCGTG CTAAGTGAAC GCAAACGACA ACGTGGTCAT
1451 CGTCGGTACC GGAAGTGGTG GCGTTGAGGT CGCCTTCGGC CTGCGCGCCA
1501 GCGGCTGGGA AGGCAATATC CGGTTGGTGG GGGATGCGAC GGTAATTCCC
1551 CATCACCTAC CACCGCTATC CAAAGCTT
```

Figure A.3 Nucleotide sequence of vector pET-30a (+).

1 ATCCGGATAT AGTTCCTCCT TTCAGCAAAA AACCCCTCAA GACCCGTTTA
51 GAGGCCCCAA GGGGTTATGC TAGTTATTGC TCAGCGGTGG CAGCAGCCAA
101 CTCAGCTTCC TTTCGGGCTT TGTTAGCAGC CGGATCTCAG TGGTGGTGGT
151 GGTGGTGCTC GAGTGCGGCC GCAAGCTTGT CGACGGAGCT CGAATTCGGA
201 TCCGATATCA GCCATGGCCT TGTCGTCGTC GTCGGTACCC AGATCTGGGC
251 TGTCCATGTG CTGGCGTTCG AATTTAGCAG CAGCGGTTTC TTTCATACCA
301 GAACCGCGTG GCACCAGACC AGAAGAATGA TGATGATGAT GGTGCATATG
351 TATATCTCCT TCTTAAAGTT AAACAAAATT ATTTCTAGAG GGGAATTGTT
401 ATCCGCTCAC AATTCCCCTA TAGTGAGTCG TATTAATTTT GCGGGATCGA
451 GATCGATCTC GATCCTCTAC GCCGGACGCA TCGTGGCCGG CATCACCGGC
501 GCCACAGGTG CGGTTGCTGG CGCCTATATC GCCGACATCA CCGATGGGGA
551 AGATCGGGCT CGCCACTTCG GGCTCATGAG CGCTTGTTTC GGCCTGGGTA
601 TGGTGGCAGG CCCCGTGGCC GGGGGACTGT TGGGCGCCAT CTCCTTGCAT
651 GCACCATTC TCGCGCGGC GGTGCTCAAC GGCCTCAACC TACTACTGGG
701 CTGCTTCCTA ATGCAGGAGT CGCATAAGGG AGAGCGTCGA GATCCCGGAC
751 ACCATCGAAT GGCGCAAAAC CTTTCGCGGT ATGGCATGAT AGCGCCCGGA
801 AGAGAGTCAA TTCAGGGTGG TGAATGTGAA ACCAGTAACG TTATACGATG
851 TCGCAGAGTA TGCCGGTGTC TCTTATCAGA CCGTTTCCCG CGTGGTGAAC
901 CAGGCCAGCC ACGTTTCTGC GAAAACGCGG GAAAAAGTGG AAGCGGCGAT
951 GGCGGAGCTG AATTACATTC CCAACCGCGT GGCACAACAA CTGGCGGGCA
1001 AACAGTCGTT GCTGATTGGC GTTGCCACCT CCAGTCTGGC CCTGCACGCG
1051 CCGTCGCAA TTGTCGCGGC GATTAAATCT CGCGCCGATC AACTGGGTGC
1101 CAGCGTGGTG GTGTCGATGG TAGAACGAAG CGGCGTCGAA GCCTGTAAAG
1151 CGGCGGTGCA CAATCTTCTC GCGCAACGCG TCAGTGGGCT GATCATTAAC
1201 TATCCGCTGG ATGACCAGGA TGCCATTGCT GTGGAAGCTG CCTGCACTAA
1251 TGTTCGGCG TTATTTCTTG ATGTCTCTGA CCAGACACCC ATCAACAGTA
1301 TTATTTTCTC CCATGAAGAC GGTACGCGAC TGGGCGTGGA GCATCTGGTC
1351 GCATTGGGTC ACCAGCAAAT CGCGCTGTTA GCGGGCCCAT TAAGTTCTGT
1401 CTCGGCGCGT CTGCGTCTGG CTGGCTGGCA TAAATATCTC ACTCGCAATC
1451 AAATTCAGCC GATAGCGGAA CGGGAAGGCG ACTGGAGTGC CATGTCCGGT
1501 TTCAACAAA CCATGCAAAT GCTGAATGAG GGCATCGTTC CCACTGCGAT
1551 GCTGGTTGCC AACGATCAGA TGGCGCTGGG CGCAATGCGC GCCATTACCG
1601 AGTCCGGGCT GCGCGTTGGT GCGGACATCT CGGTAGTGGG ATACGACGAT
1651 ACCGAAGACA GTCATGTTA TATCCCGCCG TTAACCACCA TCAAACAGGA
1701 TTTTCGCCTG CTGGGGCAAA CCAGCGTGGA CCGCTTGCTG CAACTCTCTC
1751 AGGGCCAGGC GGTGAAGGGC AATCAGCTGT TGCCCGTCTC ACTGGTGAAA
1801 AGAAAAACCA CCCTGGCGCC CAATACGCAA ACCGCCTCTC CCCGCGCGTT
1851 GGCCGATTCA TTAATGCAGC TGGCACGACA GGTTTCCCGA CTGGAAGCG

1901 GGCAGTGAGC GCAACGCAAT TAATGTAAGT TAGCTCACTC ATTAGGCACC
 1951 GGGATCTCGA CCGATGCCCT TGAGAGCCTT CAACCCAGTC AGCTCCTTCC
 2001 GGTGGGCGCG GGGCATGACT ATCGTCGCCG CACTTATGAC TGTCTTCTTT
 2051 ATCATGCAAC TCGTAGGACA GGTGCCGGCA GCGCTCTGGG TCATTTTCGG
 2101 CGAGGACCGC TTTCGCTGGA GCGCGACGAT GATCGGCCTG TCGCTTGCGG
 2151 TATTCGGAAT CTTGCACGCC CTCGCTCAAG CCTTCGTCAC TGGTCCCGCC
 2201 ACCAAACGTT TCGGCGAGAA GCAGGCCATT ATCGCCGGCA TGGCGGCCCC
 2251 ACGGGTGCGC ATGATCGTGC TCCTGTCGTT GAGGACCCGG CTAGGCTGGC
 2301 GGGGTTGCCT TACTGGTTAG CAGAATGAAT CACCGATACG CGAGCGAACG
 2351 TGAAGCGACT GCTGCTGCAA AACGTCTGCG ACCTGAGCAA CAACATGAAT
 2401 GGTCTTCGGT TTCCGTGTTT CGTAAAGTCT GGAAACGCGG AAGTCAGCGC
 2451 CCTGCACCAT TATGTTCCGG ATCTGCATCG CAGGATGCTG CTGGCTACCC
 2501 TGTGGAACAC CTACATCTGT ATTAACGAAG CGCTGGCATT GACCCTGAGT
 2551 GATTTTCTC TGGTCCCGCC GCATCCATAC CGCCAGTTGT TTACCCTCAC
 2601 AACGTTCCAG TAACCGGGCA TGTTTCATCAT CAGTAACCCG TATCGTGAGC
 2651 ATCCTCTCTC GTTTCATCGG TATCATTACC CCCATGAACA GAAATCCCCC
 2701 TTACACGGAG GCATCAGTGA CCAAACAGGA AAAAACCGCC CTTAACATGG
 2751 CCCGCTTTAT CAGAAGCCAG ACATTAACGC TTCTGGAGAA ACTCAACGAG
 2801 CTGGACGCGG ATGAACAGGC AGACATCTGT GAATCGCTTC ACGACCACGC
 2851 TGATGAGCTT TACCGCAGCT GCCTCGCGCG TTTCGGTGAT GACGGTGAAA
 2901 ACCTCTGACA CATGCAGCTC CCGGAGACGG TCACAGCTTG TCTGTAAGCG
 2951 GATGCCGGGA GCAGACAAGC CCGTCAGGGC GCGTCAGCGG GTGTTGGCGG
 3001 GTGTCGGGGC GCAGCCATGA CCCAGTCACG TAGCGATAGC GGAGTGTATA
 3051 CTGGCTTAAC TATGCGGCAT CAGAGCAGAT TGTACTGAGA GTGCACCATA
 3101 TATGCGGTGT GAAATACCGC ACAGATGCGT AAGGAGAAAA TACCGCATCA
 3151 GGCGCTCTTC CGCTTCCTCG CTCACTGACT CGCTGCGCTC GGTCGTTTCG
 3201 CTGCGGCGAG CGGTATCAGC TCACTCAAAG GCGGTAATAC GGTTATCCAC
 3251 AGAATCAGGG GATAACGCAG GAAAGAACAT GTGAGCAAAA GGCCAGCAAA
 3301 AGGCCAGGAA CCGTAAAAAG GCCGCGTTGC TGGCGTTTTT CCATAGGCTC
 3351 CGCCCCCTG ACGAGCATCA CAAAATCGA CGCTCAAGTC AGAGGTGGCG
 3401 AAACCCGACA GGAATAAAA GATACCAGGC GTTCCCCCT GGAAGCTCCC
 3451 TCGTGCGCTC TCCTGTTCCG ACCCTGCCGC TTACCGGATA CCTGTCCGCC
 3501 TTTCTCCCTT CGGGAAGCGT GCGGCTTTCT CATAGCTCAC GCTGTAGGTA
 3551 TCTCAGTTCG GTGTAGGTCG TTCGCTCCAA GCTGGGCTGT GTGCACGAAC
 3601 CCCCCGTTCA GCCCGACCGC TCGCCTTAT CCGGTAATA TCGTCTTGAG
 3651 TCCAACCCGG TAAGACACGA CTTATCGCCA CTGGCAGCAG CCACTGGTAA
 3701 CAGGATTAGC AGAGCGAGGT ATGTAGGCGG TGCTACAGAG TTCTTGAAGT
 3751 GGTGGCCTAA CTACGGCTAC ACTAGAAGGA CAGTATTTGG TATCTGCGCT
 3801 CTGCTGAAGC CAGTTACCTT CGGAAAAAGA GTTGGTAGCT CTTGATCCGG
 3851 CAAACAAACC ACCGCTGGTA GCGGTGGTTT TTTGTTTGC AAGCAGCAGA

3901 TTACGCGCAG AAAAAAAGGA TCTCAAGAAG ATCCTTTGAT CTTTTCTACG
 3951 GGGTCTGACG CTCAGTGGAA CGAAAACTCA CGTTAAGGGA TTTTGGTCAT
 4001 GAACAATAAA ACTGTCTGCT TACATAAACA GTAATACAAG GGGTGTTATG
 4051 AGCCATATTC AACGGGAAAC GTCTTGCTCT AGGCCGCGAT TAAATTCCAA
 4101 CATGGATGCT GATTTATATG GGTATAAATG GGCTCGCGAT AATGTCGGGC
 4151 AATCAGGTGC GACAATCTAT CGATTGTATG GGAAGCCCGA TGCGCCAGAG
 4201 TTGTTTCTGA AACATGGCAA AGGTAGCGTT GCCAATGATG TTACAGATGA
 4251 GATGGTCAGA CTAAACTGGC TGACGGAATT TATGCCTCTT CCGACCATCA
 4301 AGCATTTTAT CCGTACTCCT GATGATGCAT GGTTACTCAC CACTGCGATC
 4351 CCCGGGAAAA CAGCATTCCA GGTATTAGAA GAATATCCTG ATTCAGGTGA
 4401 AAATATTGTT GATGCGCTGG CAGTGTCCT GCGCCGGTTG CATTGATTC
 4451 CTGTTTGTA TTGTCCTTTT AACAGCGATC GCGTATTTTC TCTCGCTCAG
 4501 GCGCAATCAC GAATGAATAA CGGTTTGGTT GATGCGAGTG ATTTTGATGA
 4551 CGAGCGTAAT GGCTGGCCTG TTGAACAAGT CTGGAAAGAA ATGCATAAAC
 4601 TTTTGCCATT CTCACCGGAT TCAGTCGTCA CTCATGGTGA TTTCTCACTT
 4651 GATAACCTTA TTTTGTACGA GGGGAAATTA ATAGGTTGTA TTGATGTTGG
 4701 ACGAGTCGGA ATCGCAGACC GATACCAGGA TCTTGCCATC CTATGGAAC
 4751 GCCTCGGTGA GTTTTCTCCT TCATTACAGA AACGGCTTTT TCAAAAATAT
 4801 GGTATTGATA ATCCTGATAT GAATAAATTG CAGTTTCATT TGATGCTCGA
 4851 TGAGTTTTTC TAAGAATTAA TTCATGAGCG GATACATATT TGAATGTATT
 4901 TAGAAAAATA AACAAATAGG GGTTCGCGC ACATTTCCCC GAAAAGTGCC
 4951 ACCTGAAATT GTAAACGTTA ATATTTTGTT AAAATTCGCG TTAAATTTTT
 5001 GTTAAATCAG CTCATTTTTT AACCAATAGG CCGAAATCGG CAAAATCCCT
 5051 TATAAATCAA AAGAATAGAC CGAGATAGGG TTGAGTGTTG TTCCAGTTTG
 5101 GAACAAGAGT CCACTATTAA AGAACGTGGA CTCCAACGTC AAAGGGCGAA
 5151 AAACCGTCTA TCAGGGCGAT GGCCCACTAC GTGAACCATC ACCCTAATCA
 5201 AGTTTTTTTG GGTGAGGTG CCGTAAAGCA CTAAATCGGA ACCCTAAAGG
 5251 GAGCCCCCGA TTTAGAGCTT GACGGGGAAA GCCGGCGAAC GTGGCGAGAA
 5301 AGGAAGGGAA GAAAGCGAAA GGAGCGGGCG CTAGGGCGCT GCAAGTGTA
 5351 GCGGTCACGC TGC GCGTAAC CACCACACCC GCCGCGCTTA ATGCGCCGCT
 5401 ACAGGGCGCG TCCCATTCGC CA

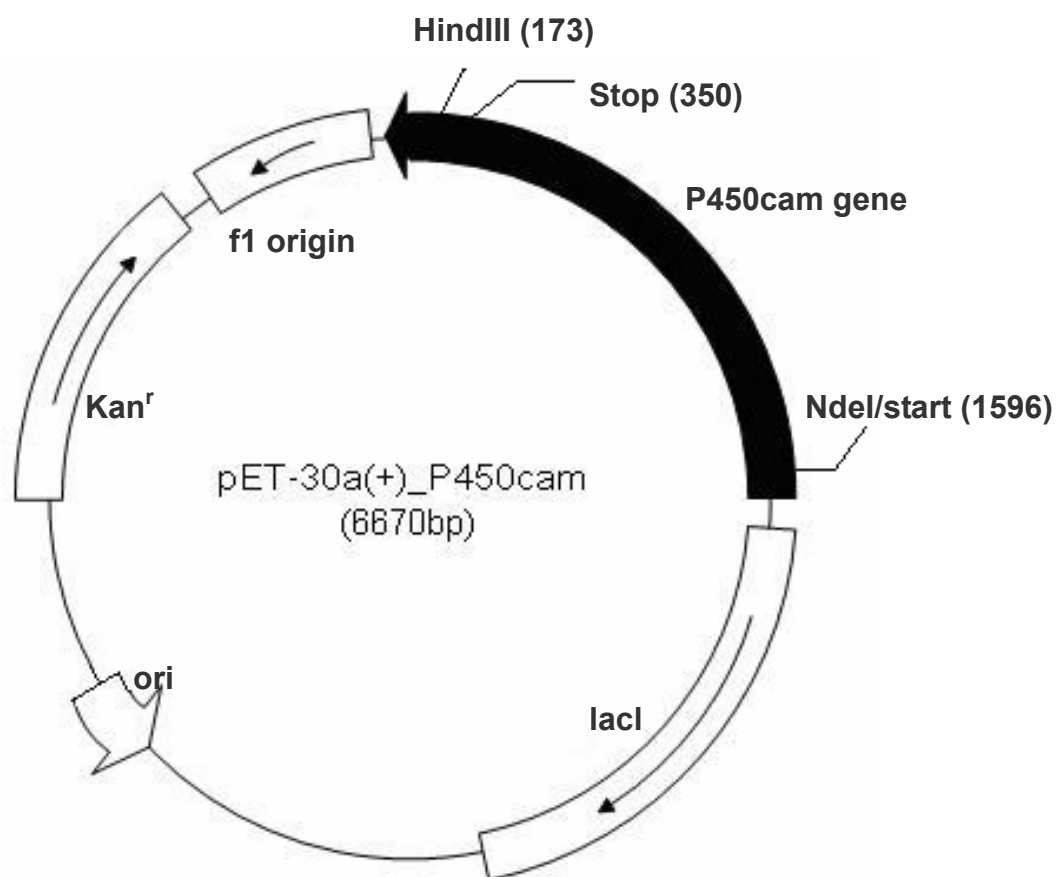


Figure A.4 Plasmid map of pET-30a (+)_P450cam.

Figure A.5 Nucleotide sequence of plasmid containing vector pET-30a(+) and WT cytochrome P450cam gene. (152+1426+5072=6670bp)

```
1 ATCCGGATAT AGTTCCTCCT TTCAGCAAAA AACCCCTCAA GACCCGTTTA
51 GAGGCCCCAA GGGGTTATGC TAGTTATTGC TCAGCGGTGG CAGCAGCCAA
101 CTCAGCTTCC TTTCGGGCTT TGTTAGCAGC CGGATCTCAG TGGTGGTGGT
151 GGTGGTGCTC GAGTGCGGCC GCAAGCTTTG GATAGCGGTG GTAGGTGATG
201 GGGAATTACC GTCGCATCCC CCACCAACCG GATATTGCCT TCCCAGCCGC
251 TGGCGCGCAG GCCGAAGGCG ACCTCAACGC CAGCCAGTCC GGTACCGACG
301 ATGACCACGT TGTCGTTTGC GTTCACTTAG CACGCACTCC CATGTGTTTA
351 TACCGCTTTG GTAGTCGCCG GATCCAGAC CAGAGGGAGT GCCTGCACGC
401 CGCTGACGAT GCCGCTCTTG TGCTGAATCT GGGCACCCGG GGCAATGGAG
451 AAGTCAGGAA TCCTGGTCAG CCATTCCTTG AGGGTGACGA TGATTTCCTG
501 GCGGGCCAGG TGCTGGCCAA GGCACAGATG GCTGCCGTGG CCAAAGGTGG
551 TGTGTGAAAC CTTTGGCGA CTGAAGTCGA CGTGCATCGG GCAGGCGTTT
601 TCGCGCTCAT CCAGGCCAGA CAGCATCTGC GGTAGCAGGA TCTGGTCACC
651 TTTCTTCAGT TGCACGCCAT GAAACTCGTA ATCGGAGGTG AGGATGCGGC
701 CATCGGCAAC CAGCGAGAAG CGCCGGAGTA GTTCCTCGCA AGCGGCTGGA
751 ATACGCTCGG GACGCTCGAT CAGCTCCTGG CGATGCTCCG GGCTTTTGGC
801 CAGGAACTCC ATGCTGAAGC TGAGGAAATT GACCACCGTA TCCAGGCCGC
851 CGACCAGTAA CAGGCCACAC ATCCTCTTGG CTTCTGCTACT GGTGATCGGT
901 CGCCCATTGA CCTGGCCGTT GGCAACGATG CTGATAGCGT CGGTTCCCGG
951 CTTCTGCCTG CGTTGCTCGA TGATCGGTAT CAGATAGTC GTAGAGCGCCT
1001 CCTTGGCCTC TGCGAAGGTC ATGCTGCCAT CCGGACGGGT CATCTGATCC
1051 GTTAGGTATT TCAAGTGCGG GATATCTTCT TCCGGTAGAC CTGCGAGCAG
1101 CATGAAGATG CGTATCGGGA AGGGTTCGGC GTAGTCCTCG GTGAAGTTGC
1151 ACTGTCCTTG CGGGCGCAGG CTCTCGATCA GCGAGCAGGC CAGCTCCTGG
1201 ATCCGGTTCT CCAGCTTATC CACCACCGGC ATGCCAACCA CTTGGTTGGC
1251 CAGCGCACGA AACTGGCGCT GCTCGGGCGG ATCCATCGAG GTGGGAATGA
1301 AGTCGTAGGC TTCGCCGGCT TCACGAGGGA TGAACGGGCA CTCGCTGGAA
1351 AAGTGGCGGT AATCTTCATA GGCCTCACGG ATCAGTTGGC CGCGAGTGGC
1401 GATCCAGTGT CCGCCGTTGC AGCGAGTCCA CACCAGATCC GGTACGTTTG
1451 ATTCTTGCAG AACTGCCCAG GCCTCCTGCA CGCCGGCAGA CAGATTCGAC
1501 GGATTGTACA TGTCGAAGTC GAATACCAGG TGCTCTGGCA CATGGGGTGG
1551 CAGAGGGGCA AGATTGGCGT TGCTTTGTAT GGTTTCAGTC GTCATATGTA
1601 TATCTCCTTC TTAAAGTTAA ACAAATTAT TTCTAGAGGG GAATTGTTAT
1651 CCGCTCACAA TTCCCCTATA GTGAGTCGTA TTAATTTTCGC GGGATCGAGA
1701 TCGATCTCGA TCCTCTACGC CGGACGCATC GTGGCCGGCA TCACCGGCGC
1751 CACAGGTGCG GTTGCTGGCG CCTATATCGC CGACATCACC GATGGGGAAG
1801 ATCGGGCTCG CCACTTCGGG CTCATGAGCG CTTGTTTCGG CGTGGGTATG
```

1851 GTGGCAGGCC CCGTGGCCGG GGGACTGTTG GGCGCCATCT CCTTGCATGC
 1901 ACCATTCTT GCGGCGGCGG TGCTCAACGG CCTCAACCTA CTACTGGGCT
 1951 GCTTCCTAAT GCAGGAGTCG CATAAGGGAG AGCGTCGAGA TCCCGGACAC
 2001 CATCGAATGG CGCAAAACCT TTCGCGGTAT GGCATGATAG CGCCCGGAAG
 2051 AGAGTCAATT CAGGGTGGTG AATGTGAAAC CAGTAACGTT ATACGATGTC
 2101 GCAGAGTATG CCGGTGTCTC TTATCAGACC GTTTCGCGG TGGTGAACCA
 2151 GGCCAGCCAC GTTCTGCGA AAACGCGGGA AAAAGTGGAA GCGGCGATGG
 2201 CGGAGCTGAA TTACATTCCC AACCGCGTGG CACAACAACCT GGCGGGCAAA
 2251 CAGTCGTTGC TGATTGGCGT TGCCACCTCC AGTCTGGCCC TGCACGCGCC
 2301 GTCGCAAATT GTCGCGGCGA TTAAATCTCG CGCCGATCAA CTGGGTGCCA
 2351 GCGTGGTGGT GTCGATGGTA GAACGAAGCG GCGTCGAAGC CTGTAAAGCG
 2401 GCGGTGCACA ATCTTCTCGC GCAACGCGTC AGTGGGCTGA TCATTAACCTA
 2451 TCCGCTGGAT GACCAGGATG CCATTGCTGT GGAAGCTGCC TGCACCTAATG
 2501 TTCCGGCGTT ATTTCTTGAT GTCTCTGACC AGACACCCAT CAACAGTATT
 2551 ATTTTCTCCC ATGAAGACGG TACGCGACTG GGCGTGGAGC ATCTGGTCGC
 2601 ATTGGGTCAC CAGCAAATCG CGCTGTTAGC GGGCCCATTA AGTTCTGTCT
 2651 CGGCGCGTCT GCGTCTGGCT GGCTGGCATA AATATCTCAC TCGCAATCAA
 2701 ATTCAGCCGA TAGCGGAACG GGAAGGCGAC TGGAGTGCCA TGTCCGGTTT
 2751 TCAACAAACC ATGCAAATGC TGAATGAGGG CATCGTTCCC ACTGCGATGC
 2801 TGGTTGCCAA CGATCAGATG GCGCTGGGCG CAATGCGCGC CATTACCGAG
 2851 TCCGGGCTGC GCGTTGGTGC GGACATCTCG GTAGTGGGAT ACGACGATAC
 2901 CGAAGACAGC TCATGTTATA TCCCGCCGTT AACCACCATC AAACAGGATT
 2951 TTCGCCTGCT GGGGCAAACC AGCGTGGACC GCTTGCTGCA ACTCTCTCAG
 3001 GGCCAGGCGG TGAAGGGCAA TCAGCTGTTG CCCGTCTCAC TGGTGAAAAG
 3051 AAAAACCACC CTGGCGCCCA ATACGCAAAC CGCCTCTCCC CGCGCGTTGG
 3101 CCGATTCATT AATGCAGCTG GCACGACAGG TTTCCCGACT GGAAAGCGGG
 3151 CAGTGAGCGC AACGCAATTA ATGTAAGTTA GCTCACTCAT TAGGCACCGG
 3201 GATCTCGACC GATGCCCTTG AGAGCCTTCA ACCCAGTCAG CTCCTTCCGG
 3251 TGGGCGCGGG GCATGACTAT CGTCGCCGCA CTTATGACTG TCTTCTTTAT
 3301 CATGCAACTC GTAGGACAGG TGCCGGCAGC GCTCTGGGTC ATTTTCGGCG
 3351 AGGACCGCTT TCGCTGGAGC GCGACGATGA TCGGCCTGTC GCTTGCGGTA
 3401 TTCGGAATCT TGCACGCCCT CGCTCAAGCC TTCGTCACTG GTCCCGCCAC
 3451 CAAACGTTTC GCGGAGAAGC AGGCCATTAT CGCCGGCATG GCGGCCCCAC
 3501 GGGTGCGCAT GATCGTGCTC CTGTCGTTGA GGACCCGGCT AGGCTGGCGG
 3551 GGTTGCCTTA CTGGTTAGCA GAATGAATCA CCGATACGCG AGCGAACGTG
 3601 AAGCGACTGC TGCTGCAAAA CGTCTGCGAC CTGAGCAACA ACATGAATGG
 3651 TCTTCGGTTT CCGTGTTTCG TAAAGTCTGG AAACGCGGAA GTCAGCGCCC
 3701 TGCACCATTA TGTTCCGGAT CTGCATCGCA GGATGCTGCT GGCTACCCTG
 3751 TGGAACACCT ACATCTGTAT TAACGAAGCG CTGGCATTGA CCCTGAGTGA
 3801 TTTTCTCTG GTCCCGCCGC ATCCATACCG CCAGTTGTTT ACCCTCACA

3851 CGTTCCAGTA ACCGGGCATG TTCATCATCA GTAACCCGTA TCGTGAGCAT
 3901 CCTCTCTCGT TTCATCGGTA TCATTACCCC CATGAACAGA AATCCCCCTT
 3951 ACACGGAGGC ATCAGTGACC AAACAGGAAA AAACCGCCCT TAACATGGCC
 4001 CGCTTTATCA GAAGCCAGAC ATTAACGCTT CTGGAGAAAC TCAACGAGCT
 4051 GGACGCGGAT GAACAGGCAG ACATCTGTGA ATCGCTTCAC GACCACGCTG
 4101 ATGAGCTTTA CCGCAGCTGC CTCGCGCGTT TCGGTGATGA CGGTGAAAAC
 4151 CTCTGACACA TGCAGCTCCC GGAGACGGTC ACAGCTTGTC TGTAAGCGGA
 4201 TGCCGGGAGC AGACAAGCCC GTCAGGGCGC GTCAGCGGGT GTTGGCGGGT
 4251 GTCGGGGCGC AGCCATGACC CAGTCACGTA GCGATAGCGG AGTGTATACT
 4301 GGCTTAATA TGCGGCATCA GAGCAGATTG TACTGAGAGT GCACCATATA
 4351 TGCGGTGTGA AATACCGCAC AGATGCGTAA GGAGAAAATA CCGCATCAGG
 4401 CGCTCTTCCG CTTCTCGCT CACTGACTCG CTGCGCTCGG TCGTTCGGCT
 4451 GCGGCGAGCG GTATCAGCTC ACTCAAAGGC GGTAATACGG TTATCCACAG
 4501 AATCAGGGGA TAACGCAGGA AAGAACATGT GAGCAAAAGG CCAGCAAAAG
 4551 GCCAGGAACC GTAAAAAGGC CGCGTTGCTG GCGTTTTTCC ATAGGCTCCG
 4601 CCCCCCTGAC GAGCATCACA AAAATCGACG CTCAAGTCAG AGGTGGCGAA
 4651 ACCCGACAGG ACTATAAAGA TACCAGGCGT TTCCCCCTGG AAGCTCCCTC
 4701 GTGCGCTCTC CTGTTCCGAC CCTGCCGCTT ACCGGATACC TGTCCGCCTT
 4751 TCTCCCTTCG GGAAGCGTGG CGCTTTCTCA TAGCTCACGC TGTAGGTATC
 4801 TCAGTTCGGT GTAGGTCGTT CGCTCCAAGC TGGGCTGTGT GCACGAACCC
 4851 CCGGTTGAGC CCGACCGCTG CGCCTTATCC GGTAAGTATC GTCTTGAGTC
 4901 CAACCCGGTA AGACACGACT TATCGCCACT GGCAGCAGCC ACTGGTAACA
 4951 GGATTAGCAG AGCGAGGTAT GTAGGCGGTG CTACAGAGTT CTTGAAGTGG
 5001 TGGCCTAACT ACGGCTACAC TAGAAGGACA GTATTTGGTA TCTGCGCTCT
 5051 GCTGAAGCCA GTTACCTTCG GAAAAAGAGT TGGTAGCTCT TGATCCGGCA
 5101 AACAAACCAC CGCTGGTAGC GGTGGTTTTT TTGTTTGCAA GCAGCAGATT
 5151 ACGCGCAGAA AAAAAGGATC TCAAGAAGAT CCTTTGATCT TTTCTACGGG
 5201 GTCTGACGCT CAGTGGAACG AAAACTCACG TTAAGGGATT TTGGTCATGA
 5251 ACAATAAAAC TGTCTGCTTA CATAAACAGT AATACAAGGG GTGTTATGAG
 5301 CCATATTCAA CGGGAAACGT CTTGCTCTAG GCCGCGATTA AATTCCAACA
 5351 TGGATGCTGA TTTATATGGG TATAAATGGG CTCGCGATAA TGTCGGGCAA
 5401 TCAGGTGCGA CAATCTATCG ATTGTATGGG AAGCCCGATG CGCCAGAGTT
 5451 GTTTCTGAAA CATGGCAAAG GTAGCGTTGC CAATGATGTT ACAGATGAGA
 5501 TGGTCAGACT AAAGTGGCTG ACGGAATTTA TGCCTCTTCC GACCATCAAG
 5551 CATTTTATCC GTACTCCTGA TGATGCATGG TTAATCACCA CTGCGATCCC
 5601 CGGGAAAACA GCATTCCAGG TATTAGAAGA ATATCCTGAT TCAGGTGAAA
 5651 ATATTGTTGA TGCCTGGCA GTGTTCTGCG GCCGGTTGCA TTCGATTCCT
 5701 GTTTGTAATT GTCCTTTTAA CAGCGATCGC GTATTTGTC TCGCTCAGGC
 5751 GCAATCACGA ATGAATAACG GTTTGGTTGA TGCGAGTGAT TTTGATGACG
 5801 AGCGTAATGG CTGGCCTGTT GAACAAGTCT GGAAAGAAAT GCATAAACTT

5851 TTGCCATTCT CACCGGATTC AGTCGTCAC T CATGGTGATT TCTCACTTGA
5901 TAACCTTATT TTTGACGAGG GGAAATTAAT AGGTTGTATT GATGTTGGAC
5951 GAGTCGGAAT CGCAGACCGA TACCAGGATC TTGCCATCCT ATGGAAGTGC
6001 CTCGGTGAGT TTTCTCCTTC ATTACAGAAA CGGCTTTTTC AAAAATATGG
6051 TATTGATAAT CCTGATATGA ATAAATTGCA GTTTCATTG ATGCTCGATG
6101 AGTTTTTCTA AGAATTAATT CATGAGCGGA TACATATTTG AATGTATTTA
6151 GAAAAATAAA CAAATAGGGG TTCCGCGCAC ATTTCCCCGA AAAGTGCCAC
6201 CTGAAATTGT AAACGTTAAT ATTTTGTTAA AATTCGCGTT AAATTTTGT
6251 TAAATCAGCT CATTTTTTAA CCAATAGGCC GAAATCGGCA AAATCCCTTA
6301 TAAATCAAAA GAATAGACCG AGATAGGGTT GAGTGTTGTT CCAGTTTGGA
6351 ACAAGAGTCC ACTATTAAAG AACGTGGACT CCAACGTCAA AGGGCGAAAA
6401 ACCGTCTATC AGGGCGATGG CCCACTACGT GAACCATCAC CCTAATCAAG
6451 TTTTTTGGGG TCGAGGTGCC GTAAAGCACT AAATCGGAAC CCTAAAGGGA
6501 GCCCCCGATT TAGAGCTTGA CGGGGAAAGC CGGCGAACGT GGCGAGAAAG
6551 GAAGGGAAGA AAGCGAAAGG AGCGGGCGCT AGGGCGCTGG CAAGTGTAGC
6601 GGTCACGCTG CGCGTAACCA CCACACCCGC CGCGCTTAAT GCGCCGCTAC
6651 AGGGCGCGTC CCATTGCGCA

APPENDIX B

Sequences of Sperm Whale Myoglobin and pET-30a (+) Vector

General information

The sperm whale myoglobin includes 154 amino acids.

Figure B.1 lists the amino acid sequence of full-length, wild-type sperm whale myoglobin.

Figure B.1 lists the nucleotide sequence of the synthesized sperm whale myoglobin gene as designed from the amino acid sequence including the ribosome binding site. (Springer, B. *et al*, *Proc Natl Acad Sci USA*, 1987, 84, 8961-8965)

Figure B.3 displays a map of plasmid pET-30a (+)_Mb, which is the pET-30a (+) vector with the sperm whale myoglobin gene cloned in.

Figure B.4 lists the nucleotide sequence of plasmid pET-30a (+)_Mb containing vector pET-30a(+) and wild-type sperm whale myoglobin gene cloned into NdeI (5'-end, nucleotide position 713 in the pET-30a (+) vector sequence) and KpNI (3'-end, nucleotide position 238 in the pET-30a (+) vector sequence). The numbering is correspondent to that of Figure B.4.

Figure B.1 Amino acid sequence of full-length of sperm whale myoglobin (154aa).

1 MVLSEGEWQL VLHVWAKVEA DVAGHGQDIL IRLFKSHPET LEKFDRFKHL
51 KTEAEMKASE DLKKHGVTVL TALGAILKKK GHHEAELKPL AQSHATKHKI
101 PIKYLEFISE AIIHVLHSRH PGNFGADAQG AMNKALELFR KDIAAKYKEL
151 GYQG

Figure B.2 Nucleotide sequence of full-length sperm whale myoglobin (507bp).

1 CTGCAGATAA CTA ACTAAAG GAGAACAACA ACAATGGTTC TGTCTGAAGG
51 TGAATGGCAG CTGGTTCTGC ATGTTTGGGC TAAAGTTGAA GCTGACGTCG
101 CTGGTCATGG TCAGGACATC TTGATTCGAC TGTTCAAATC TCATCCGGAA
151 ACTCTGGAAA AATTCGATCG TTTCAAACAT CTGAAAACCTG AAGCTGAAAT
201 GAAAGCTTCT GAAGATCTGA AAAAACATGG TGTTACCGTG TTAAGTCCCC
251 TAGGTGCTAT CCTTAAGAAA AAAGGGCATC ATGAAGCTGA GCTCAAACCG
301 CTTGCGCAAT CGCATGCTAC TAAACATAAG ATCCCGATCA AATACCTGGA
351 ATTCATCTCT GAAGCGATCA TCCATGTTCT GCATTCTAGA CATCCAGGTA
401 ACTTCGGTGC TGACGCTCAG GGTGCTATGA ACAAAGCTCT CGAGCTGTTC 451
CGTAAAGATA TCGCTGCTAA GTACAAAGAA CTGGGTTACC AGGGTTAATG
501 AGGTACC

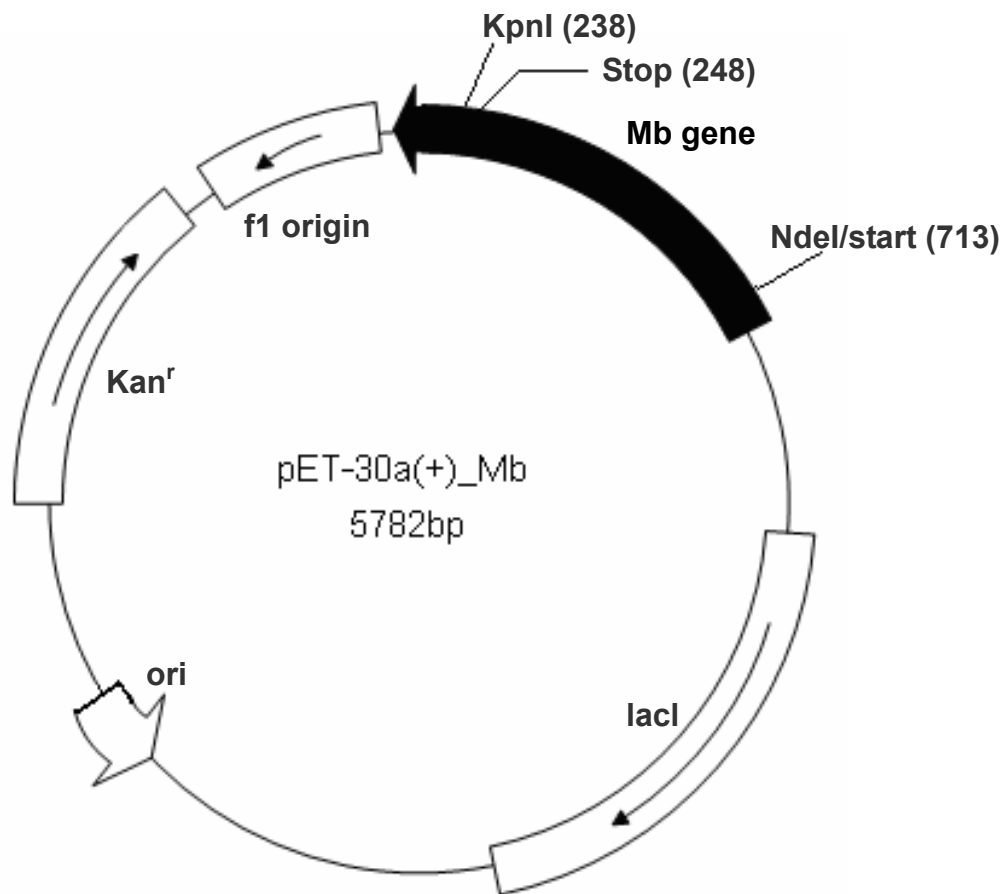


Figure B.3 Plasmid map of pET-30a (+)_Mb.

Figure B.4 Nucleotide sequence of plasmid containing vector pET-30a (+) and sperm whale myoglobin gene (5782bp).

```
1 ATCCGGATAT AGTTCCTCCT TTCAGCAAAA AACCCCTCAA GACCCGTTTA
51 GAGGCCCCAA GGGGTTATGC TAGTTATTGC TCAGCGGTGG CAGCAGCCAA
101 CTCAGCTTCC TTTCGGGCTT TGTTAGCAGC CGGATCTCAG TGGTGGTGGT
151 GGTGGTGCTC GAGTGCGGCC GCAAGCTTGT CGACGGAGCT CGAATTCGGA
201 TCCGATATCA GCCATGGCCT TGTCGTCGTC GTCGGTACCT CATTAACCCT
251 GGTAACCCAG TTCTTTGTAC TTAGCAGCGA TATCTTTACG GAACAGCTCG
301 AGAGCTTTGT TCATAGCACC CTGAGCGTCA GCACCGAAGT CACCTGGATG
351 TCTAGAATGC AGAACATGGA TGATCGCTTC AGAGATGAAT TCCAGGTATT
401 TGATCGGGAT CTTATGTTTA GTAGCATGCG ATTGCGCAAG CGGTTTGAGC
451 TCAGCTTCAT GATGCCCTTT TTTCTTAAGG ATAGCACCTA GGGCAGTTAA
501 CACGGTAACA CCATGTTTTT TCAGATCTTC AGAAGCTTTC ATTTCAGCTT
551 CAGTTTTTCAG ATGTTTGAAA CGATCGAATT TTTCCAGAGT TTCCGGATGA
601 GATTTGAACA GTCGAATCAA GATGTCCTGA CCATGACCAG CGACGTCAGC
651 TTCAACTTTA GCCCAAACAT GCAGAACCAG CTGCCATTCA CCTTCAGACA
701 GAACCATATG TATATCTCCT TCTTAAAGTT AAACAAAATT ATTTCTAGAG
751 GGGAAATTGTT ATCCGCTCAC AATTCCCCTA TAGTGAGTCG TATTAATTTT
801 GCGGGATCGA GATCGATCTC GATCCTCTAC GCCGGACGCA TCGTGGCCGG
851 CATCACCGGC GCCACAGGTG CGGTTGCTGG CGCCTATATC GCCGACATCA
901 CCGATGGGGA AGATCGGGCT CGCCACTTCG GGCTCATGAG CGCTTGTTTC
951 GGCGTGGGTA TGGTGGCAGG CCCCCTGGCC GGGGGACTGT TGGGCGCCAT
1001 CTCCTTGCAT GCACCATTCC TTGCGGCGGC GGTGCTCAAC GGCCTCAACC
1051 TACTACTGGG CTGCTTCCTA ATGCAGGAGT CGCATAAGGG AGAGCGTCGA
1101 GATCCCGGAC ACCATCGAAT GGCGCAAAAC CTTTCGCGGT ATGGCATGAT
1151 AGCGCCCGGA AGAGAGTCAA TTCAGGGTGG TGAATGTGAA ACCAGTAACG
1201 TTATACGATG TCGCAGAGTA TGCCGGTGTC TCTTATCAGA CCGTTTCCCG
1251 CGTGGTGAAC CAGGCCAGCC ACGTTTCTGC GAAAACGCGG GAAAAAGTGG
1301 AAGCGGCGAT GGCAGGAGCTG AATTACATTC CCAACCGCGT GGCACAACAA
1351 CTGGCGGGCA AACAGTCGTT GCTGATTGGC GTTGCCACCT CCAGTCTGGC
1401 CCTGCACGCG CCGTCGCAA TGTGTCGCGC GATTAAATCT CGCGCCGATC
1451 AACTGGGTGC CAGCGTGGTG GTGTCGATGG TAGAACGAAG CGGCGTCGAA
1501 GCCTGTAAAG CGGCGGTGCA CAATCTTCTC GCGCAACGCG TCAGTGGGCT
1551 GATCATTAAC TATCCGCTGG ATGACCAGGA TGCCATTGCT GTGGAAGCTG
1601 CCTGCACTAA TGTTCCGGCG TTATTTCTTG ATGTCTCTGA CCAGACACCC
1651 ATCAACAGTA TTATTTTCTC CCATGAAGAC GGTACGCGAC TGGGCGTGGA
1701 GCATCTGGTC GCATTGGGTC ACCAGCAAAT CGCGCTGTGA GCGGGCCCAT
1751 TAAGTTCTGT CTCGGCGCGT CTGCGTCTGG CTGGCTGGCA TAAATATCTC
1801 ACTCGCAATC AAATTCAGCC GATAGCGGAA CGGGAAGGCG ACTGGAGTGC
```

1851 CATGTCCGGT TTTCAACAAA CCATGCAAAT GCTGAATGAG GGCATCGTTC
 1901 CCACTGCGAT GCTGGTTGCC AACGATCAGA TGGCGCTGGG CGCAATGCGC
 1951 GCCATTACCG AGTCCGGGCT GCGCGTTGGT GCGGACATCT CGGTAGTGGG
 2001 ATACGACGAT ACCGAAGACA GCTCATGTTA TATCCCGCCG TTAACCACCA
 2051 TCAAACAGGA TTTTCGCCTG CTGGGGCAAA CCAGCGTGGA CCGCTTGCTG
 2101 CAACTCTCTC AGGGCCAGGC GGTGAAGGGC AATCAGCTGT TGCCCGTCTC
 2151 ACTGGTGAAA AGAAAAACCA CCCTGGCGCC CAATACGCAA ACCGCCTCTC
 2201 CCCGCGCGTT GGCCGATTCA TTAATGCAGC TGGCACGACA GGTTTCCCGA
 2251 CTGGAAAGCG GGCAGTGAGC GCAACGCAAT TAATGTAAGT TAGCTCACTC
 2301 ATTAGGCACC GGGATCTCGA CCGATGCCCT TGAGAGCCTT CAACCCAGTC
 2351 AGCTCCTTCC GGTGGGCGCG GGGCATGACT ATCGTCGCCG CACTTATGAC
 2401 TGTCTTCTTT ATCATGCAAC TCGTAGGACA GGTGCCGGCA GCGCTCTGGG
 2451 TCATTTTCGG CGAGGACCGC TTTCGCTGGA GCGCGACGAT GATCGGCCTG
 2501 TCGCTTGCGG TATTCGGAAT CTTGCACGCC CTCGCTCAAG CTTTCGTAC
 2551 TGGTCCCGCC ACCAAACGTT TCGGCGAGAA GCAGGCCATT ATCGCCGGCA
 2601 TGGCGGCCCC ACGGGTGCGC ATGATCGTGC TCCTGTCGTT GAGGACCCGG
 2651 CTAGGCTGGC GGGGTTGCCT TACTGGTTAG CAGAATGAAT CACCGATACG
 2701 CGAGCGAACG TGAAGCGACT GCTGCTGCAA AACGTCTGCG ACCTGAGCAA
 2751 CAACATGAAT GGTCTTCGGT TTCCGTGTTT CGTAAAGTCT GGAAACGCGG
 2801 AAGTCAGCGC CCTGCACCAT TATGTTCCGG ATCTGCATCG CAGGATGCTG
 2851 CTGGCTACCC TGTGGAACAC CTACATCTGT ATTAACGAAG CGCTGGCATT
 2901 GACCCTGAGT GATTTTTCTC TGGTCCCGCC GCATCCATAC CGCCAGTTGT
 2951 TTACCCTCAC AACGTTCCAG TAACCGGGCA TGTTTCATCAT CAGTAACCCG
 3001 TATCGTGAGC ATCCTCTCTC GTTTCATCGG TATCATTACC CCCATGAACA
 3051 GAAATCCCCC TTACACGGAG GCATCAGTGA CCAAACAGGA AAAAACCGCC
 3101 CTTAACATGG CCCGCTTAT CAGAAGCCAG ACATTAACGC TTCTGGAGAA
 3151 ACTCAACGAG CTGGACGCGG ATGAACAGGC AGACATCTGT GAATCGCTTC
 3201 ACGACCACGC TGATGAGCTT TACCGCAGCT GCCTCGCGCG TTTCGGTGAT
 3251 GACGGTGAAA ACCTCTGACA CATGCAGCTC CCGGAGACGG TCACAGCTTG
 3301 TCTGTAAGCG GATGCCGGGA GCAGACAAGC CCGTCAGGGC GCGTCAGCGG
 3351 GTGTTGGCGG GTGTCGGGGC GCAGCCATGA CCCAGTCACG TAGCGATAGC
 3401 GGAGTGTATA CTGGCTTAAC TATGCGGCAT CAGAGCAGAT TGTACTGAGA
 3451 GTGCACCATA TATGCGGTGT GAAATACCGC ACAGATGCGT AAGGAGAAAA
 3501 TACCGCATCA GGCGCTCTTC CGCTTCCTCG CTCACTGACT CGCTGCGCTC
 3551 GGTCGTTTCGG CTGCGGCGAG CGGTATCAGC TCACTCAAAG GCGGTAATAC
 3601 GGTTATCCAC AGAATCAGGGGATAACGCAG GAAAGAACATGTGAGCAAAA
 3651 GGCCAGCAAA AGGCCAGGAA CCGTAAAAAG GCCGCGTTGC TGGCGTTTTT
 3701 CCATAGGCTC CGCCCCCTG ACGAGCATCA CAAAAATCGA CGCTCAAGTC
 3751 AGAGGTGGCG AAACCCGACA GGACTATAAA GATACCAGGC GTTTCCCCT
 3801 GGAAGCTCCC TCGTGCGCTC TCCTGTTCCG ACCCTGCCGC TTACCGGATA

3851 CCTGTCCGCC TTTCTCCCTT CGGGAAGCGT GCGCTTTCT CATAGCTCAC
 3901 GCTGTAGGTA TCTCAGTTCG GTGTAGGTCG TTCGCTCCAA GCTGGGCTGT
 3951 GTGCACGAAC CCCCCGTTCA GCCCGACCGC TCGCCTTAT CCGGTAAC TA
 4001 TCGTCTTGAG TCCAACCCGG TAAGACACGA CTTATCGCCA CTGGCAGCAG
 4051 CCACTGGTAA CAGGATTAGC AGAGCGAGGT ATGTAGGCGG TGCTACAGAG
 4101 TTCTTGAAGT GGTGGCCTAA CTACGGCTAC ACTAGAAGGA CAGTATTTGG
 4151 TATCTGCGCT CTGCTGAAGC CAGTTACCTT CGGAAAAAGA GTTGGTAGCT
 4201 CTTGATCCGG CAAACAAACC ACCGCTGGTA GCGGTGGTTT TTTTGTTCG
 4251 AAGCAGCAGA TTACGCGCAG AAAAAAGGA TCTCAAGAAG ATCCTTTGAT
 4301 CTTTTCTACG GGGTCTGACG CTCAGTGGAA CGAAAACTCA CGTTAAGGGA
 4351 TTTTGGTCAT GAACAATAAA ACTGTCTGCT TACATAAACA GTAATACAAG
 4401 GGGTGTTATG AGCCATATTC AACGGGAAAC GTCTTGCTCT AGGCCGCGAT
 4451 TAAATTCCAA CATGGATGCT GATTATATG GGTATAAATG GGCTCGCGAT
 4501 AATGTCGGGC AATCAGGTGC GACAATCTAT CGATTGTATG GGAAGCCCGA
 4551 TCGCCAGAG TTGTTTCTGA AACATGGCAA AGGTAGCGTT GCCAATGATG
 4601 TTACAGATGA GATGGTCAGA CTAACTGGC TGACGGAATT TATGCCTCTT
 4651 CCGACCATCA AGCATTTTAT CCGTACTCCT GATGATGCAT GGTTACTCAC
 4701 CACTGCGATC CCCGGGAAAA CAGCATTCCA GGTATTAGAA GAATATCCTG
 4751 ATTCAGGTGA AAATATTGTT GATGCGCTGG CAGTGTTCCCT GCGCCGGTTG
 4801 CATTGATTC CTGTTTGTA TGTCTTTT AACAGCGATC GCGTATTTTCG
 4851 TCTCGCTCAG GCGCAATCAC GAATGAATAA CGGTTTGGTT GATGCGAGTG
 4901 ATTTTGATGA CGAGCGTAAT GGCTGGCCTG TTGAACAAGT CTGGAAAGAA
 4951 ATGCATAAAC TTTTGCCATT CTCACCGGAT TCAGTCGTCA CTCATGGTGA
 5001 TTTCTCACTT GATAACCTTA TTTTGACGA GGGGAAATTA ATAGGTTGTA
 5051 TTGATGTTGG ACGAGTCGGA ATCGCAGACC GATACCAGGA TCTTGCCATC
 5101 CTATGGA ACT GCCTCGGTGA GTTTTCTCCT TCATTACAGA AACGGCTTTT
 5151 TCAAAAATAT GGTATTGATA ATCCTGATAT GAATAAATTG CAGTTTCATT
 5201 TGATGCTCGA TGAGTTTTTC TAAGAATTAA TTCATGAGCG GATACATATT
 5251 TGAATGTATT TAGAAAAATA AACAAATAGG GGTTCCGCGC ACATTTCCCC
 5301 GAAAAGTGCC ACCTGAAATT GTAAACGTTA ATATTTTGTT AAAATTGCGC
 5351 TTAAATTTTT GTTAAATCAG CTCATTTTTT AACCAATAGG CCGAAATCGG
 5401 CAAATCCCT TATAAATCAA AAGAATAGAC CGAGATAGGG TTGAGTGTG
 5451 TTCCAGTTTG GAACAAGAGT CCACTATTAA AGAACGTGGA CTCCAACGTC
 5501 AAAGGGCGAA AAACCGTCTA TCAGGGCGAT GGCCCACTAC GTGAACCATC
 5551 ACCCTAATCA AGTTTTTTGG GGTGAGGTG CCGTAAAGCA CTAAATCGGA
 5601 ACCCTAAAGG GAGCCCCCGA TTAGAGCTT GACGGGGAAA GCCGGCGAAC
 5651 GTGGCGAGAAAGGAAGGGAAGAAAGCGAAA GGAGCGGGCG CTAGGGCGCT
 5701 GCAAGTGTA GCGGTCACGC TCGCGTAAC CACCACACC GCCGCGCTTA
 5751 ATGCGCCGCT ACAGGGCGCG TCCATTCGC CA

APPENDIX C

General information

Table C1 and C2 list all the primers designed for wild type cytochrome P450cam and sperm whale myoglobin and their mutants in this dissertation study.

Table C1. Primers layout for P450cam and its mutants

Primer names	Primes
P450-1 (primer with NdeI)	5'- CCA CAT ATG ACG ACT GAA ACC -3' (21bp)
P450-2 (primer with HindIII)	5'- CCC AAG CTT TGG ATA GCG GTG GTA -3' (24bp)
P450-3 (L244/245/246K)	5'- AGG ATG TGT GGC AAG AAA AAG GTC GGC GGC CTG -3' (33bp)
P450-4 (complementary of P450-3)	5'- CAG GCC GCC GAC CTT TTT CTT GCC ACA CAT CCT -3' (33bp)
P450-5(L250K/ T252H/V253A/V254R)	5'- AAG GTC GGC GGC AAG GAT CAC GCC CGC AAT TTC CTC A -3' (37bp)
P450-6(complementary of P450-5)	5'- T GAG GAA ATT GCG GGC GTG ATC CTT GCC GCC GAC CTT -3' (37bp)
P450-7 (P450H: 7a.a. mutation)	5'- TG TGT GGC AAG AAA AAG GTC GGC GGC AAG GAT CAC GCC CGC AAT TTC CTC -3' (50bp)
P450-8 (complementary of P450-7)	5'- GAG GAA ATT GCG GGC GTG ATC CTT GCC GCC GAC CTT TTT CTT GCC ACA CA -3' (50bp)
P450-9 (C357H)	5'- AGC CAT CTG CAT CTT GGC CAG CAC -3' (24bp)
P450-10 (complementary of P450-9)	5'- GTG CTG GCC AAG ATG CAG ATG GCT -3' (24bp)
P450-11 (L244K)	5'- ATG TGT GGC AAG TTA CTG GTC GGC -3' (24bp)
P450-12 (complementary of P450-11)	5'- GCC GAC CAG TAA CTT GCC ACA CAT -3' (24bp)
P450-13 (L244/245K)	5'- ATG TGT GGC AAG AAG CTG GTC GGC -3' (24bp)
P450-14 (complementary of P450-13)	5'- GCC GAC CAG CTT CTT GCC ACA CAT -3' (24bp)
P450-17 (L245K)	5'- ATG TGT GGC CTG AAA CTG GTC GGC -3' (24bp)
P450-18 (complementary of P450-17)	5'- GCC GAC CAG TTT CAG GCC ACA CAT -3' (24bp)
P450-19 (L246K)	5'- ATG TGT GGC CTG TTA AAG GTC GGC -3' (24bp)
P450-20 (complementary of P450-19)	5'- GCC GAC CTT TAA CAG GCC ACA CAT -3' (24bp)

Table C1. Primer layout for P450cam and its mutants (continued).

Primer names	Primes
P450-21 (H352G/H355G/361G)	5' - TTT GGC GGT GGC AGC GGT CTG TGC CTT GGC CAG GCA CTG GCC C -3' (43bp)
P450-22 (complementary of P450-21)	5' - G GGC CAG TGC CTG GCC AAG GCA CAG ACC GCT GCC ACC GCC AAA -3' (43bp)
P450-23 (L244H.)	5' - ATG TGT GGC CAT TTA CTG GTC GGC -3' (24bp)
P450-24 (complementary of P450-23)	5' - GCC GAC CAG TAA ATG GCC ACA CAT -3' (24bp)
P450-25 (V247H)	5' - CTG TTA CTG CAT GGC GGC CTG GAT -3' (24bp)
P450-26 (complementary of P450-25)	5' - ATC CAG GCC GCC ATG CAG TAA CAG -3' (24bp)
P450-27 (G248H)	5' - TTA CTG GTC CAT GGC CTG GAT ACG -3' (24bp)
P450-28 (complementary of P450-27)	5' - CGT ATC CAG GCC ATG GAC CAG TAA -3' (24bp)
P450-29 (C357G)	5' - AGC CAT CTG GGT CTT GGC CAG CAC CT -3' (26bp)
P450-30 (complementary of P450-29)	5' - AG GTG CTG GCC AAG ACC CAG ATG GCT -3' (26bp)
P450-31 (L246R)	5' - ATG TGT GGC CTG TTA CGT GTC GGC -3' (24bp)
P450-32 (complementary of P450-31)	5' - GCC GAC ACG TAA CAG GCC ACA CAT -3' (24bp)
P450-33 (G243R/V247H)	5' - ATG TGT CGT CTG TTA CTG CAT GGC GGC -3' (27bp)
P450-34 (complementary of P450-33)	5' - GCC GCC ATG CAG TAA CAG ACG ACA CAT -3' (27bp)
P450-35 (G248R/T252H)	5' - A CTG GTC CGT GGC CTG GAT CAT GTG GTC AA -3' (30bp)
P450-36 (complementary of P450-35)	5' - TT GAC CAC ATG ATC CAG GCC ACG GAC CAG T -3' (30bp)
P450-37 (L244R/V247H)	5' - ATG TGT GGC CGT TTA CTG CAT GGC GGC -3' (27bp)
P450-38 (complementary of P450-37)	5' - GCC GCC ATG CAG TAA ACG GCC ACA CAT -3' (27bp)

Table C2. Primer layout for Mb and its mutants.

Primer names	Primers
Mb-1 (P450 mimic with 8a.a. mutation)	5' - GGT TCT CGT CTG TGC CTG GGT CAG CAT AAG ATC CCG ATC AA -3' (41bp)
Mb-2 (reverse direction)	5' - CGG TTT GAG CTC AGC TTC ATG ATG C -3' (25bp)
Mb-3 (primer with NdeI)	5' - CCA CAT ATG GTT CTG TCT GAA GGT G -3' (25bp)
Mb-4 (primer with KpNI)	5' - CTA GGT ACC TCA TTA ACC CTG GTA -3' (24bp)
Mb-5 (CPO mimic with 8a.a. mutation)	5' - TCT CGT GCT CCT TGC CCA GCT CTG CAT AAG ATC CCG ATC AA -3' (41bp)
Mb-8 (H64G)	5' - CTG AAA AAA GGT GGT GTT ACC GTG-3' (24bp)
Mb-9 (complementary of Mb-8)	5' - CAC GGT AAC ACC ACC TTT TTT CAG -3' (24bp)
Mb-10 (H64E)	5' - CTG AAA AAA GAA GGT GTT ACC GTG-3' (24bp)
Mb-11 (complementary of Mb-10)	5' - CAC GGT AAC ACC TTC TTT TTT CAG -3' (24bp)
Mb-12 (H97A of MbP)	5' - CTG GGT CAG GCT AAG ATC CCG ATC-3' (24bp)
Mb-13 (complementary of Mb-12)	5' - GAT CGG GAT CTT AGC CTG ACC CAG -3' (24bp)
Mb-14 (H97A of MbO)	5' - CCA GCT CTG GCT AAG ATC CCG ATC-3' (24bp)
Mb-15 (complementary of Mb-14)	5' - GAT CGG GAT CTT AGC CAG AGC TGG -3' (24bp)
Mb-16 (V68C)	5' - AA CAT GGT GTT ACC TGC TTA ACT GCC-3' (26bp)
Mb-17 (complementary of Mb-16)	5' - GGC AGT TAA GCA GGT AAC ACC ATG TT -3' (26bp)

VITA

HUI TIAN

May 19, 1981

Born, Hebei, China

1999-2003

Bachelor, Chemical Engineering and Technology
Hebei University of Technology, China

2010

Doctoral Candidate in Chemistry
Florida International University
Miami, Florida

PUBLICATIONS AND PRESENTATIONS

Tian, Hui; Wang, Zhonghua; Terentis, Andrew; Wang, Xiaotang. *Relative stability of iron-sulfur bond vs iron-nitrogen bond in heme thiolate protein: Evidence from an engineered cytochrome P450cam with a novel heme iron ligand set*. Abstracts of Papers, 237th ACS National Meeting, Washington D.C., United States, August 17-22, 2009

Tian, Hui; Wang, Zhonghua; Terentis, Andrew; Wang, Xiaotang. *Single amino acid switch turns P450cam from a monooxygenase to an efficient peroxidase*. Abstracts of Papers, 237th ACS National Meeting, Salt Lake City, UT, United States, March 22-26, 2009

Tian, Hui; Jiang, Yucheng; Wang, Xiaotang. *Engineering P450 into P420 with catalytic activities*. Abstracts of Papers, 235th ACS National Meeting, New Orleans, LA, United States, April 6-10, 2008

Mulchandani, Avani; Tian, Hui; Wang, Xiaotang; Li, Chenzhong. *Nanomaterials functionalized device for redox studies of cytochrome P450cam L246K*. Abstracts of Papers, Biotech 2008, Miami, FL, United States, April 24, 2008

Wang, Xiaotang; Wang, Zheng; Jiang, Yucheng; Tian, Hui. *Catalytic roles of Phe103 at the substrate-binding pocket of chloroperoxidase: Remote control of heme chemistry in heme-thiolate proteins*. Abstracts of Papers, 234th ACS National Meeting, Boston, MA, United States, August 19-23, 2007

Wang, Xiaotang; Jiang, Yucheng; Zhang, Chengxiao; Wang, Zheng; Tian, Hui. *Structure of the green prosthetic group in chloroperoxidase following mechanism-based modification with terminal alkenes*. Abstracts of Papers, 232nd ACS National Meeting, San Francisco, CA, United States, Sept. 10-14, 2006